Structure and Dynamics of Chemically Modified Cellulose Ethers in Aqueous Solution

2020. 3

Department of Symbiotic Science of Environment and Natural Resources

United Graduate School of Agricultural Science

Tokyo University of Agriculture and Technology

Kengo Arai

Acknowledgements:

This thesis is carried out from 2014 to 2020 under the direction of Professor Toshiyuki Shikata at the Department of Symbiotic Science of Environment and Natural Resources, United Graduate School of Agricultural Science, Tokyo University of Agriculture and Technology.

First, I would like to express my sincere gratitude to Professor Toshiyuki Shikata for his invaluable guidance, kindest support and encouragement throughout my research and studies.

I also would like to thank Professor Masao Takayanagi, Professor Shinso Yokota, Associate Professor Natsuki Kasuya and Associate Professor Yoshiki Horikawa for their valuable discussions.

I am also grateful to all members of Shikata laboratory for their helpful discussion and sharing the precious time.

I would like to thank Shin-Etsu Chemical Co. Ltd. for kindly supplying the cellulose ether samples and providing their technical information. I also would like to express my gratitude to Dr. Kazuhisa Hayakawa of Shin-Etsu Chemical for providing helpful advices and useful discussions about the cellulose ethers. I would also like to thank Daicel Corporation for kindly supplying hydroxyethyl cellulose samples. I am also grateful to The Dow Chemical Company for kindly providing the hydroxyethyl cellulose samples. I would also like to thank Nippon Soda Co., Ltd. for kindly supplying the hydroxypropyl cellulose samples.

Finally, I am deeply grateful to my family for their unwavering support and warmest encouragement.

Kengo Arai

Contents

Chapter 1: General Introduction

1.1 Overview

Cellulose is the most abundant natural organic resource on the globe, and annual production of cellulose in nature is estimated to be 10^{14} – 10^{15} kg.[1] Cellulose is a high-molecular weight linear polysaccharide which consists of D-glucopyranose unit via β-(1,4) glycosidic linkage. The repeating units do not lie in a plane structure, rather they possess a chair conformation with succeeding glucose residues rotated by 180º on the molecular axis and possessing hydroxy groups in an equatorial position.[2] Cellulose fibers are bundles of microfibrils, and the cellulose molecules are always biosynthesized in the form of nanosized fibrils. The cellulose fibers work as the load-bearing constituents in plants.[3] The major industrial applications of cellulose are paper and textile ones. In addition, cellulose nanocrystals (CNCs) and cellulose nanofibers (CNFs) have been used as new materials due to their unique properties such as high mechanical characteristics and low density.[4,5] However, native cellulose is insoluble into most usual solvents, including water, due to highly developed inter- and intramolecular hydrogen bonding between its hydrophilic groups.[6,7] This insolubility has highly limited industrial applications of cellulose as a nature-friendly eco-material.

A series of chemically modified celluloses, such as water-soluble nonionic methyl, hydroxypropyl, hydroxyethyl and hydroxypropylmethyl cellulose ethers, anionic sodium carboxymethyl cellulose ether, and organic solvent-soluble ethyl and cyanoethyl cellulose ethers, and cellulose nitrate and cellulose acetate, have been developed by several chemical companies.[3] These chemically modified cellulose samples exhibit useful properties, such as viscosity thickening, surfactant activity, film formation, adhesion, and so on. Then, they have been widely used in various

areas such as pharmaceutical productions, foods, construction agents, cosmetics, oil drilling, and paint.[3,8] In spite of their wide application range, the reasons why these chemically modified cellulose samples can be dissolved in solvent have not been fully understood so far. Moreover, when one pays attention to the characteristics of aqueous solutions of non-ionic water-soluble cellulose ether samples (WSCEs), such as methyl, hydroxypropyl, hydroxyethyl, hydroxypropylmethyl and hydroxyethylmethyl cellulose ethers, illustrated in Scheme 1.1, one frequently encounters the complicated solution behavior that the solubilities of these cellulose ethers are highly dependent on temperature. Although the WSCEs well dissolve into water below room temperature, ca. 25 ºC, most of them lose their high solubility and sometimes become turbid gels at high temperatures, i.e., they have lower critical solution temperatures (LCST), which are strongly dependent on their substitution conditions by hydroxypropyl, hydroxyethyl and methyl groups.[9–11] However, the mechanism of losing water solubility for WSCEs with increasing temperature have not been clarified. Understanding the water solubility of WSCEs is very important to bring out their higher potential to be used in broader practical applications rather than they are currently used.

Scheme 1.1 Chemical structure of water-soluble cellulose ether samples

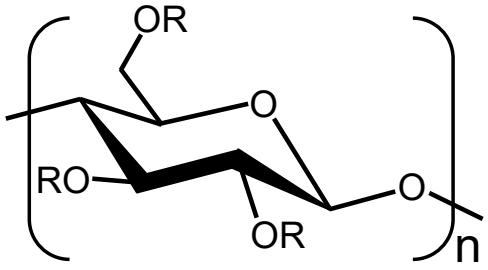

R = -H, -CH_3, -$CH_2CH(OH)CH_3$ or -CH_2CH_2OH

The water solubility of materials is one of the important fundamental properties. Water soluble compounds are usually called hydrophilic compounds. The essential reason for water solubility of the hydrophilic compounds is considered to be the hydration of hydrophilic groups in solute molecules and water molecules, resulted from the formation of intermolecular hydrogen

bonding between the hydrophilic groups and water molecules. However, the relation between hydration behavior and water solubility of the hydrophilic compounds has not been fully understood. Then, many studies have been carried out to explore the hydration behavior of various hydrophilic compounds in order to clarify the reasons why hydrophilic compounds are dissolved into water using various methods, such as extended depolarized light scattering (EDLS),[12–16] nuclear magnetic resonance (NMR),[17–19] neutron scattering (NS),[20] time-resolved fluorescence decay,[21] dielectric spectroscopy (DS)[15,22–27] and molecular dynamics simulation (MD)[28–31] techniques. These studies have revealed that the dynamics of hydrated water molecules in aqueous systems is affected by the solute molecules. In discussion on the water solubility of materials, many scientists believe that the hydration number for solute molecules in aqueous solution is a key parameter.

The dielectric spectroscopy measurement is one of the most useful methods to determine the amount of water molecules hydrated to solute molecules because the measurement is highly sensitive to a difference in the rates of rotational molecular motions of water molecules. The hydration numbers of hydrophilic chemical groups, such as ether,[22] hydroxy,[32] ester,[33] carbonyl,[33] cyano[34] and nitro[34] groups, have been determined by using the dielectric techniques to discuss the relationship between hydration number and their water solubility. Moreover, not only the hydration number of one hydrophilic group but also that of the complicated compounds which bear multiple hydrophilic groups would give important and indispensable information to understand the water solubility. This is because the solubility of the complicated compounds cannot be determined simply by the number of hydrophilic groups of them. Each hydrophilic group of the complicated compounds does not effectively demonstrate their potential hydration ability in water, because they would form inter- and intramolecular hydrogen bonding between themselves. For example, although glucose is the constituent monomer of cellulose and possesses high water solubility, native cellulose is completely insoluble in water. On the other hand, native dextran and pullulan which consist of α-1,6-D-glucopyranose unit and α-1,6-linked maltotriose molecule, respectively, well dissolve in water.[35]

Moreover, the water soluble cellulose ethers, WSCEs, are soluble in water below room temperature, whereas many kinds of them lose solubility at high temperatures. Ono et al.[23] have determined the temperature dependence of hydration numbers for poly(*N*-isopropylacrylamide) (PNIPAm) which is typical synthetic water-soluble polymer showing the LCST type phase behavior in aqueous solution, and clarified the temperature dependent hydration numbers are closely related to its solubility. Then, the dependence of hydration number for the WSCEs on temperature would have relation to their solubility in water and provide an important information to understand the water solubility of hydrophilic compounds.

On the other hand, dynamics and conformation of solute molecules in aqueous solution are considerably affected by water molecules. Thus, in order to fully understand the hydration behavior in aqueous solution, it is important to clarify the dynamics of solute molecules in aqueous solution. The dynamics of polymer molecules in solution can be observed by dynamic mechanical analysis (DMA) measurements using rheometers. The DMA measurements can precisely detect the mechanical behavior of tested solution samples in a frequency range from 10^{-2} to 10^{2} s^{-1} which are much lower than the frequency range for the dynamics of water molecules. Then, many studies have discussed the dynamics, phase separation and gelation behavior for solutions of polymeric compounds by using DMA measurements.

Briscoe et al.[36] have investigated the rheological properties of aqueous poly(vinyl alcohol), PVA, solutions and the effects of the degree of polymer hydrolysis, temperature, pressure and addition of electrolytes on rheological behavior of the solutions. They have concluded that these conditions alter the contribution of two types of hydrogen bonding, between the polymer chains and water molecules, and inter- and intra- polymer chains, in aqueous solutions, and the contribution determines the rheological properties of the solution.

Lessard et al.[37] have investigated the phase separation of aqueous poly(*N*,*N*-

diethylacrylamide) (PDEA) solution by using rheological and dynamic light scattering techniques. They reported that the aqueous systems show a coil-globule transition with increasing temperature before phase separation and finally demonstrated an aggregation phenomenon at a higher temperature.

Zhang et al.[38] have determined the molecular weight dependent the gelation concentration point, c_{gel}, for aqueous solutions of lentinan which consists of a β-1,3-D-glucan with a side chain of β-1,6-D-glucan and possesses triple helical structure, by using rheological measurements. They reported that obtained c_{gel} for the aqueous solution of lentinan with a high molecular weight was much lower than other many polymer solutions because of the high stiffness of triple helical structure and strong intra- and intermolecular interactions between lentinan molecules.

Although it is important to investigate the phase separation and gelation behavior of the polymer solutions directly, other fundamental information on solute polymer molecules, such as the conformation of the polymer molecules in the solution, is also indispensable to fully understand the complicated behavior. DMA measurements are one of the useful methods to explore the conformation of solute molecules. Doi and Edwards[39] have proposed famous theoretical models for polymer systems that predict the viscoelastic properties of the polymer systems dependent on conformation of polymer molecules. Ferry[40] has experimentally investigated the viscoelastic behavior of polymer systems in detail and discussed the dependence of the viscoelastic properties on many variables, such as temperature, molecular weight and concentration.

In my doctoral thesis, the hydration behavior of water soluble cellulose ether samples (WSCEs), such as methyl cellulose (MC), hydroxypropylmethyl cellulose (HpMC), hydroxyethylmethyl cellulose (HeMC), hydroxypropyl cellulose (HpC) and hydroxyethyl cellulose (HeC), in aqueous solution will be discussed from two different perspectives. The first one is the dynamics of water molecules in aqueous WSCEs solutions observed using dielectric spectroscopy measurements. The second one is the dynamics of solute cellulose molecules dissolved in aqueous

systems using dynamic viscoelastic techniques.

In Chapter 2, the temperature dependence of hydration numbers for HeC, MC, HpMC, HeMC, HpC samples with various substitution conditions and molecular weights in aqueous solution is determined by using extremely high-frequency dielectric spectroscopy techniques. The dependence of hydration numbers on the substitution conditions and molecular weight will be fully discussed.

In Chapter 3, the temperature dependence of viscoelastic behavior for aqueous solutions of MC and HpMC samples is investigated to understand the gelation mechanism of these solutions from the rheological point of view. The differences of temperature dependent viscoelasticity between aqueous solutions of MC and HpMC are discussed in relation to the hydration numbers of them. The concentration and molecular weight dependence of viscoelastic behavior for aqueous HpMC solution is investigated at a low temperature. The obtained results will be fully discussed to clarify the conformation of HpMC molecules in aqueous solution.

In Chapter 4, the temperature dependence of viscoelastic behavior for aqueous solutions of HpC and HeC samples is investigated to understand the gelation mechanism of the aqueous HpC system and confirm whether the HeC molecules are perfectly dissolved in water over a wide temperature range by using dynamic viscoelastic measurements. Moreover, I investigated the concentration and molecular weight dependence of viscoelastic behavior for aqueous solutions of HeC with a wide molecular weight range at a low temperature. The obtained results provide the information on the conformation of HeC molecules in aqueous solution. In addition, the differences of the viscoelastic behavior between aqueous solutions of HeC and HpMC at a low temperature will be discussed.

In Chapter 5, I summarize the results and discussion described in Chapter 2 to 4 and conclude the hydration behavior of aqueous WSCEs systems.

References

(1) Klemm, D.; Philipp, B.; Heinze, T.; Heinze, U.; Wagenknect, W. *Comprehensive Cellulose Chemistry. Vol. 2*; Wiley-VCH: Weinheim, 1998.

(2) Klemm, D.; Heublein, B.; Fink, H.-P.; Bohn, A. Cellulose: Fascinating Biopolymer and Sustainable Raw Material. *Angew. Chemie Int. Ed.* **2005**, *44* (22), 3358–3393.

(3) Kalia, S.; Kaith, B. S.; Inderjeet Kaur. *Cellulose Fibers : Bio- and Nano-Polymer Composites ; Green Chemistry and Technology*; Springer, 2011.

(4) Abdul Khalil, H. P. S.; Davoudpour, Y.; Islam, M. N.; Mustapha, A.; Sudesh, K.; Dungani, R.; Jawaid, M. Production and Modification of Nanofibrillated Cellulose Using Various Mechanical Processes: A Review. *Carbohydr. Polym.* **2014**, *99*, 649–665.

(5) Salas, C.; Nypelö, T.; Rodriguez-Abreu, C.; Carrillo, C.; Rojas, O. J. Nanocellulose Properties and Applications in Colloids and Interfaces. *Curr. Opin. Colloid Interface Sci.* **2014**, *19* (5), 383–396.

(6) Nishiyama, Y.; Langan, P.; Chanzy, H. Crystal Structure and Hydrogen-Bonding System in Cellulose Iβ from Synchrotron X-Ray and Neutron Fiber Diffraction. *J. Am. Chem. Soc.* **2002**, *124* (31), 9074–9082.

(7) Li, Y.; Liu, X.; Zhang, Y.; Jiang, K.; Wang, J.; Zhang, S. Why Only Ionic Liquids with Unsaturated Heterocyclic Cations Can Dissolve Cellulose: A Simulation Study. *ACS Sustain. Chem. Eng.* **2017**, *5* (4), 3417–3428.

(8) Clasen, C.; Kulicke, W. M. Determination of Viscoelastic and Rheo-Optical Material Functions of Water-Soluble Cellulose Derivatives. *Progress in Polymer Science (Oxford)*. 2001.

(9) Sarkar, N. Thermal Gelation Properties of Methyl and Hydroxypropyl Methylcellulose. *J. Appl. Polym. Sci.* **1979**, *24* (4), 1073–1087.

(10) Sarkar, N.; Walker, L. C. Hydration-Dehydration Properties of Methylcellulose and Hydroxypropylmethylcellulose. *Carbohydr. Polym.* **1995**, *27* (3), 177–185.

(11) Feller, R.; Wilt, M. *Evaluation of Cellulose Ethers for Conservation*; 1990; Vol. 3.

(12) Lupi, L.; Comez, L.; Paolantoni, M.; Perticaroli, S.; Sassi, P.; Morresi, A.; Ladanyi, B. M.; Fioretto, D. Hydration and Aggregation in Mono- and Disaccharide Aqueous Solutions by

Gigahertz-to-Terahertz Light Scattering and Molecular Dynamics Simulations. *J. Phys. Chem. B* **2012**, *116* (51), 14760–14767.

(13) Lupi, L.; Comez, L.; Paolantoni, M.; Fioretto, D.; Ladanyi, B. M. Dynamics of Biological Water: Insights from Molecular Modeling of Light Scattering in Aqueous Trehalose Solutions. *J. Phys. Chem. B* **2012**, *116* (25), 7499–7508.

(14) Comez, L.; Paolantoni, M.; Sassi, P.; Corezzi, S.; Morresi, A.; Fioretto, D. Molecular Properties of Aqueous Solutions: A Focus on the Collective Dynamics of Hydration Water. *Soft Matter* **2016**, *12* (25), 5501–5514.

(15) Perticaroli, S.; Nakanishi, M.; Pashkovski, E.; Sokolov, A. P. Dynamics of Hydration Water in Sugars and Peptides Solutions. *J. Phys. Chem. B* **2013**, *117* (25), 7729–7736.

(16) Corezzi, S.; Sassi, P.; Paolantoni, M.; Comez, L.; Morresi, A.; Fioretto, D. Hydration and Rotational Diffusion of Levoglucosan in Aqueous Solutions. *J. Chem. Phys.* **2014**, *140* (18).

(17) Denisov, V. P.; Halle, B. Protein Hydration Dynamics in Aqueous Solution. *Faraday Discuss.* **1996**, *103*, 227–244.

(18) Steinhoff, H. J.; Kramm, B.; Hess, G.; Owerdieck, C.; Redhardt, A. Rotational and Translational Water Diffusion in the Hemoglobin Hydration Shell: Dielectric and Proton Nuclear Relaxation Measurements. *Biophys. J.* **1993**, *65*, 1486–1495.

(19) Winther, L. R.; Qvist, J.; Halle, B. Hydration and Mobility of Trehalose in Aqueous Solution. *J. Phys. Chem. B* **2012**, *116* (30), 9196–9207.

(20) Perticaroli, S.; Ehlers, G.; Stanley, C. B.; Mamontov, E.; O'Neill, H.; Zhang, Q.; Cheng, X.; Myles, D. A. A.; Katsaras, J.; Nickels, J. D. Description of Hydration Water in Protein (Green Fluorescent Protein) Solution. *J. Am. Chem. Soc.* **2017**, *139* (3), 1098–1105.

(21) Pal, S. K.; Zewail, A. H. Dynamics of Water in Biological Recognition. *Chem. Rev.* **2004**, *104* (4), 2099–2124.

(22) Shikata, T.; Okuzono, M.; Sugimoto, N. Temperature-Dependent Hydration/Dehydration Behavior of Poly(Ethylene Oxide)s in Aqueous Solution. *Macromolecules* **2013**, *46* (5), 1956–1961.

(23) Ono, Y.; Shikata, T. Hydration and Dynamic Behavior of Poly(*N* -Isopropylacrylamide)s in Aqueous Solution: A Sharp Phase Transition at the Lower Critical Solution Temperature. *J. Am. Chem. Soc.* **2006**, *128* (31), 10030–10031.

(24) Arai, K.; Okuzono, M.; Shikata, T. Reason for the High Solubility of Chemically Modified Poly(Vinyl Alcohol)s in Aqueous Solution. *Macromolecules* **2015**, *48* (5), 1573–1578.

(25) Shiraga, K.; Suzuki, T.; Kondo, N.; Tajima, T.; Nakamura, M.; Togo, H.; Hirata, A.; Ajito, K.; Ogawa, Y. Broadband Dielectric Spectroscopy of Glucose Aqueous Solution: Analysis of the Hydration State and the Hydrogen Bond Network. *J. Chem. Phys.* **2015**, *142* (23), 234504.

(26) Shiraga, K.; Suzuki, T.; Kondo, N.; De Baerdemaeker, J.; Ogawa, Y. Quantitative Characterization of Hydration State and Destructuring Effect of Monosaccharides and Disaccharides on Water Hydrogen Bond Network. *Carbohydr. Res.* **2015**, *406*, 46–54.

(27) Shiraga, K.; Adachi, A.; Nakamura, M.; Tajima, T.; Ajito, K.; Ogawa, Y. Characterization of the Hydrogen-Bond Network of Water around Sucrose and Trehalose: Microwave and Terahertz Spectroscopic Study. *J. Chem. Phys.* **2017**, *146* (10), 105102.

(28) Deshmukh, S. A.; Sankaranarayanan, S. K. R. S.; Suthar, K.; Mancini, D. C. Role of Solvation Dynamics and Local Ordering of Water in Inducing Conformational Transitions in Poly(*N* -Isopropylacrylamide) Oligomers through the LCST. *J. Phys. Chem. B* **2012**, *116* (9), 2651–2663.

(29) Marchi, M.; Sterpone, F.; Ceccarelli, M. Water Rotational Relaxation and Diffusion in Hydrated Lysozyme. *J. Am. Chem. Soc.* **2002**, *124* (23), 6787–6791.

(30) Sterpone, F.; Stirnemann, G.; Laage, D. Magnitude and Molecular Origin of Water Slowdown Next to a Protein. *J. Am. Chem. Soc.* **2012**, *134* (9), 4116–4119.

(31) Tomobe, K.; Yamamoto, E.; Yasui, M.; Yasuoka, K. Effects of Temperature, Concentration, and Isomer on the Hydration Structure in Monosaccharide Solutions. *Phys. Chem. Chem. Phys.* **2017**, *19* (23), 15239–15246.

(32) Shikata, T.; Okuzono, M. Hydration/Dehydration Behavior of Polyalcoholic Compounds Governed by Development of Intramolecular Hydrogen Bonds. *J. Phys. Chem. B* **2013**, *117* (9), 2782–2788.

(33) Shikata, T.; Okuzono, M. Are All Polar Molecules Hydrophilic? Hydration Numbers of Ketones and Esters in Aqueous Solution. *J. Phys. Chem. B* **2013**, *117* (25), 7718–7723.

(34) Shikata, T.; Sagawa, N. Are All Polar Molecules Hydrophilic? -Hydration Numbers of Nitro Compounds and Nitriles in Aqueous Solution. *Phys. Chem. Chem. Phys.* **2014**, *16*, 13262–

13270.

(35) Eckelt, J.; Sugaya, R.; Wolf, B. A. Pullulan and Dextran: Uncommon Composition Dependent Flory-Huggins Interaction Parameters of Their Aqueous Solutions. *Biomacromolecules* **2008**, *9* (6), 1691–1697.

(36) Briscoe, B.; Luckham, P. The Effects of Hydrogen Bonding upon the Viscosity of Aqueous Poly(Vinyl Alcohol) Solutions. *Polymer (Guildf).* **2000**, *41* (10), 3851–3860.

(37) Lessard, D. G.; Ousalem, M.; Zhu, X. X.; Eisenberg, A.; Carreau, P. J. Study of the Phase Transition of Poly(N,N-Diethylacrylamide) in Water by Rheology and Dynamic Light Scattering. *J. Polym. Sci. Part B Polym. Phys.* **2003**, *41* (14), 1627–1637.

(38) Zhang, Y.; Xu, X.; Xu, J.; Zhang, L. Dynamic Viscoelastic Behavior of Triple Helical Lentinan in Water: Effects of Concentration and Molecular Weight. *Polymer (Guildf).* **2007**, *48* (22), 6681–6690.

(39) M. Doi and S. F. Edwards. *The Theory of Polymer Dynamics*; Oxford, 1986.

(40) Ferry, J. D. *Viscoelastic Properties of Polymers*, 3rd ed.; Wiley & Sons: New York, 1980.

Chapter 2: Hydration Behavior of Chemically Modified Cellulose Ethers in Aqueous Solution

2.1 Introduction

In this chapter, I focus on the dynamics of hydrated water molecules to water-soluble chemically modified cellulose ethers in aqueous solution in order to understand the hydration behavior of cellulose ethers. Although the water soluble cellulose ethers possess high water solubility below room temperature, ca. 25 ºC, most of them lose it and sometimes become turbid gels at high temperatures.[1–3] Takeshita et al.[4] have investigated the structure formation of aqueous methyl cellulose solution with increasing temperature by using small-angle X-ray scattering and light scattering techniques and reported that the liquid-liquid separation occurred before gelation. Bajwa et al.[5] have discussed the gelation process of aqueous hydroxypropylmethyl cellulose solution with increasing temperature by using infrared spectroscopic, rheological and turbidimetric measurements and found the increase of hydrophobic interactions between hydroxypropylmethyl cellulose molecules during the gelation process. Bodvik et al.[6] have discussed differences in aggregation kinetics and structure formation between aqueous solutions of methyl cellulose and hydroxypropylmethyl cellulose with increasing temperature by using scattering and viscometric measurements and cryogenic transmission electron microscopic techniques. Lott et al.[7,8] have investigated the structure formed by methyl cellulose in aqueous solution and gel state at temperatures higher than the gel points, and found a fibril structure in gels using cryogenic transmission electron microscopic and small-angle neutron scattering techniques.

The lowest temperature at which homogeneous clear solutions turn into turbid

inhomogeneous dispersed systems, i.e., a phase transition, is thermodynamically defined as “the lower critical solution temperature” (LCST).[9] Many scientists believe that the temperature dependence of the hydration number for solute molecules in aqueous solution should be a key parameter in controlling the fundamental physical characteristics related to the whole phase behavior. For both poly(oxyethylene) (POE) and poly(*N*-isopropylacrylamide) (PNIPAm), which are typical synthetic water-soluble polymers demonstrating the LCST type phase behavior in aqueous solution, the hydration number per monomeric unit has been determined as a function of temperature by using extremely high-frequency dielectric spectroscopic (DS) techniques.[10,11] In the case of PNIPAm, the hydration number exhibits a plateau value in a lower temperature range than the room temperature and is followed by a drastic decrease just below the LCST at 32 °C.[11] This temperature dependence is successfully explained by a theoretical model proposed by Matsuyama and Tanaka[12] that assumes a high cooperativity in the hydration/dehydration process governed by solute molecular characteristics.[11] On the other hand, the temperature dependence of the hydration number for POE in aqueous solution was much gentler than that for PNIPAm, which could be explained by the theory assuming a lower cooperativity in the hydration/dehydration process than that of PNIPAm.[10–12]

In the case of the LCST type phase transition behavior frequently observed in aqueous cellulose ethers systems, the hydration number should also be a key parameter to investigate the temperature dependence of phase behavior uniquely. So far, there have been few reports on the temperature dependence of hydration number for cellulose ethers. Koda et al.[13] tried to measure the hydration number of methyl cellulose samples in aqueous solution as a function of temperature using sound velocity measuring techniques. They concluded that the value of the hydration number is reduced with increasing temperature and with increasing the degree of substitution at the same temperature.[13] However, they did not discuss the molecular weight dependence of the hydration number and the critical hydration number that is necessary for the methyl cellulose sample to be dissolved into water.

It has been reported that the hydroxyethyl cellulose samples possess high solubility in water over a wide temperature range including high temperatures.[14] Koda et al.[15] have compared the water retention capacity between MC, HeC and HpC by using compression method and differential scanning calorimetry measurement and reported that the capacity of HeC is the strongest. This study was conducted at room temperature and 0 ºC, and very few studies have focused on the influence of temperature on aqueous HeC systems. However, the reason why the HeC samples maintain their water solubility at high temperatures has not been fully understood.

In a previous study, the temperature dependence of the hydration numbers for poly(vinyl alcohol) (PVA) and partially chemically modified PVA (ChPVA) which shows much higher water solubility than PVA was determined by using DS techniques.[16] The hydration number of ChPVA was larger than that of PVA over all temperature ranges examined in the study. This result suggested that the hydration number of the HeC samples determined by using extremely high-frequency DS measurements provides an important information on their water solubility.

In this chapter, the temperature dependence of the hydration numbers for chemically modified cellulose ethers, such as hydroxyethyl, methyl, hydroxypropylmethyl, hydroxyethylmethyl and hydroxypropyl cellulose, bearing various substitution conditions and molecular weights in aqueous solution is determined by using extremely high-frequency DS techniques over a wide temperature range from 10 to 70 ºC or their cloud point temperatures. The temperature dependent hydration/dehydration behavior will be discussed as a function of the substitution condition of the examined cellulose ethers. The critical hydration number, which is necessary to be dissolved into water, for cellulose ethers will be determined in relation to the substitution conditions. Moreover, the reason why HeC samples possess high water-solubility even at high temperatures will be also discussed.

2.2 Experimental

Materials

A series of methyl cellulose (MC), hydroxypropylmethyl cellulose (HpMC) and hydroxyethylmethyl cellulose (HeMC) samples were kindly supplied by Shin-Etsu Chemical Co. Ltd. (Tokyo). Moreover, a series of hydroxyethyl cellulose (HeC) samples were kindly supplied by Daicel Co. (Osaka) and Dow Chemical Japan Ltd. (Tokyo), and hydroxypropyl cellulose (HpC) samples were kindly supplied by Nippon Soda Co., Ltd. (Tokyo). These cellulose ether samples were coded as MC(m:M_w/10^3), HpMC(hp:m:M_w/10^3), HeMC(he:m:M_w/10^3), HeC(he:M_w/10^3) and HpC(hp:M_w/10^3) with numerical quantities, m, hp, he and M_w, which represent the degree of substitution of the three hydroxy groups per glucopyranose unit by methyl groups, the molar substitution number by hydroxypropyl groups, the molar substitution number by hydroxyethyl groups, and the weight-average molecular weight, respectively. Table 2.1 summarizes characteristics of all cellulose ether samples examined in this chapter. The molecular weight distribution indexes given by a ratio of M_w to the number-average molecular weight (M_n) were not so sharp and in a range from 2 to 3. MC, HpMC, HeMC and HpC samples were used without further purification. HeC samples were purified by dialysis and freeze-dried because they include a lot of ionic impurities which generate enormously large noise in dielectric spectra. Triethylene glycol (TEG) (>98%) was purchased from Tokyo Chemical Industry Co., Ltd. (Tokyo). TEG was used as a model compound of hydroxyethyl group. Tripropylene glycol mono methyl ether (TPGM) (>97%) was purchased from FUJIFILM Wako Pure Chemical Co. (Osaka). TPGM was used as a model compound of hydroxypropyl group. Highly deionized water with the specific resistance higher than 18 MΩ·cm, generated by a Direct-Q UV3 (Millipore-Japan, Tokyo), was used as a solvent.

The concentrations of aqueous cellulose ethers solutions ranged from 1.0 to 10 wt%.

Table 2.1 Characteristics of cellulose ethers used in this chapter

sample codes	molar substitution number by hydroxypropyl groups	molar substitution number by hydroxyethyl groups	degree of substitution by methyl groups	$M_w/10^3$
MC (1.8:$M_w/10^3$)	0	0	1.8	95, 150
HpMC (0.25:1.9:$M_w/10^3$)	0.25	0	1.9	20, 75, 300
HpMC (0.15:1.8:$M_w/10^3$)	0.15	0	1.8	75
HpMC (0.20:1.4:$M_w/10^3$)	0.20	0	1.4	95
HeMC (0.20:1.5:$M_w/10^3$)	0	0.20	1.5	300
HeC (1.3:$M_w/10^3$)	0	1.3	0	90
HeC (2.0:$M_w/10^3$)	0	2.0	0	220
HeC (3.6:$M_w/10^3$)	0	3.6	0	70
HpC (2.8:$M_w/10^3$)	2.8	0	0	140

Methods

Dielectric spectroscopy measurements: Two measuring systems were used to determine the dielectric spectra of aqueous solutions of the cellulose ethers over a frequency range from 1 MHz to 50 GHz. A dielectric probe kit, 8507E, equipped with a network analyzer, N5230C, an ECal module N4693A, and performance probe 05 (Agilent Technologies, Santa Clara, CA), was used for DS measurements over a frequency range from 50 MHz to 50 GHz ($3.14 \times 10^8 - 3.14 \times 10^{11}$ s^{-1} in angular frequency (ω)). The probe, with a diameter of 9.7 mm, was inserted into a glass vial possessing an inner diameter of ca. 16 mm, and the distance from the probe edge to the bottom of the vial was maintained at greater than 3 mm. The volume of tested liquid sample was ca. 2 mL. The real and imaginary parts (ε' and ε'') of the electric permittivity were automatically calculated from the reflection coefficients measured by the network analyzer via a program supplied by Agilent Technologies. A three-point calibration procedure using *n*-hexane, 3-pentanone, and water as the standard materials was performed prior to all the dielectric measurements at each measuring temperature.

In the lower frequency range from 1 MHz to 3 GHz ($\omega = 6.28 \times 10^6 - 1.88 \times 10^{10}$ s^{-1}), an RF

LCR meter 4287A (Agilent) equipped with a homemade electrode cell with a vacant electric capacity of C_0 = 0.23 pF was used, which consisted of center and outer electrodes made of gold-covered brass insulated by poly(tetrafluoroethylene). The electrode cell possesses inner and outer conductor diameters of 3.04 and 7.00 mm, respectively, which are the same as those of an impedance matching an APC7 connector with the characteristic resistance of 50 Ω. A short part of the APC7 was used as a counter electrode against the inner conductor electrode with a flat surface. The separation between inner and counter electrodes was 0.5 mm. Open (air), short (0 Ω, a gold plate with the thickness of 0.5 mm), and load (water) calibration procedures were performed prior to sample measurements at each measuring temperature. Dielectric measurements were performed at temperatures ranged from T = 10 to 70 °C or the cloud points of each sample solution with the accuracy of ± 0.1 °C using a temperature controlling unit made of a Peltier device.

Density measurements: Density measurements for all the sample solutions were conducted using a digital density meter, DMA4500 (Anton Paar, Graz), to determine the partial molar volumes of the cellulose ethers at the same temperature as the performed dielectric measurements.

2.3 Theoretical Background

Dielectric spectroscopy measurements

The dielectric spectroscopy (DS) measurements are able to detect rotational motions of dipoles of the whole molecules and polar groups attached to the molecules. DS technique in an extremely wide frequency range ($f = 10^{-6} – 10^{12}$ Hz) has become one of the useful spectroscopy tools to investigate the dynamic behavior of liquids and solids.[17] The data obtained by using DS measurements (angular frequency, ω, dependence of dielectric permittivity, ε', and loss, ε'',) provide the information of the properties of the individual constituents in the tested systems which is related

to the characteristics of their bulk properties. For example, the relaxation times, τ, of the individual molecules in the tested systems obtained by DS techniques via various analytical methods, such as Debye-type relaxation function fit, lead to the time necessary for the dipolar molecules (or group) to rotate and alter their direction. Moreover, the magnitude of permittivity is proportional to the number density of dipolar molecules in the tested systems and the amount of their dipole moment.[18] The water molecules possess the permanent characteristic electric dipole moment of 1.8 D, and the dielectric spectra of their collective rotational relaxation process are well described with a single Debye-type mode at the relaxation time of τ_w = 9.0 ps at T = 20 ºC in pure liquid water.[19] Therefore, extremely high-frequency DS measurements can directly observe the rotational motions of water molecules in aqueous systems and is quite useful to discuss the dynamics of the water molecules in the systems.

2.4 Results and Discussion

2.4.1 Dielectric Behavior of Aqueous HeC Solution

Dielectric spectra (ε' and ε'' vs ω) for the aqueous solution of HeC(1.3:90) at c = 0.23 mol L^{-1} (M) and 20 ºC are shown in Figure 2.1(a) as typical examples. The dependence of ε' and ε'' on ω was well described with the summation of five Debye-type relaxations as follows:

$$\varepsilon' = \sum_{j=1}^{5} \frac{\varepsilon_j}{1+\omega^2\tau_j^2} + \varepsilon_\infty \quad , \quad \varepsilon'' = \sum_{j=1}^{5} \frac{\varepsilon_j \omega\tau_j}{1+\omega^2\tau_j^2} \qquad (2\text{-}1)$$

where ε_j, τ_j, and ε_∞ represent the relaxation strength and time for a mode j and the high-frequency limiting electric permittivity, respectively. The broken lines drawn in the figure represent the constituent Debye-type relaxation mode ε_j' and ε_j'' (j = 1 to 5 from the fastest relaxation mode due to the shortest relaxation time). To confirm the validity of decomposition into five Debye-type relaxation modes for the spectra, the residuals of $\varepsilon' - \varepsilon_1' - \varepsilon_\infty$ and $\varepsilon'' - \varepsilon_1''$ are also plotted in the same

figure with small closed symbols, which clearly demonstrate the presence of modes j =2, 3, 4 and 5. The G_{DC} values for all the measured samples were not so high, but lower than 400 μS.

A variety of useful methods were proposed to explore hydration behavior of solute molecules including large biomacromolecules like proteins and DNAs, such as extended depolarized light scattering (EDLS),[20–23] nuclear magnetic resonance (NMR),[24,25] neutron scattering (NS),[26] time-resolved fluorescence decay,[27] dielectric spectroscopy (DS)[10,11,16,23,28–30] and molecular dynamics simulation (MD)[31–33] techniques. The DS technique is one of the most useful methods for the purpose because it directly probes dynamics of water molecules quite precisely.[10,11,16,23,28–30] Dielectric spectra for aqueous solutions of solute molecules are exactly described as the summation of Debye-type relaxation mode of free water molecules, additional Debye-type relaxation mode(s) assigned to the rotational process of hydrated water molecules and that of dipoles attached to solute molecules in aqueous systems.[10,11,16,23,28–30] Then, I used the summation of Debye-type relaxation modes given by eq. 2-1 to describe the dielectric spectra obtained in this study.

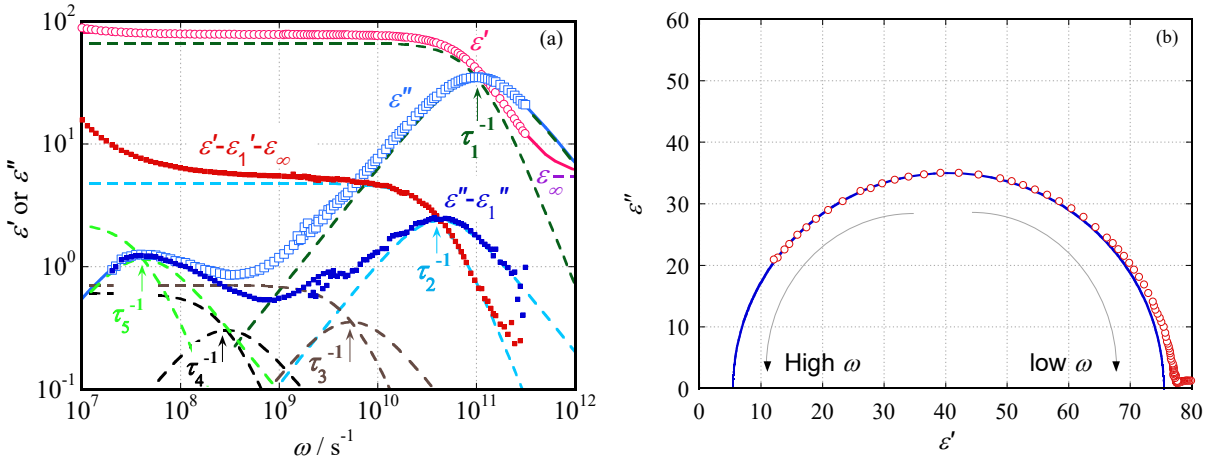

Figure 2.1 (a) Dielectric spectra (ε' and ε'' vs ω) for an aqueous solution of HeC(1.3:90) at c = 0.23 M and 20 °C. Broken lines represent constituent relaxation modes from j = 1 to 5. The residuals of $\varepsilon' - \varepsilon_1' - \varepsilon_\infty$ and $\varepsilon'' - \varepsilon_1''$ are also plotted in the same figure with small closed symbols. (b) A Cole–Cole plot for the data shown in (a). A solid semicircle represents single Debye-type presentation for the major dielectric dispersion observed at $\omega \sim 10^{11}$ s^{-1}.

It has been well-known that the Cole−Cole[34] and Cole−Davidson[35] models are also useful to describe dielectric behaviors showing non-single Debye-type dielectric spectra. Figure 2.1(b) represents a so-called Cole−Cole plot for the data shown in Figure 2.1(a) together with the best fit single Debye-type behavior represented by a solid semicircle for major dielectric dispersion observed at $\omega \sim 10^{11}$ s^{-1}. Small but non-negligible deviation from the sloid circle is recognized in data points in a lower frequency side, which demonstrates the additional minor contribution described by the modes j = 3, 4 and 5. Although the agreement between the solid semicircle and data points in the major dispersion portion seems rather well, the Cole−Cole or Cole−Davidson model is not the best way to express such DS spectra showing a slight deviation from a single Debye-type behavior observed in this study. Then, I did not use the models to analyze dielectric behavior observed in this study. However, it is worth to note that the Cole−Davidson model is also quite useful to describe the broad frequency dependence of susceptibility of aqueous solutions determined by spectroscopic methods other than the DS method to explore hydration behavior, such as EDLS[20–23] and NS[26] techniques.

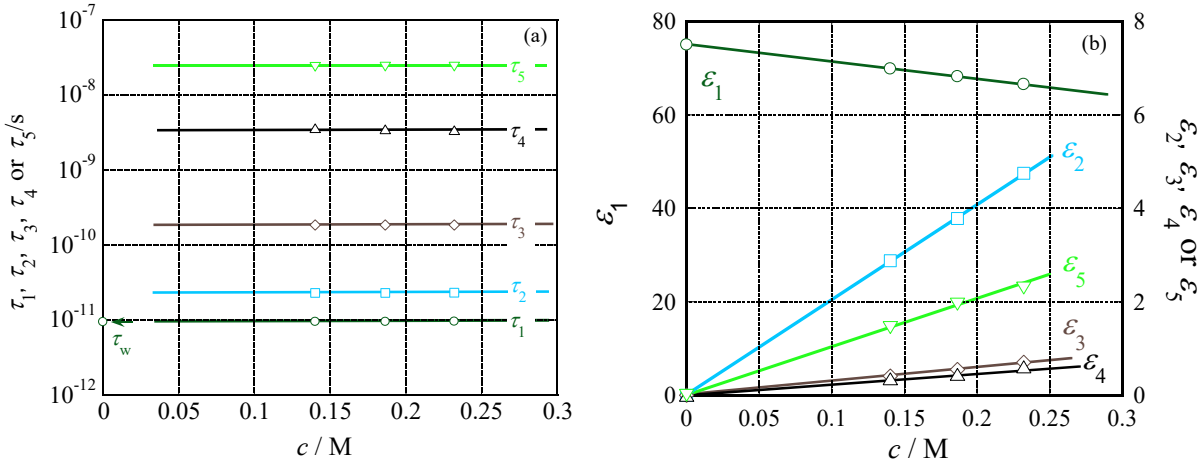

Figure 2.2 Concentration dependence of dielectric relaxation times (a) and strength (b) for each mode observed in aqueous solution of HeC(1.3:90) at T = 20 ºC shown in Figure 2.1(a).

Figures 2.2(a) and 2.2(b) show the concentration dependence of the dielectric relaxation times and strength for each mode obtained from the aqueous solution of HeC(1.3:90). The fastest relaxation time, τ_1, was identical to the value of the rotational relaxation time, τ_w, of water molecules in the pure liquid state as shown in Figure 2.2(a). Then, the mode $j = 1$ is easily attributed to the rotational relaxation mode of free water molecules in the aqueous solution of HeC(1.3:90). The value of ε_1 considerably decreased with increasing concentration, c, as shown in Figure 2.2(b). The amount of free water molecules in aqueous solution was substantially reduced by the presence of solute HeC(1.3:90) molecules which possess a certain volume fraction in the aqueous solution and the effect of hydration behavior. In a later section, the number of water molecules hydrated to a glucopyranose unit of the HeC(1.3:90) molecules (hydration number, n_H) will be calculated from the c dependence of ε_1.

The second relaxation mode $j = 2$ possesses the relaxation time $\tau_2 \sim 2.4\tau_1$ and the strength ε_2 is the second largest and proportional to c as shown in Figures 2.2(a),(b). According to the previous reports of several water-soluble substances,[10,11,16,23,28–30] MD simulation studies,[31–33] and DS and EDLS studies,[23] the mode $j = 2$ is assigned to the exchange process of hydrated water molecules by free ones in the solution. The obtained relaxation time, τ_2, usually possesses longer relaxation time for some factors than the value of τ_1, and the ratio of τ_2/τ_1 has been called a retardation ratio (or slowdown factor). The observed value of τ_1 was very close to that of τ_w, then, the evaluated value of τ_2/τ_1 is essentially identical to that of τ_2/τ_w in this study. Since the value of $\tau_2 \sim 2.4\tau_1$ seen in Figure 2.2(a) and also in other aqueous cellulose ether systems examined in this study is fairly similar to that reported for aqueous solutions of some saccharides, such as glucose, fructose, sucrose determined using EDLS and DS techniques,[23,28–30] the characteristics of hydration behavior observed in aqueous cellulose ether systems are not so different from those of mono- and disaccharide molecules. The fact that the value of $n_H c(\varepsilon_w/55.6)$ for aqueous HeC solution, which is the estimation of dielectric relaxation strength for hydrated water molecules assuming that the relaxation strength of

the molecules is same as free water molecules, is close to the value of ε_2 strongly supports the validity of this assignment.

The third relaxation mode $j = 3$ of the relaxation time τ_3 is 180 ps as seen in Figure 2.2(a). Although the strength of mode $j = 3$ is considerably smaller than that of mode $j = 2$, the value is proportional to c as shown in Figure 2.2(b). Since HeC(1.3:90) molecules have a few kinds of polar groups bearing finite dipole moments, such as hydroxy and ether groups (−OH and $-CH_2OCH_2-$), the rotational motions of these polar groups would be the origin of dielectric relaxation. The value of relaxation time ($\tau_3 \sim 180$ ps) for HeC is similar to that for MC and HpMC ($\tau_3 \sim 220$ ps). Figure 2.3(a) shows the molar substitution number (*MS*) dependence of relaxation strength per one mol of glucopyranose ring, $\varepsilon_3 c^{-1}$, and the value of $\varepsilon_3 c^{-1}$ is proportional to *MS*. The fact that the intercept value of $\varepsilon_3 c^{-1}$ for HeC ($\varepsilon_3 c^{-1} \sim 2.5$) is almost the same value of $\varepsilon_3 c^{-1}$ for pullulan ($\varepsilon_3 c^{-1} \sim 2.6$), which is a natural glucan, powerfully supports the validity of this assignment. The rotational relaxation time of a hydroxy group would be governed by the lifetime of intramolecular hydrogen bonding between two hydroxy groups, and a hydroxy group and an ether group. There are two types of ether groups: a native ether group (ether group-N) that cellulose possesses natively and an additional ether group (ether group-S) which is given by the substitution. The rotational relaxation time of ether group-N would be longer than that of ether group-S because the rotational motion of ether group-N requires rotating the glucopyranose ring. On the other hand, the ether group-S can rotate without rotating the glucopyranose ring. Then, τ_3 would be assigned to the rotational relaxation time of hydroxy groups and ether groups-S controlled by the lifetime of intramolecular hydrogen bonding.

The fourth and fifth relaxation modes, $j = 4$ and 5, showed the relaxation times of $\tau_4 \sim 3.5$ ns and $\tau_5 \sim 24$ ns, respectively. The relaxation magnitudes of these modes, ε_4 and ε_5, are proportional to c as ε_2 and ε_3 as seen in Figures 2.2(a),(b). Figure 2.3(b) shows the c dependence of the magnitudes, ε_4 and ε_5, for HeC(1.3:90), HeC(2.0:220) and HeC(3.6:70). The c dependent the magnitudes, ε_4 and ε_5, are independent of molecular weight and *MS* of HeC. Then, the strength would be affected only

by the dipole moment of the whole glucopyranose ring and irrespective of the dipole moment for individual polar groups of the glucopyranose ring. The relaxation times of these modes, τ_4 and τ_5, for HeC(2.0:220) are ca. 5.5 ns and 50 ns, respectively, and these values are longer than that of HeC(1.3:90) and HeC(3.6:70). These observations suggest that the fourth and fifth relaxation modes, j = 4 and 5, are the rotational modes of the segments in HeC polymer, and the size of segments becomes larger with increasing molecular weight. The main purpose of this chapter is a basic argument about the hydration/dehydration behavior of the cellulose ethers in aqueous solution. To clarify the assignments of fourth and fifth relaxation modes, it is quite helpful to use a wide M_w range of HeC samples with monodisperse ($M_w/M_n \sim 1$) molecular weight distribution.

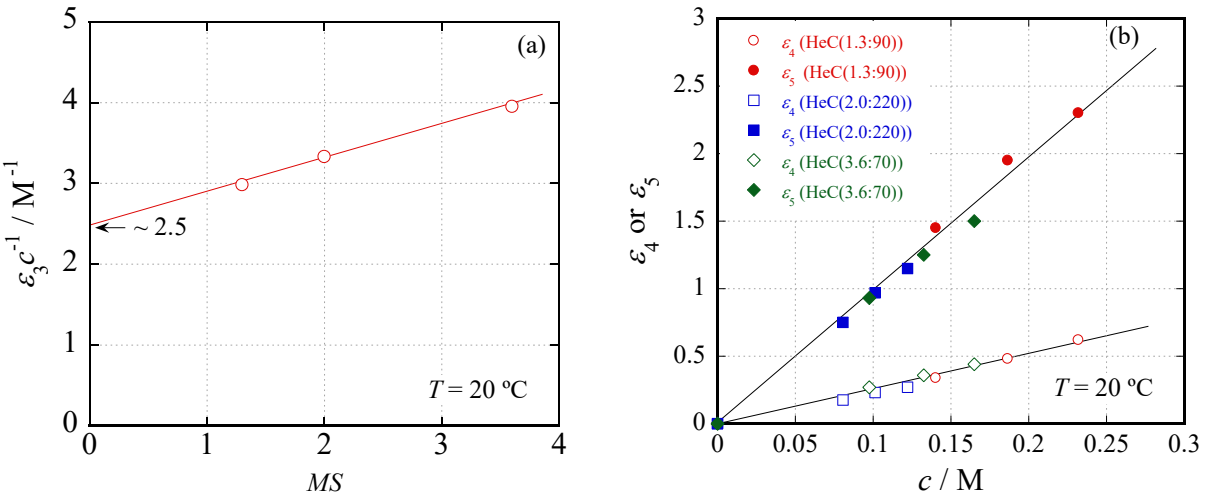

Figure 2.3 (a) Molar substitution (*MS*) dependence of normalized dielectric relaxation strength for mode j = 3 ($\varepsilon_3 c^{-1}$). (b) Concentration dependence of dielectric relaxation strength for mode j = 4 and 5 observed in aqueous solutions of HeC(1.3:90), HeC(2.0:220) and HeC(3.6:70).

Figure 2.4 shows dependence of dielectric relaxation times, τ_1 and τ_2, and the retardation ratio, τ_2/τ_1, on the reciprocal temperature, T^{-1}, for an aqueous solution of HeC(1.3:90) at c = 0.23 M as an example. The activation energy of the mode j = 1 is evaluated to be 17.1 kJ mol^{-1} from the slope of the τ_1 data shown in Figure 2.4. The fact that this value is close to that of the rotational relaxation

time, τ_w, of the pure liquid water verifies the validity of the assignment for the mode j = 1. The activation energy of the mode j = 2 was 17.8 kJ mol^{-1}, which is slightly greater than that of mode j = 1. This is because the interaction energy between a hydrated water molecule and a hydration spot of HeC(1.3:90) molecules is slightly greater than that between water molecules in the pure liquid state. Similar temperature dependence of τ_1 and τ_2 values was also obtained from aqueous solutions of HeC(2.0:220) and HeC(3.6:70).

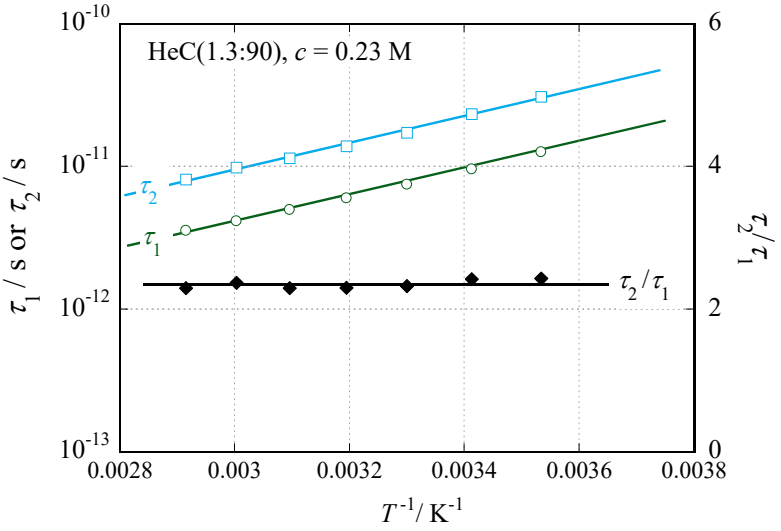

Figure 2.4 Temperature dependence of dielectric relaxation times, τ_1 and τ_2, and the retardation ratio, τ_2/τ_1, for aqueous solution of HeC(1.3:90) at c = 0.23 M.

The τ_2/τ_1 value is kept at 2.2-2.4 for HeC(1.3:90) and other HeC samples in the temperature range examined. This retardation ratio reasonably agrees with the values previously reported for hydrated water molecules in aqueous solutions of saccharides determined at room temperature using EDLS and DS techniques,[23,28–30] and aqueous solution of MC and HpMC in the same temperature range as in this study using DS techniques.[36] In the case of HpMC in aqueous solution, the T^{-1} dependence of the τ_2/τ_1 value showed a bending with increasing T above 30 ºC.[36] The T^{-1} dependence of the τ_2/τ_1 value for the aqueous HeC systems does not show a bending in the measured T range.

The differences between them would be related to the dehydration behavior discussed in a later section.

The retardation ratio of hydrated water molecules was reported at two different temperatures, 7 and 30 ºC, in aqueous solution of green fluorescent protein using NS techniques. Although the retardation ratio was not influenced by temperature, the ratio was ranged from 3 to 7 depending on the scattering vector.[26] The retardation ratios of hydration water molecules in aqueous solutions of other proteins like lysozyme and oligo peptides were also reported to be 3 to 7 using various methods, such as EDLS,[23] DS,[23,37] NMR[24,25] techniques and MD[32,33] simulations. It seems that amide groups forming oligo peptides and proteins possess considerably greater retardation ratios of hydration water molecules than ether and hydroxy groups constructing polysaccharides as described above.

2.4.2 Hydration Behavior of HeC in Aqueous Solution

The c dependence of ε_1 allows us to determine the hydration number, n_H, per glucopyranose unit using equation 2-2, as follows: [10,11,16]

$$\frac{\varepsilon_1}{\varepsilon_w} = \frac{1-10^{-3}V_m c}{1+10^{-3}V_m c/2} - 10^{-3}V_w c n_H \qquad (2\text{-}2)$$

where V_m and V_w represent the partial molar volumes of a glucopyranose unit and water molecule, respectively, at each measured temperature in the units of $cm^3\ mol^{-1}$. The V_m value was calculated from the density data of examined aqueous sample solution, and precisely determined V_w values are available in literature. The first term of eq. 2-2 represents the contribution of the volume excluded by the presence of solute (organic) molecules and the second term represents the contribution of the hydration effect to the solute molecules.

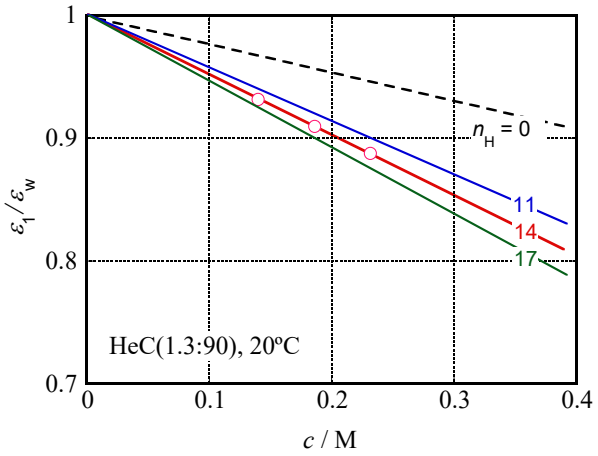

Figure 2.5 Relationship between the values of $\varepsilon_1/\varepsilon_w$ and concentration, c, for aqueous solution of HeC(1.3:90) at T = 20 ºC.

Figure 2.5 shows the concentration, c, dependence of the $\varepsilon_1/\varepsilon_w$ values for an aqueous solution of HeC(1.3:90) at 20 ºC as a typical example. The experimentally obtained $\varepsilon_1/\varepsilon_w$ data points are far from a theoretically calculated line via eq. 2-2 assuming n_H = 0. However, the agreement between the $\varepsilon_1/\varepsilon_w$ data and a solid line calculated assuming n_H = 14 is perfect over the entire examined c range. Then, it is concluded that the hydration number, n_H, of HeC(1.3:90) at 20 ºC is 14. According to the same procedure, the n_H value was determined successfully from 10 to 70 ºC for all the aqueous solutions of HeC samples examined.

Figure 2.6 represents the temperature, T, dependence of n_H for aqueous HeC(1.3:90) solution obtained in a concentration range from 0.14 to 0.23 M. Agreement between the n_H value determined from aqueous HeC solutions at different concentrations looks perfect at each temperature. Then, one might conclude that the n_H value is successfully determined and has quite weak c dependence in the range examined. Furthermore, the n_H value is ca. 15 at 10 °C and then gently reduces with increasing temperature to ca. 10 at 70 °C. The HeC sample possessed water solubility even in a higher temperature range and did not demonstrate a cloud point and gelation in the examined T range.

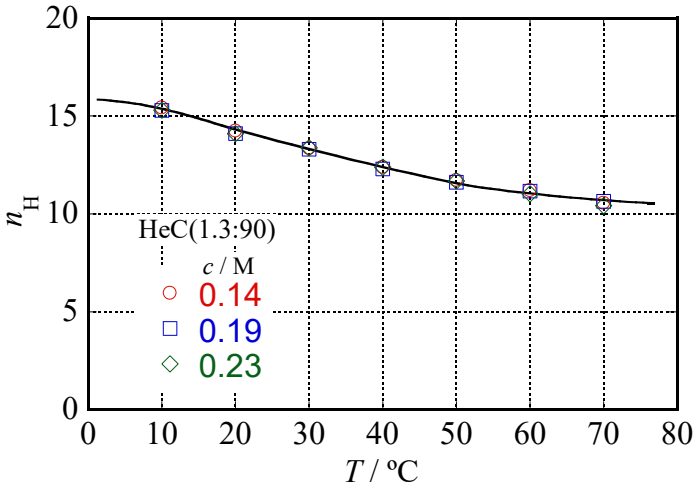

Figure 2.6 Temperature, T, dependence of the hydration number, n_H, per glucopyranose unit for aqueous HeC(1.3:90) solutions at several c values ranged from 0.14 to 0.23 M.

Figure 2.7 shows temperature, T, dependence of hydration number, n_H, per glucopyranose unit for aqueous solutions of HeC(1.3:90), HeC(2.0:220) and HeC(3.6:70), which possess different molar substitution number, MS, by hydroxyethyl groups (He groups). All the examined HeC samples keep high water solubility over a wide T range and never demonstrate a cloud point even in a high T range. As the MS by He groups increases, the values of n_H increase. This is because the number of hydrophilic ether groups per glucopyranose unit increases with increasing MS by He groups and the number of hydroxy groups per glucopyranose is kept at the same value of natural cellulose. The increase of the n_H value resulted from the additional substitution by He groups is more remarkable in a low T range; the increase coefficient of the n_H value per MS by He groups at 10 ºC is evaluated to be $\frac{\partial n_H}{\partial MS}$ = 3.3. The effect on the n_H value by increase of MS in a high T range looks weaker than that in a low T range; the increase coefficient of the n_H value per MS by He groups at 70 ºC is 2.2. Then, the T dependence of n_H for HeC is substantially affected by the MS value.

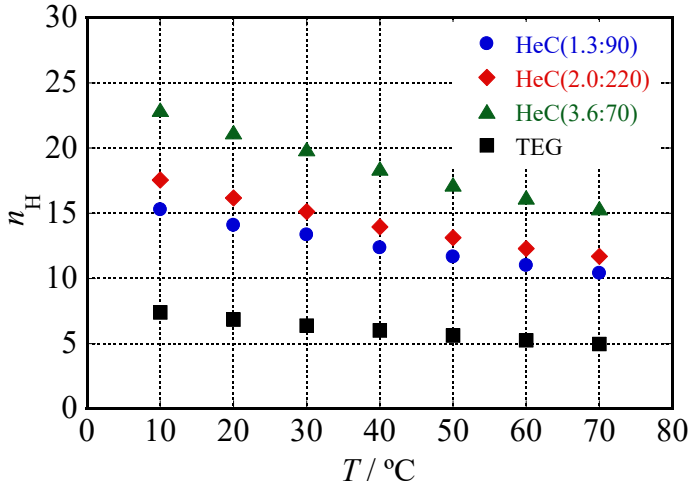

Figure 2.7 Temperature, T, dependence of hydration number, n_H, per glucopyranose unit for HeC(1.3:90), HeC(2.0:220), HeC(3.6:70) and that for triethylene glycol per molecule.

The temperature, T, dependence of hydration number, n_H, for triethylene glycol (TEG) was investigated as a model molecule of the substitution groups for HeC. Scheme 2.1 shows the chemical structure of TEG. Since the structure of TEG is the same as that of a molecule which is constructed by connecting two hydroxyethoxy groups (-$CH_3OCH_2CH_2OH$), TEG is a reasonable model to compare the hydration behavior of the substitution groups and that of HeC. The T dependence of n_H per molecule for TEG is also shown in Figure 2.7. In order to compare the temperature dependence of hydration/dehydration behavior for HeC and TEG, the n_H values of each temperature are normalized by the n_H value at 20 ºC. Then, I name the obtained value a characteristic hydration number, n_H*. Figure 2.8 shows temperature, T, dependence of n_H* for aqueous solutions of HeC(1.3:90), HeC(2.0:220), HeC(3.6:70) and TEG. The T dependence of n_H* for all samples agrees very well with each other. Therefore, the substitution groups of HeC, hydroxyethoxy groups, essentially control the temperature dependence of hydration number for HeC in aqueous solution, even that for HeC(1.3:90) with the *MS* of only 1.3.

Scheme 2.1 Chemical Structure of Triethylene Glycol (TEG).

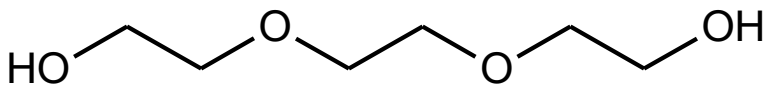

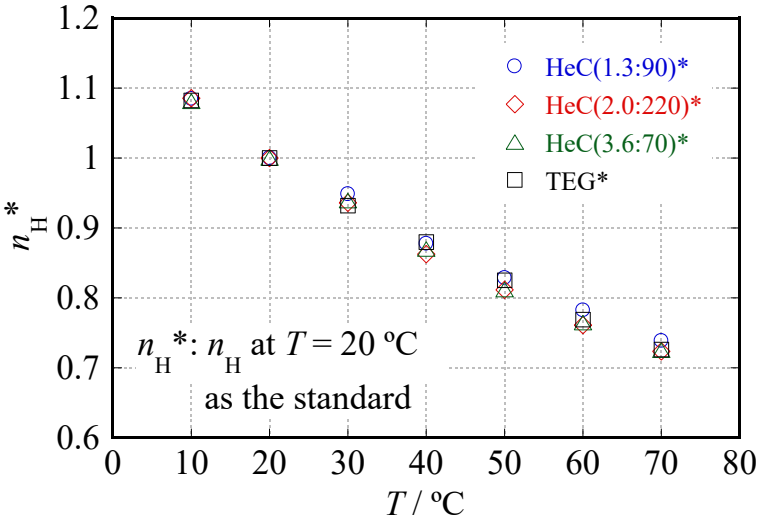

Figure 2.8 Temperature, T, dependence of characteristic hydration numbers, n_H*, taking the n_H at T = 20 ºC as the standard for each hydroxyethyl cellulose sample and triethylene glycol.

2.4.3 Hydration Behavior of Mainly Methylated Cellulose Ethers in Aqueous Solution

In the previous section, the hydration behavior of HeC, which does not show a cloud point and gelation, was discussed. However, most of nonionic cellulose ether samples demonstrate cloud points with increasing temperature.[1–3] Here, I investigated the hydration behavior of methyl cellulose (MC), hydroxypropylmethyl cellulose (HpMC) and hydroxyethylmethyl cellulose (HeMC), which are mainly methylated cellulose ethers. Figure 2.9(a) shows the temperature, T, dependence of n_H for aqueous HpMC(0.25:1.9:75) solutions in a c range from 0.11 to 0.37 M obtained by the same procedures as in aqueous HeC solution. Hydration number, n_H, retains the value of ca. 14 at 10 ºC

and then decreases remarkably with increasing temperature down to 5 at 53 ºC. The distinct dehydration behavior with increasing temperature well corresponds to the presence of a cloud point, which was observed at 53 °C irrespective of the c values, i.e., the LCST for aqueous HpMC(0.25:1.9:75) solution as shown in Figure 2.9(a).

Figure 2.9(b) represents the temperature, T, dependence of the hydration number, n_H, for aqueous solutions of HpMC(0.25:1.9:$M_w/10^3$) with various molecular weight, M_w. The T dependence of n_H and cloud points for aqueous solutions of HpMC(0.25:1.9:$M_w/10^3$) is independent of M_w in the examined M_w range. Then, the T dependent hydration behavior of HpMC depends only on the substitution conditions such as substitution groups and the degree of substitution. The temperature dependence of n_H in the dehydration behavior shown in Figure 2.9 is not as sharp as that observed in aqueous PNIPAm solution,[11] but it is similar to the slow behavior observed in aqueous POE solution.[10] Thus, the cooperativity in the hydration/dehydration process for cellulose ethers in aqueous solution is not as high as in the case of PNIPAm.

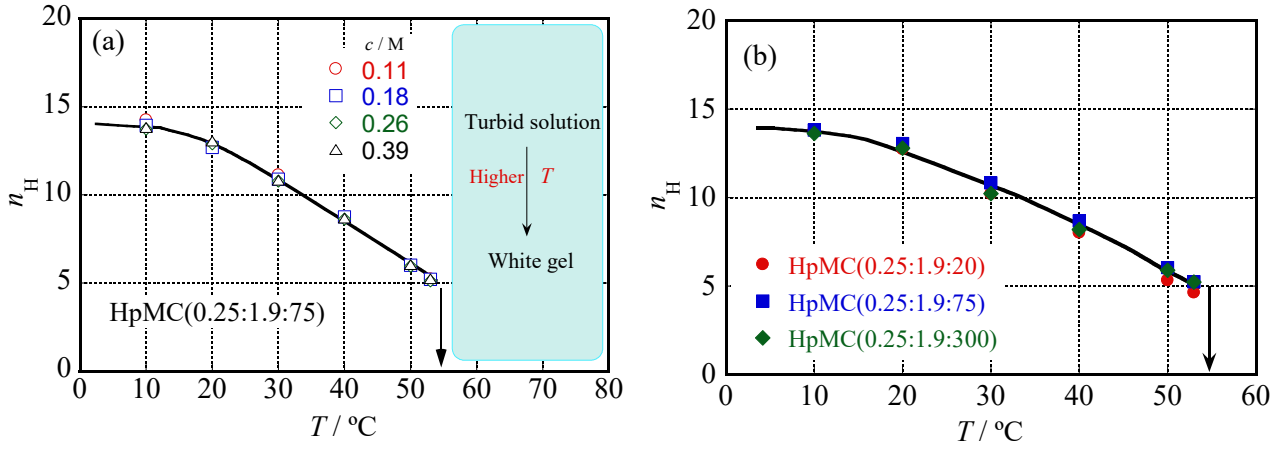

Figure 2.9 (a) Temperature, T, dependence of n_H for aqueous HpMC(0.25:1.9:75) solutions in a concentration range from 0.11 to 0.37 M. The arrow in this figure represents the lowest cloud point observed in a high concentration side, i.e., LCST. (b) T dependence of n_H for aqueous solutions of HpMC(0.25:1.9:$M_w/10^3$) with various molecular weight, M_w. The LCST value shown with an arrow is independent of M_w.

Figure 2.10 shows the T dependence of the n_H values for aqueous solutions of MC(1.8:95) at 0.32 M and MC(1.8:150) at 0.16M. The n_H data of two MC samples demonstrate essentially identical T dependence. Then, the T dependence of the n_H value is not affected by a difference in the M_w values over the examined M_w range as in the case of HpMC samples as discussed above. The cloud point temperature for the aqueous solution of MC is strongly dependent on the concentration than that for the aqueous solution of HpMC. Arvidson et al.[38] also reported the gel point of MC decreases with increasing concentration, though it is virtually independent of the molecular weight. A broken arrow in Figure 2.10 shows the cloud point of aqueous MC(1.8:150) solution at a dilute condition of c = 0.16 M. As the value of c increased, the cloud point temperature of MC(1.8:150) in aqueous solution decreased and approached the LCST at 38 ºC, as shown by a black solid arrow in the condition of c > 0.3 M. Since the temperature is identical to the LCST of aqueous MC(1.8:95) solution, the LSCT is not affected by the M_w values for the MC samples examined in this study. It seems that the n_H value just below the LCST is close to 5 similarly in the case of the aqueous HpMC(0.25:1.9:M_w/10^3) solution as shown in Figures 2.9(a),(b).

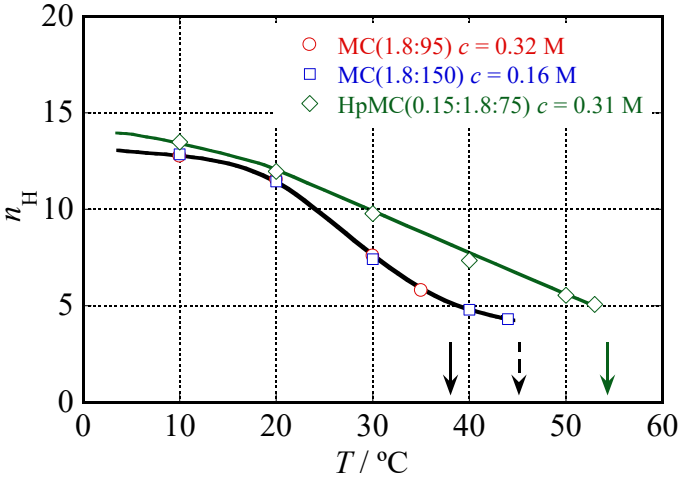

Figure 2.10 Temperature, T, dependence of n_H for aqueous solutions of MC(1.8:95) at 0.32 M, MC(1.8:150) at 0.16 M and HpMC(0.15:1.8:75) at 0.31 M. A black solid arrow in this figure represents the LCST value for MC(1.8:95) and MC(1.8:150) independent of M_w value, and a broken arrow represents a cloud point for MC(1.8:150) observed at a dilute condition of c = 0.16 M, and a green solid arrow represents a cloud point for HpMC(0.15:1.8:75) independent of c value.

Figure 2.10 also shows the T dependence of the n_H value for an aqueous solution of HpMC(0.15:1.8:75) at 0.31 M. As the molar substitution by hydroxypropyl groups is increased slightly from 0 to 0.15 for MC(1.8:95) sample with same degree of substitution by methyl groups and similar molecular weight, the dehydration behavior of HpMC(0.15:1.8:75) with increasing T becomes less sharp. As a result, the LCST value of HpMC(0.15:1.8:75) increases considerably from 38 up to 53 °C (by 15 °C). These results suggest that an additional small amount of substitution by hydroxypropyl groups effectively increases the LCST values. Although the substitution of hydroxy groups of cellulose by hydroxypropyl groups decreases the number of native hydroxy groups forming intra- and intermolecular hydrogen bonds, the number of hydroxy groups per glucopyranose unit is kept at the original value. Then, the hydrophilicity or solubility of the cellulose ethers would be effectively increased by an additional substitution by hydroxypropyl groups in the examined range.

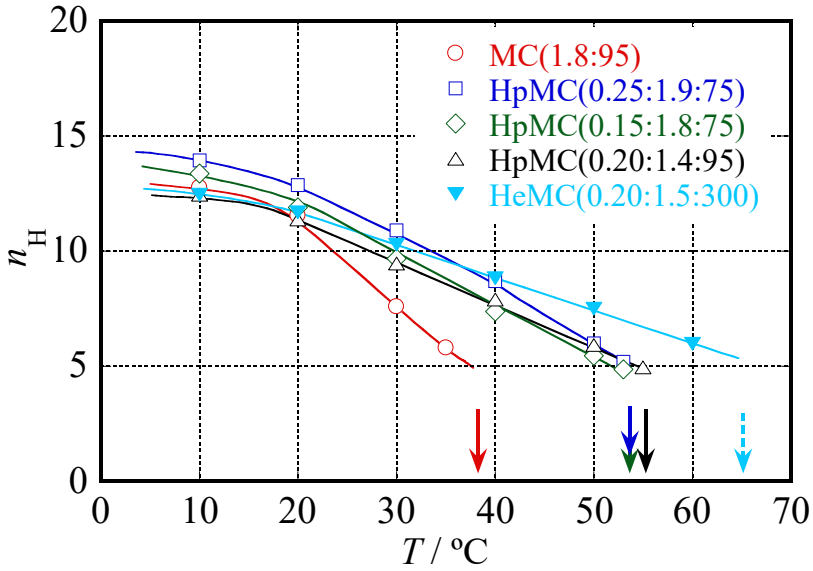

Figure 2.11 Temperature, T, dependence of n_H for aqueous solutions of MC(1.8:95), HpMC(0.25:1.9:75), HpMC(0.15:1.8:75), HpMC(0.20:1.4:95) and HeMC(0.20:1.5:300). Solid arrows in this figure represent the LCST value for each cellulose ether sample in aqueous solution. A dotted arrow represents gelation point without turning into the turbid state for aqueous solution of HeMC(0.20:1.5:300) at 0.1 M.

Figure 2.11 shows the T dependence of the n_H data for MC(1.8:95), HpMC(0.25:1.9:75), HpMC(0.15:1.8:75), HpMC(0.20:1.4:95) and HeMC(0.20:1.5:300) in aqueous solution examined in this study. The n_H data shown in this figure are the average ones calculated from the data obtained at various concentrations from 0.05 to 0.37 M. When the n_H values of the cellulose ethers at 10 °C are compared each other, the values increase in the order of the summation of the degree of substitution by methyl groups and the molar substitution number by hydroxypropyl or hydroxyethyl groups, i.e., the total substitution number. This result reveals that the total substitution determines the hydration number to the fully hydrated state, which is reached by lowering the temperature down to 10 °C, irrespective of the kinds of substitution groups.

The n_H values in a lower T range than 40 ºC for three HpMC samples at different degrees of substitution by methyl groups (1.4 – 1.9) and different molar substitution number by hydroxypropyl groups (0.15 – 0.25) are slightly different from each other. However, the three HpMC samples demonstrate almost same LCST values (53 – 55 ºC) irrespective of the degree of substitution by methyl groups and molar substitution number by hydroxypropyl groups in the examined ranges. This result suggests that the combination of substitution groups, such as only methyl group, methyl group and hydroxypropyl group, etc., determine the LCST values for cellulose ethers examined in this study. The n_H values obtained just below the LCST values are found to be ca. 5, irrespective of the molar substitution up to 0.25 by hydroxypropyl groups for each HpMC sample. Therefore, one might conclude that the n_H value of ca. 5 is the critical hydration number for the MC and HpMC samples that is necessary to be dissolved into water.

Although the LCST value for the aqueous solution of HpMC(0.20:1.4:95) was 53 ºC, HeMC(0.20:1.5:300), which bears almost same molar substitution number and degree of substitution, did not demonstrate a cloud point in aqueous solution at c = 0.1 M. The aqueous HeMC solution turned into a transparent gel above 65 °C as shown by a dotted arrow in Figure 2.11. Aqueous solutions of HeMC(0.2:1.5:300) at concentrations higher than 0.1 M showed distinct viscoelastic

behavior in a low temperature range and turned into transparent gels also approximately at 65 °C without showing clouding behavior. This result strongly suggests that the substitution by hydroxyethyl groups (−CH_2CH_2OH) has a higher ability to expand the water-soluble temperature range than hydroxypropyl groups (−$CH_2CH(OH)CH_3$). In addition, because a decrease in the n_H value for HeMC(0.20:1.5:300) with increasing T is markedly smaller than that of HpMC(0.20:1.4:95) in a temperature range higher than 30 °C, the essential reason for the higher water-soluble ability of HeMC than HpMC given by hydroxyethyl groups is keeping the high n_H values. The n_H value observed just below the LCST for aqueous solution of HpMC(0.20:1.4:95) was ca. 5, and the n_H value for HeMC(0.20:1.5:300) just below the gelation point was also ca. 5. These quantities were not influenced by a difference in the substitution groups: hydroxypropyl or hydroxyethyl group. Consequently, it is likely that the quantity of ca. 5 is the critical n_H value for MC, HpMC and HeMC samples examined in this study, which is necessary for the cellulose ether samples to dissolve into water.

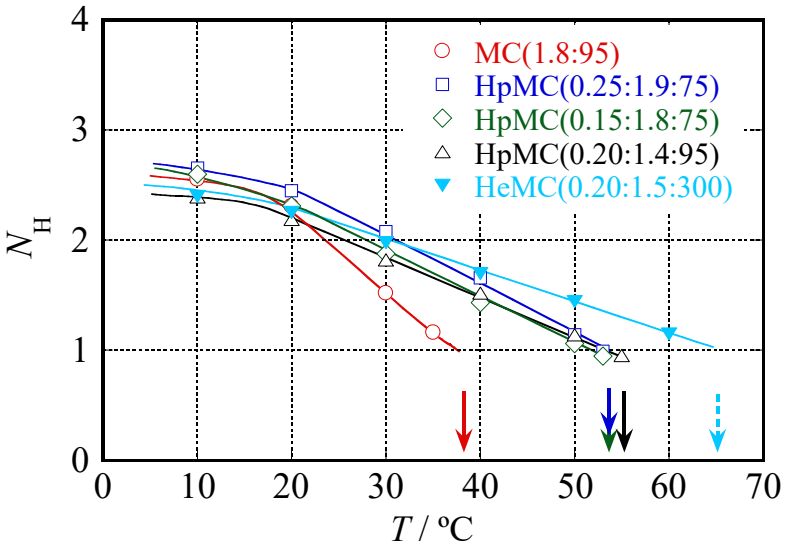

Figure 2.12 Temperature, T, dependence of hydration number per hydrophilic groups, N_H, for aqueous solutions of MC(1.8:95), HpMC(0.25:1.9:75), HpMC(0.15:1.8:75), HpMC(0.20:1.4:95) and HeMC(0.20:1.5:300). Solid arrows and a dotted arrow are the same as in Figure 2.11.

Figure 2.12 represents temperature, T, dependence of hydration number per hydrophilic groups: hydroxy (−OH) and ether (−O−) groups, N_H, for aqueous solutions of MC(1.8:95), HpMC(0.25:1.9:75), HpMC(0.15:1.8:75), HpMC(0.20:1.4:95) and HeMC(0.20:1.5:300). When the N_H values of the cellulose ethers at 10 °C are compared each other, the values have little dependence on the total substitution number. In a higher T range, the N_H values observed just below the LCST for aqueous solutions of MC and HpMC were ca. 1, and the N_H values for HeMC(0.20:1.5:300) just below the gelation point was also ca. 1. The situation in which the N_H value is less than ca. 1 means that unhydrated hydrophilic groups exist in the aqueous systems. Then, the unhydrated hydrophilic groups easily form intra- and intermolecular hydrogen bonds each other. As a result, the aqueous cellulose ether systems including unhydrated hydrophilic groups form molecular association and demonstrate a cloud point or gelation point at the temperature showing the N_H value less than ca.1. In conclusion, the quantity of ca. 1 is the critical hydration number per hydrophilic groups, N_H, for MC, HpMC and HeMC samples examined in this study, which is necessary for the samples to be dissolved into water.

In order to compare the hydration behavior of mainly methylated cellulose ethers and hydroxyethyl cellulose, Figure 2.13(a) shows temperature, T, dependence of n_H for aqueous solutions of HeC(1.3:90), MC(1.8:95), HpMC(0.15:1.8:75) and HeMC(0.20:1.5:300). The data shown in this figure are the average ones calculated from data obtained at a variety of concentrations from 0.05 to 0.37 M. In a temperature range lower than room temperature, the n_H value of HeC(1.3:90), which has the lowest total substitution number, is the largest in the four examined cellulose ether samples. Figure 2.13(b) shows temperature, T, dependence of the N_H value of HeC(1.3:90), MC(1.8:95), HpMC(0.15:1.8:75) and HeMC(0.20:1.5:300) in aqueous solution. Although the n_H value of HeC(1.3:90) is the largest in the four cellulose ether samples, the N_H values of these cellulose ethers in a low T range gather into the same value of ca. 2.5 irrespective of sample species. Although the number of ether groups for HeC increases with increasing molar substitution number by hydroxyethyl,

He, group, the number of hydroxy groups per glucopyranose unit for HeC is kept at the original value of natural cellulose with increasing *MS* by He groups. Then, the reason for the highest n_H values of HeC(1.3:90) in the four cellulose ethers is that the number of hydrophilic groups per glucopyranose unit for HeC(1.3:90): 6.3, is larger than that for other cellulose ethers, such as MC(1.8:95): 5.0, HpMC(0.15:1.8:75): 5.15, and HeMC(0.20:1.5:300): 5.2. Koda et al.[15] reported that the water retention capacity of HeC is higher than that of MC by using compression method and differential scanning calorimetry measurement. The higher n_H values of HeC would affect the higher water retention capacity of HeC than that of MC.

The decreasing rate of hydration number for HeC(1.3:90) with increasing temperature is clearly lower than that for other three cellulose ethers as seen in Figure 2.13(a). The HeC(1.3:90) keeps high n_H value even in a high temperature range (n_H ~ 10 at T = 70 ºC), and the n_H value of HeC(1.3:90) is always much higher than that of other three cellulose ethers in the examined T range. The value of N_H for HeC(1.3:90) is ca. 1.7 at T = 70 ºC as shown in Figure 2.13(b), and the value is much larger than the critical hydration number per hydrophilic groups, ca. 1, for series of cellulose ether samples. Therefore, the HeC(1.3:90) can keep the high solubility in water even in a high T range. The values of n_H per hydrophilic groups for HeC(2.0:220) and HeC(3.6:70) at T = 70 ºC are also much larger than the critical hydration number per hydrophilic groups for cellulose ethers; the value of HeC(2.0:220) is ca. 1.7 and that of HeC(3.6:70) is ca. 1.8 at T = 70 ºC. The substitution groups of HeC (He groups) determine the temperature dependence of n_H for HeC as discussed in Section 2.4.2, and the decrease in n_H for HeC with increasing T is substantially weaker than that for other cellulose ethers examined in this study. Consequently, the HeC samples in aqueous solution possess high water solubility over a wide T range and never demonstrate a cloud point and gelation behavior even in a high T range as the MC, HpMC and HeMC samples in aqueous solution.

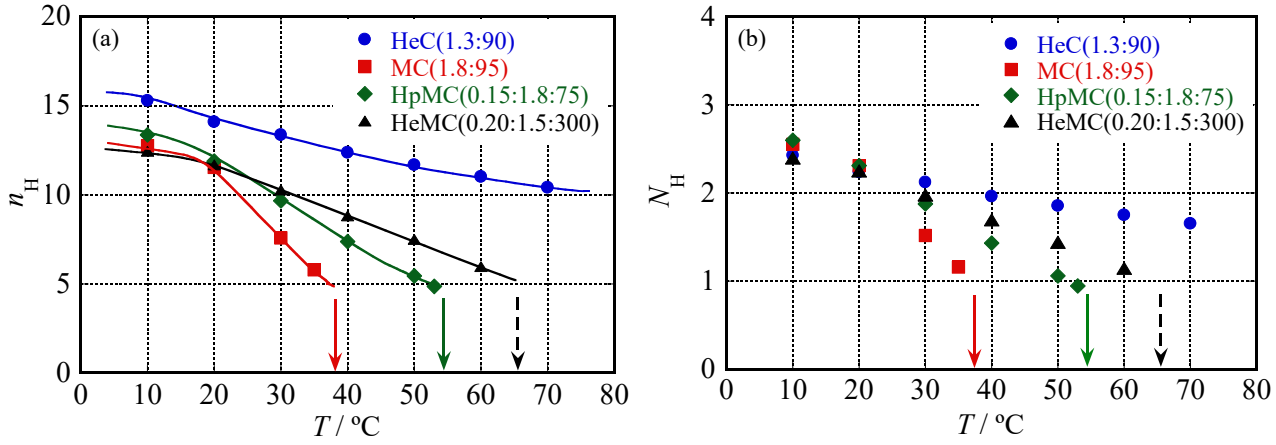

Figure 2.13 (a) Temperature, T, dependence of the n_H values for HeC(1.3:90), MC(1.8:95), HpMC(0.15:1.8:75) and HeMC(0.20:1.5:300) in aqueous solution. Solid arrows and a dotted arrow are the same as in Figure 2.11. (b) T dependence of the N_H values for each chemically modified cellulose ether sample.

2.4.4 Hydration Behavior of HpC in Aqueous Solution

Dehydration behavior of HpMC in aqueous solution with increasing temperature was substantially more gently than that of MC because of an additional substitution by hydroxypropyl groups (Hp groups) as discussed above. In order to clarify the effect of Hp groups on hydration behavior of cellulose ethers, temperature dependence of hydration number for hydroxypropyl cellulose (HpC), which is substituted only by Hp groups, was investigated. Figure 2.14(a) shows the T dependence of n_H for HpC(2.8:140), MC(1.8:95) and HpMC(0.15:1.8:75) in aqueous solution. The n_H value of HpC(2.8:140) is much larger than that of MC and HpMC over all T range. This is because that the molar substitution number by Hp groups of HpC(2.8:140) is larger than the total substitution number of MC(1.8:95) and HpMC(0.15:1.8:75), and the Hp group bears hydroxy group. Then, the number of hydrophilic groups per glucopyranose unit for HpC is larger than that for MC and HpMC. Moreover, the hydration number per hydrophilic group, N_H, of HpC at T = 10 ºC is also higher than

that of MC and HpMC; the values of HpC(2.8:140), MC(1.8:95) and HpMC(0.15:1.8:75) are 3.6, 2.6 and 2.6, respectively at T = 10 ºC. This observation proposes that Hp groups possess large hydration number leading to the n_H of HpC. The n_H value of HpC(2.8:140) is 28 at 10 ºC and the value decreased remarkably with increasing T. The distinct dehydration behavior with increasing T well corresponds to the presence of a cloud point, which is observed at 46 °C irrespective of the c values, i.e., the LCST for aqueous HpC(2.8:140) solution as shown in Figure 2.14(a). However, the n_H value of HpC(2.8:140) obtained just below the LCST value is ca. 20 and the n_H value is much larger than the critical hydration number of ca. 5 for MC, HpMC and HeMC as discussed above. I speculate that the mechanism of insolubilization with increasing T for HpC in aqueous solution differs from that for MC, HpMC and HeMC in aqueous solution.

The temperature, T, dependence of hydration number, n_H, for tripropylene glycol monomethylether (TPGM) was investigated as a model molecule of substitution groups of HpC. Scheme 2.2 shows the chemical structure of TPGM. Since the structure of TPGM is almost the same as that of the trimer of hydroxypropoxy groups (-$OCH_2CH(OH)CH_3$), TPGM is a reasonable model compound for substituted hydroxypropoxy groups to compare the hydration behavior of the substituted Hp groups and HpC. The T dependence of n_H for TPGM is also shown in Figure 2.14(a). The hydration number per hydrophilic group of TPGM at T = 10 ºC is calculated to be 3.6, and the value is similar to that of HpC(2.8:140): 3.6. Then, the reason why the hydration number per hydrophilic group of HpC(2.8:140) at 10 ºC is much larger than that of MC(1.8:95) and HpMC(0.15:1.8:75) would be the large hydration number per hydrophilic group of Hp.

In order to compare the temperature dependence of hydration behavior for HpC(2.8:140) and TPGM, the n_H value at each temperature is normalized by the n_H value at 20 ºC, and the obtained value is named a characteristic hydration number, n_H*. Figure 2.14(b) shows temperature, T, dependence of n_H* for aqueous solutions of HpC(2.8:140), MC(1.8:95), HpMC(0.15:1.8:75) and TPGM. The T dependence of n_H* for HpC(2.8:140) and TPGM very well agrees with one another in

a T range from 10 to 40 ºC. Then, Hp groups, which are the substitution groups of HpC, essentially control the temperature dependence of hydration number for HpC(2.8:140) and the hydrated water molecules to HpC would mainly dehydrate from hydration sites in Hp groups with increasing T. Although the n_H value of HpC(2.8:140) obtained just below the LCST value is much larger than the critical hydration number, the hydrophobicity of substitution groups markedly increases with increasing T by the dehydration. In a high T range, the hydrophilic groups in Hp groups, which are less hydrated than ones in a low T range, would form intermolecular hydrogen bonding each other and the hydrophobic groups in Hp groups interact with each other due to the hydrophobic interaction. Jing et al.[39] investigated the phase transition of concentrated aqueous HpC solution with increasing T by using infrared and near infrared spectroscopic methods. They concluded that hydrophobic interaction between C–H groups are the driving force of coil-globule transition of HpC, and intermolecular hydrogen bonding between O–H groups is the driving force of the sol-gel transition of aqueous HpC systems.

The T dependence of n_H and n_H* for HeC(3.6:70) and TEG are also shown in Figures 2.14(a),(b). Although TPGM and TEG possess the same number of hydrophilic groups, the n_H value of TPGM is substantially higher than that of TEG over all T range. Moreover, the T dependence of n_H for both HpC and HeC is essentially controlled by the property of substitution groups as discussed above. The fact that the hydration number per hydrophilic groups, N_H, of HpC(2.8:140) is 2.7 at 40 ºC and that of HeC(3.6:70) is 2.1 at the same temperature reveals that the hydrophobic interaction between Hp groups is the main driving force of insolubilization of HpC in aqueous solution with increasing T. Although the n_H value of HpC is obviously larger than that of HeC, an addition of a hydrophobic methyl group remarkably strengthens the hydrophobicity of substitution groups. Desai et al.[40] reported the cloud points of aqueous HpC solutions decrease with increasing molar substitution number by Hp groups. This result suggests that the increase of Hp groups in HpC effectively increase the hydrophobic interaction between HpC molecules.

Finally, the aqueous HpC(2.8:140) solution forms molecular association and demonstrates a cloud point at 46 ºC despite of its large n_H value at the temperature. Consequently, not only higher n_H values of HpC than the critical hydration number, ca 5, but also the large n_H values of each hydrophilic group of HpC are necessary to keep the water solubility of HpC over a wide temperature range. These results propose that in the case of cellulose ethers substituted by slightly hydrophobic groups like Hp groups, the required hydration number for them to be dissolved in water becomes substantially larger than the standard critical hydration number of ca .5.

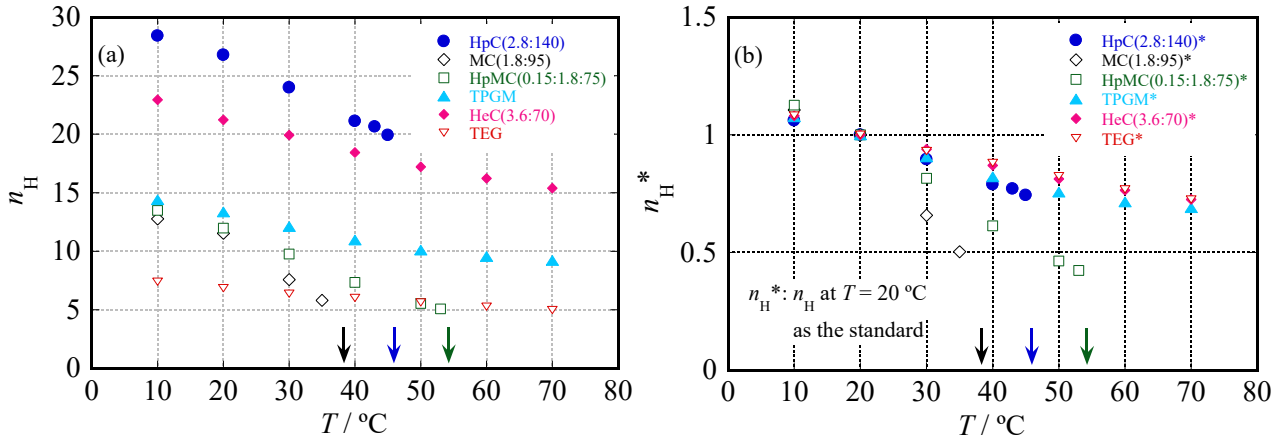

Figure 2.14 (a) Temperature, T, dependence of hydration number, n_H, per glucopyranose unit for HpC(2.8:140), MC(1.8:95), HpMC(0.15:1.8:75) and HeC(3.6:70), and that for TPGM and TEG per molecule. (b) Temperature, T, dependence of characteristic hydration numbers, n_H*, taking the n_H value at T = 20 ºC as the standard for each cellulose ether sample, TPGM and TEG. Solid arrows represent the LCST values for each cellulose ether sample.

Scheme 2.2 Chemical Structure of Tripropylene Glycol Monomethylether (TPGM).

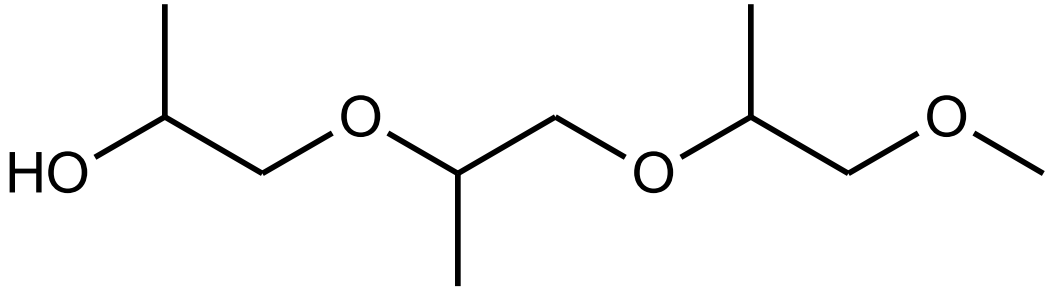

2.5 Conclusions

Hydration/dehydration behavior of hydroxyethyl cellulose, HeC, in aqueous solution was investigated by using dielectric spectroscopic measurements in a temperature range from $T = 10 – 70$ ºC. Although the hydration number per glucopyranose unit of HeC decreases with increasing temperature, the aqueous HeC solution never demonstrates a cloud point. As the molar substitution number by hydroxyethyl groups of HeC increases, the hydration number increases, and dehydration behavior becomes obvious with increasing temperature. The temperature dependence of n_H for triethylene glycol, TEG, which is a model compound of substitution group of HeC, was also investigated. The temperature dependence of characteristic hydration number values for aqueous solutions of HeC(1.3:90), HeC(2.0:220), HeC(3.6:70) and TEG well agrees with each other. Therefore, the substitution groups of HeC, hydroxyethoxy groups, determine the temperature dependence of hydration number for HeC in aqueous solution.

Hydration/dehydration behavior of methyl cellulose, MC, hydroxypropylmethyl cellulose, HpMC, and hydroxyethylmethyl cellulose, HeMC, in aqueous solution was also investigated. The hydration numbers of these cellulose ether samples in a low temperature range are governed by the total substitution number by methyl, hydroxypropyl and hydroxyethyl groups. Additional substitution to MC by hydroxypropyl or hydroxyethyl groups effectively extends solubility into water, i.e., increases the cloud point temperature. The effect of hydroxyethyl groups on increasing the hydration number is greater than that of hydroxypropyl groups. The critical hydration number for these cellulose ether samples necessary to obtain solubility into water are evaluated to be ca. 5 because the hydration numbers observed just below their lower critical soluble temperatures are close to 5 irrespective of molecular weights and substitution conditions for MC, HpMC and HeMC. The hydration number of HeC(1.3:90) is ca. 10 at 70 ºC and the value is much larger than critical hydration number. Consequently, the HeC samples keep their high water solubility even in a high temperature range.

Hydration/dehydration behavior of hydroxypropyl cellulose, HpC, in aqueous solution was also investigated. HpC possesses much higher hydration number than other examined cellulose ethers over all examined T range. Although the hydration number of HpC(2.8:140) obtained just below its LCST value of T = 45 ºC is much larger than the critical hydration number of MC, HpMC and HeMC, the aqueous HpC solution demonstrates a cloud point at 46 ºC. The T dependence of n_H for tripropylene glycol monomethylether, TPGM, which is a model molecule of substitution group of HpC, was investigated. The temperature dependence of characteristic hydration number for aqueous solutions of HpC(2.8:140) and TPGM agrees very well. The substitution groups of HpC determine the hydration/dehydration behavior of HpC in aqueous solution. The substitution groups of HpC dehydrate with increasing T and then the HpC forms molecular association due to the intermolecular interaction between substitution groups. Finally, the aqueous HpC solution demonstrates a cloud point at a high temperature of 46 ºC.

In conclusion, higher hydration numbers of cellulose ethers than their critical hydration numbers are necessary to keep their water solubility over a wide temperature range. When the hydrophobicity of the substitution groups is slightly high, the required hydration number to dissolve in water becomes substantially large.

References

(1) Sarkar, N. Thermal Gelation Properties of Methyl and Hydroxypropyl Methylcellulose. *J. Appl. Polym. Sci.* **1979**, *24* (4), 1073–1087.

(2) Sarkar, N.; Walker, L. C. Hydration-Dehydration Properties of Methylcellulose and Hydroxypropylmethylcellulose. *Carbohydr. Polym.* **1995**, *27* (3), 177–185.

(3) Feller, R.; Wilt, M. *Evaluation of Cellulose Ethers for Conservation*; 1990; Vol. 3.

(4) Takeshita, H.; Saito, K.; Miya, M.; Takenaka, K.; Shiomi, T. Laser Speckle Analysis on

Correlation between Gelation and Phase Separation in Aqueous Methyl Cellulose Solutions. *J. Polym. Sci. Part B Polym. Phys.* **2010**, *48* (2), 168–174.

(5) Bajwa, G. S.; Sammon, C.; Timmins, P.; Melia, C. D. Molecular and Mechanical Properties of Hydroxypropyl Methylcellulose Solutions during the Sol:Gel Transition. *Polymer (Guildf).* **2009**, *50* (19), 4571–4576.

(6) Bodvik, R.; Dedinaite, A.; Karlson, L.; Bergström, M.; Bäverbäck, P.; Pedersen, J. S.; Edwards, K.; Karlsson, G.; Varga, I.; Claesson, P. M. Aggregation and Network Formation of Aqueous Methylcellulose and Hydroxypropylmethylcellulose Solutions. *Colloids Surfaces A Physicochem. Eng. Asp.* **2010**, *354* (1–3), 162–171.

(7) Lott, J. R.; McAllister, J. W.; Arvidson, S. A.; Bates, F. S.; Lodge, T. P. Fibrillar Structure of Methylcellulose Hydrogels. *Biomacromolecules* **2013**, *14* (8), 2484–2488.

(8) Lott, J. R.; McAllister, J. W.; Wasbrough, M.; Sammler, R. L.; Bates, F. S.; Lodge, T. P. Fibrillar Structure in Aqueous Methylcellulose Solutions and Gels. *Macromolecules* **2013**, *46* (24), 9760–9771.

(9) Atkins, P.; de Paula, J. *Physical Chemistry*, 10th ed.; W.H. Freeman, Ed.; New York, 2014.

(10) Shikata, T.; Okuzono, M.; Sugimoto, N. Temperature-Dependent Hydration/Dehydration Behavior of Poly(Ethylene Oxide)s in Aqueous Solution. *Macromolecules* **2013**, *46* (5), 1956–1961.

(11) Ono, Y.; Shikata, T. Hydration and Dynamic Behavior of Poly(*N* -Isopropylacrylamide)s in Aqueous Solution: A Sharp Phase Transition at the Lower Critical Solution Temperature. *J. Am. Chem. Soc.* **2006**, *128* (31), 10030–10031.

(12) Matsuyama, A.; Tanaka, F. Theory of Solvation-Induced Reentrant Phase Separation in Polymer Solutions. *Phys. Rev. Lett.* **1990**, *65* (3), 341–344.

(13) Koda, S.; Hori, T.; Nomura, H.; Kawaizumi, F. Hydration of Methyl Cellulose. *Polymer (Guildf).* **1991**, *32* (15), 2806–2810.

(14) CELLOSIZE Hydroxyethyl Cellulose https://nshosting.dow.com/doc-archive/industry/building_construction/Cellosize_brochure.pdf.

(15) Koda, S.; Uemura, E.; Nomura, H.; Iwata, M.; Onda, Y. Water Retention Capacity of Cellulose Derivatives by the Compression Method. *Macromol. Chem. Phys.* **1998**, *199* (8), 1489–1493.

(16) Arai, K.; Okuzono, M.; Shikata, T. Reason for the High Solubility of Chemically Modified Poly(Vinyl Alcohol)s in Aqueous Solution. *Macromolecules* **2015**, *48* (5), 1573–1578.

(17) Feldman, Y.; Puzenko, A.; Ryabov, Y. Dielectric Relaxation Phenomena in Complex Materials. In *Advances in Chemical Physics, Fractals, Diffusion and Relaxation in Disordered Complex Systems*; Wiley Blackwell, 2005; Vol. 133, pp 1–125.

(18) Hübner, C.; Kaatze, U. *Electromagnetic Moisture Measurement. Principles and Applications*; 2016.

(19) Pottel, R. Dielectric Properties. In *Water: a comprehensive treatise. Vol. 3, Aqueous solutions of simple electrolytes*; Francs, F., Ed.; Plenum: New York, 1973; pp 401–431.

(20) Lupi, L.; Comez, L.; Paolantoni, M.; Perticaroli, S.; Sassi, P.; Morresi, A.; Ladanyi, B. M.; Fioretto, D. Hydration and Aggregation in Mono- and Disaccharide Aqueous Solutions by Gigahertz-to-Terahertz Light Scattering and Molecular Dynamics Simulations. *J. Phys. Chem. B* **2012**, *116* (51), 14760–14767.

(21) Lupi, L.; Comez, L.; Paolantoni, M.; Fioretto, D.; Ladanyi, B. M. Dynamics of Biological Water: Insights from Molecular Modeling of Light Scattering in Aqueous Trehalose Solutions. *J. Phys. Chem. B* **2012**, *116* (25), 7499–7508.

(22) Comez, L.; Paolantoni, M.; Sassi, P.; Corezzi, S.; Morresi, A.; Fioretto, D. Molecular Properties of Aqueous Solutions: A Focus on the Collective Dynamics of Hydration Water. *Soft Matter* **2016**, *12* (25), 5501–5514.

(23) Perticaroli, S.; Nakanishi, M.; Pashkovski, E.; Sokolov, A. P. Dynamics of Hydration Water in Sugars and Peptides Solutions. *J. Phys. Chem. B* **2013**, *117* (25), 7729–7736.

(24) Denisov, V. P.; Halle, B. Protein Hydration Dynamics in Aqueous Solution. *Faraday Discuss.* **1996**, *103*, 227–244.

(25) Steinhoff, H. J.; Kramm, B.; Hess, G.; Owerdieck, C.; Redhardt, A. Rotational and Translational Water Diffusion in the Hemoglobin Hydration Shell: Dielectric and Proton Nuclear Relaxation Measurements. *Biophys. J.* **1993**, *65*, 1486–1495.

(26) Perticaroli, S.; Ehlers, G.; Stanley, C. B.; Mamontov, E.; O'Neill, H.; Zhang, Q.; Cheng, X.; Myles, D. A. A.; Katsaras, J.; Nickels, J. D. Description of Hydration Water in Protein (Green Fluorescent Protein) Solution. *J. Am. Chem. Soc.* **2017**, *139* (3), 1098–1105.

(27) Pal, S. K.; Zewail, A. H. Dynamics of Water in Biological Recognition. *Chem. Rev.* **2004**,

104 (4), 2099–2124.

(28) Shiraga, K.; Suzuki, T.; Kondo, N.; Tajima, T.; Nakamura, M.; Togo, H.; Hirata, A.; Ajito, K.; Ogawa, Y. Broadband Dielectric Spectroscopy of Glucose Aqueous Solution: Analysis of the Hydration State and the Hydrogen Bond Network. *J. Chem. Phys.* **2015**, *142* (23), 234504.

(29) Shiraga, K.; Suzuki, T.; Kondo, N.; De Baerdemaeker, J.; Ogawa, Y. Quantitative Characterization of Hydration State and Destructuring Effect of Monosaccharides and Disaccharides on Water Hydrogen Bond Network. *Carbohydr. Res.* **2015**, *406*, 46–54.

(30) Shiraga, K.; Adachi, A.; Nakamura, M.; Tajima, T.; Ajito, K.; Ogawa, Y. Characterization of the Hydrogen-Bond Network of Water around Sucrose and Trehalose: Microwave and Terahertz Spectroscopic Study. *J. Chem. Phys.* **2017**, *146* (10), 105102.

(31) Deshmukh, S. A.; Sankaranarayanan, S. K. R. S.; Suthar, K.; Mancini, D. C. Role of Solvation Dynamics and Local Ordering of Water in Inducing Conformational Transitions in Poly(*N* -Isopropylacrylamide) Oligomers through the LCST. *J. Phys. Chem. B* **2012**, *116* (9), 2651–2663.

(32) Marchi, M.; Sterpone, F.; Ceccarelli, M. Water Rotational Relaxation and Diffusion in Hydrated Lysozyme. *J. Am. Chem. Soc.* **2002**, *124* (23), 6787–6791.

(33) Sterpone, F.; Stirnemann, G.; Laage, D. Magnitude and Molecular Origin of Water Slowdown Next to a Protein. *J. Am. Chem. Soc.* **2012**, *134* (9), 4116–4119.

(34) Cole, K. S.; Cole, R. H. *Dispersion and Absorption in Dielectrics 1. Alternating Current Characteristics**; 1941; Vol. 9.

(35) Davidson, D. W.; Cole, R. H. Dielectric Relaxation in Glycerol, Propylene Glycol, and n-Propanol. *J. Chem. Phys.* **1951**, *19* (12), 1484–1490.

(36) Arai, K.; Shikata, T. Hydration/Dehydration Behavior of Cellulose Ethers in Aqueous Solution. *Macromolecules* **2017**, *50* (15), 5920–5928.

(37) Shikata, T.; Minakawa, A.; Okuyama, K. Structure, Dynamics, and Hydration of a Collagen Model Polypeptide, (L-Prolyl-L-ProlylGlycyl) 10, in Aqueous Media: A Chemical Equilibrium Analysis of Triple Helix-to-Single Coil Transition. *J. Phys. Chem. B* **2009**, *113* (43), 14504–14512.

(38) Arvidson, S. A.; Lott, J. R.; McAllister, J. W.; Zhang, J.; Bates, F. S.; Lodge, T. P.; Sammler,

R. L.; Li, Y.; Brackhagen, M. Interplay of Phase Separation and Thermoreversible Gelation in Aqueous Methylcellulose Solutions. *Macromolecules* **2013**, *46* (1), 300–309.

(39) Jing, Y.; Wu, P. Study on the Thermoresponsive Two Phase Transition Processes of Hydroxypropyl Cellulose Concentrated Aqueous Solution: From a Microscopic Perspective. *Cellulose* **2013**, *20* (1), 67–81.

(40) Desai, D.; Rinaldi, F.; Kothari, S.; Paruchuri, S.; Li, D.; Lai, M.; Fung, S.; Both, D. Effect of Hydroxypropyl Cellulose (HPC) on Dissolution Rate of Hydrochlorothiazide Tablets. *Int. J. Pharm.* **2006**, *308* (1–2), 40–45.

Chapter 3: Dynamic Viscoelastic Behavior of Methyl Cellulose and Hydroxypropylmethyl Cellulose in Aqueous Solution

3.1 Introduction

In the previous chapter, the mechanism of insolubilization for methyl cellulose, MC, and hydroxypropylmethyl cellulose, HpMC, in aqueous solution was discussed from the view point of hydrated water molecules to cellulose ethers. The gelation behavior for aqueous solutions of MC and HpMC will be discussed by using rheological measurements in this chapter. A number of rheological studies have focused on the gelation behavior of aqueous MC and HpMC solutions. Wang et al.[1] have investigated the molecular weight and concentration dependence of elasticity in gel state and gelation mechanism for aqueous solution of methylcellulose. Silva et al.[2] have focused on the correlation between polymer hydrophobicity and rheological behavior and explored the effect of shear strain on thermal gelation behavior for aqueous hydroxypropylmethyl cellulose solutions. Shahin et al.[3] have investigated temperature and concentration dependence of the viscoelastic behavior for aqueous solution of hydroxypropylmethyl cellulose and proposed the structure that is formed in the system. Arvidson et al.[4] have discussed the relationship between phase behavior and mechanical properties related to gel formation for aqueous solutions of methyl celluloses possessing various molecular weights. McAllister et al.[5,6] have determined the fibril structure formed by methyl cellulose in aqueous solution at temperatures higher than 40 °C during annealing processes for long periods, such as several weeks, and they developed thermodynamics of the formed fibrils and coiled methyl cellulose. Lodge et al.[7] have drawn a consistent picture of phase separation and gelation for aqueous solutions of hydroxypropylmethyl cellulose by using turbidimetry, rheology, cryoTEM, SANS, SAXS and light scattering techniques. Here, I will discuss the temperature dependence of viscoelastic

behavior for aqueous MC and HpMC solutions. The gelation mechanism of these solutions will be discussed on the basis of rheological behavior in relation to hydration behavior of MC and HpMC in aqueous solution as discussed in Chapter 2.

Many studies on aqueous solutions of MC and HpMC have mainly focused on temperature dependence of their properties because these solutions demonstrate clear gelation behavior with increasing temperature. However, in order to obtain full understanding on the complicated behavior of these solutions with increasing temperature, such as phase separation and gelation behavior, it is necessary to obtain the fundamental knowledge of aqueous MC and HpMC solutions in a low temperature range where these cellulose ethers are well dissolved in water. Then, I will try to clarify the conformation of HpMC molecules in aqueous solution by using rheological measurements. There have been several theoretical predictions of relationship between the viscoelastic properties and the conformation of polymer molecules in various states, such as melt, solution and dispersion.[8,9] Moreover, a number of studies have investigated the viscoelastic behavior of polymer solutions and discussed the conformation of polymer molecules.[10–13] The viscoelastic behavior for aqueous solutions of several HpMC samples with a wide molecular weight range from M_w = 75,000 to 300,000 will be discussed at a low temperature of 10 ºC. The concentration and molecular weight dependence of the viscoelastic behavior for aqueous HpMC solutions will be fully discussed to clarify the conformation of HpMC molecules well dissolved in aqueous solution.

3.2 Experimental

Materials: A series of methyl cellulose (MC) and hydroxypropylmethyl cellulose (HpMC) samples were kindly supplied by Shin-Etsu Chemical Co. Ltd. (Tokyo). These cellulose ether samples were coded in the same way as Chapter 2. Table 3.1 summarizes characteristics of all cellulose ether samples discussed in this chapter. All the MC and HpMC samples were used without further

purification. Highly deionized water with a specific resistance higher than 18.2 MΩ·cm obtained by a Direct-Q 3UV system (Millipore-Japan, Tokyo) was used as the solvent for the aqueous sample solution preparation.

The concentrations, c, of aqueous MC and HpMC solutions for the viscoelastic measurements are ranged from 1.5 to 12 wt%.

Table 3.1 Characteristics of MC and HpMC samples used in this chapter

Sample codes	Molar substitution number by hydroxypropyl groups	Degree of substitution by methyl groups	$M_w/10^3$
MC(1.8:$M_w/10^3$)	0	1.8	300
HpMC(0.15:1.8:$M_w/10^3$)	0.15	1.8	75, 150, 220, 300

Methods: Dynamic viscoelastic measurements were conducted using a rheometer MCR301(Anton Paar) equipped with a coaxial cylinder (internal radius: 16.7mm, external radius: 18mm, height: 25mm) and a Peltier temperature control. The measurements were performed at strain amplitude of $\gamma = 10$ % over an angular frequency range from $\omega = 10^{-2}$ to 10^2 s^{-1} and in a temperature range from T = 10 to 70 °C. The waiting time before measurements at each temperature was 20 minutes and a thin liquid layer of tetradecane was placed on the top surface of the samples to prevent the evaporation of the solvent water.

Many materials are viscoelastic, and their mechanical behavior cannot be described with only viscous or elastic properties when they undergo deformation and flow. The rheological techniques are quite useful methods to investigate the mechanical properties of complex materials, such as viscoelastic fluids and solids. Dynamic viscoelastic measurement is one of the rheological measurements and provides information on mechanical responses (dynamic modulus or viscosity) under sinusoidal strains for the tested systems as function of frequency. In the conventional rheometers, strain amplitudes applied to samples are ranged from 0.01 to 100, and a frequency range from 10^{-2} to 10^2 s^{-1} are used.

3.3 Results and Discussion

3.3.1 Viscoelastic Behavior for Aqueous solutions of MC and HpMC Samples

Figures 3.1 (a) and (b) show the obtained angular frequency, ω, dependence of storage modulus, G', and loss modulus, G'', for aqueous solutions of MC(1.8:300) and HpMC(0.15:1.8:300) at the concentration of c = 3 wt% and the temperature of T = 10 ° C as typical examples. The HpMC and MC solutions behave as typical flowing fluids showing G' proportional to $\omega^{\sim 2}$ and G'' to ω in an ω range lower than $\omega = 10^{-1}$ s^{-1}. This flowing behavior suggests that most of solute cellulose molecules in the examined system are in the relaxed state in the frequency range. However, small shoulders are observed in G' data in a low frequency range $\omega \sim 10^{-2}$ s^{-1} in both the systems. Although it has been considered that the HpMC and MC molecules well dissolve in cold water around T = 10 ° C as described in Chapter 2, a small part of polymer chains forms a weak network structure possessing a long relaxation time. I speculate that a similar behavior is also observed in the systems discussed here, which are consisting of different molecular weight samples in a different concentration range.

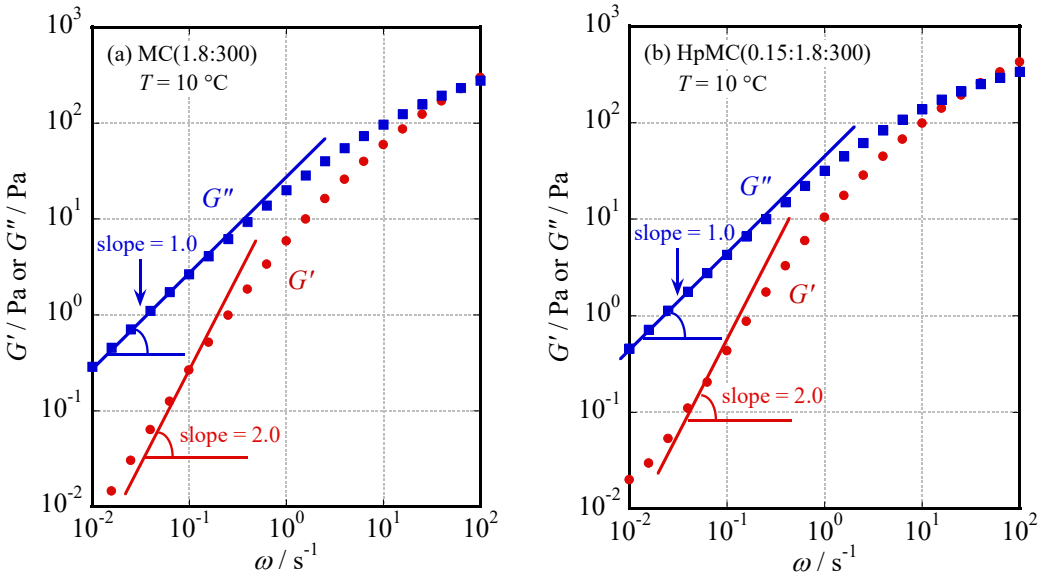

Figure 3.1 Angular frequency, ω, dependence of storage and loss modulus, G' and G'', for aqueous solutions of MC(1.8:300) (a) and HpMC(0.15:1.8:300) (b) at c = 3 wt% and T = 10 ºC.

3.3.2 Temperature Dependence of Viscoelastic Behavior for Aqueous Solutions of MC and HpMC Samples

The aqueous solutions of MC and HpMC form a weak network structure even at the low temperature of T = 10 ºC as discussed above. MC and HpMC molecules dissolved in aqueous solution dehydrate and show a phase transition from transparent solution to turbid gel with increasing T as discussed in Chapter 2. To clarify the mechanism of gelation in the system from the viewpoint of viscoelastic behavior, T dependence of G' and G'' for aqueous solutions of MC and HpMC was investigated over a T range from 10 ºC to the observed gelation temperatures. Figure 3.2 shows dynamic viscoelastic behavior of aqueous solution of HpMC(0.15:1.8:300) at 3 wt% in a T range from 10 to 70 ºC. The small shoulder observed in a G' curve at 10 ºC markedly grows to apparent plateau with increasing T. G'' curves also exhibit a similar growth from a small shoulder to plateau with increasing T. At a high temperature of T = 70 ºC, the G' and G'' curves show rather flat plateau with very weak ω dependence. Shahin et al.[3] reported a similar dynamic viscoelastic behavior for the aqueous system of a different type of HpMC.

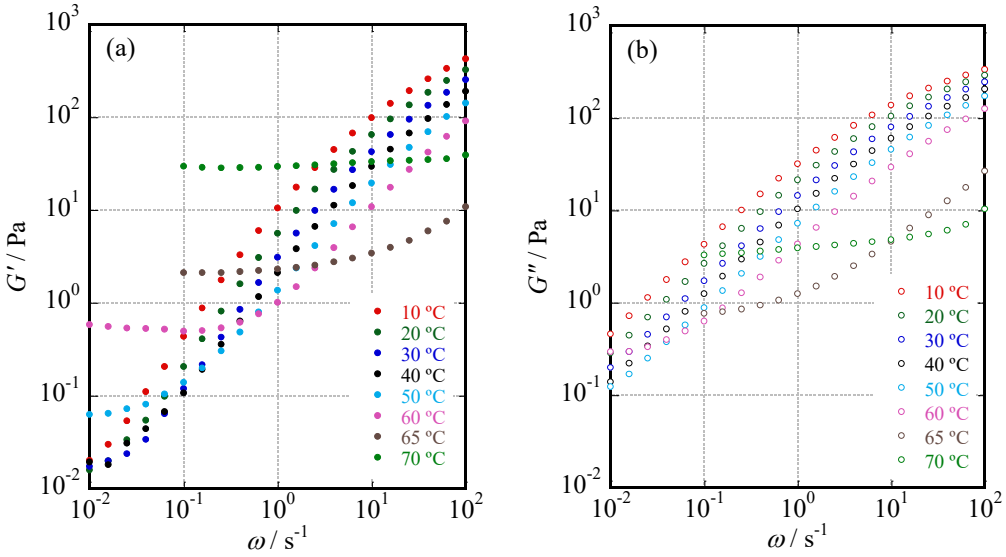

Figure 3.2 Temperature, T, dependence of storage modulus G' (a) and loss modulus G'' (b) as functions of ω for an aqueous solution of HpMC(0.15:1.8:300) obtained at c = 3 wt% over a temperature range from 10 to 70 ºC.

To discuss the T dependence of viscoelastic behavior observed in Figure 3.2 in detail, I tried to apply the time-temperature superposition principle to the frequency, ω, dependence of G' and G'' for the aqueous solution of HpMC(0.15:1.8:300) seen in Figure 3.2. The superposition was applied to both G' and G'' curves taking the data of 10 ºC as the standards. Figure 3.3 shows the obtained master curves of G' and G'' for the solution. The horizontal (ω axis) shift factor and the vertical (modulus axis) shift factor are defined as a_T and b_T, respectively. The time-temperature superposition works well in the data for the aqueous HpMC solution especially in a high-frequency (fast mode) region except for data obtained at high temperatures T = 60 and 70 ºC as seen in Figure 3.3. Figure 3.4 shows the dependence of the horizontal shift factor a_T on the reciprocal of temperature, T^{-1}, necessary to obtain the master curves in Figure 3.3 for aqueous solution of HpMC(0.15:1.8:300) at c = 3 wt% in the T range from 10 to 50 ºC in which the superposition works well in the fast mode. The obtained T dependence of a_T showed Arrhenius type one. Then, the T dependence of relaxation time of the fast mode is also the Arrhenius type because T dependence of the horizontal shift factor a_T is equivalent to T dependence of relaxation time of the system. The activation energy of the fast mode, E_f*, was evaluated from the slope of a straight line in Figure 3.4 to be E_f* = 26.9 kJ mol^{-1}. If molecular motions in the system is governed only by the viscosity η_m of the medium, the relaxation time, τ, is given as $\tau \propto \eta_m \alpha T^{-1}$, where α means the size effect of molecules.[8] The activation energy, E_m*, of the medium viscosity, η_m, is evaluated from the next equation assuming the origins of G' and G'' are governed by diffusive molecular motion of HpMC molecules;

$$a_T \propto \frac{\exp\left(\frac{E_m^*}{RT}\right)}{RT} \qquad (3\text{-}1)$$

The obtained value of E_m* for HpMC is 24.4 kJ mol^{-1}. On the other hand, the activation energy of viscosity of pure water, E_w*, is calculated to be E_w* = 15.4 kJ mol^{-1} by using viscosity data of water.[14] The reason why the E_m* value is higher than the E_w* value by 9 kJ mol^{-1} would be intermolecular

interaction between HpMC molecules and hydration of the solute molecules in aqueous solution.

The vertical shift factor b_T is also used to obtain the master curves of G' and G'' for the HpMC solution. Figure 3.5 shows T dependence of the reciprocal value of b_T in a T range from 10 to 50 ºC in which the superposition of the fast relaxation mode is well performed. The value of b_T^{-1} means how many HpMC molecules contribute to the fast mode seen in high-frequency range relative to the number of HpMC molecules contributing to the fast mode at T = 10 ºC. The value of b_T^{-1} decreased gradually with increasing T and reduced to ca. 0.8 at T = 50 ºC. This means that ca. 20 % of HpMC molecules existing freely at T = 10 ºC participate in a network structure formed at T = 50 ºC.

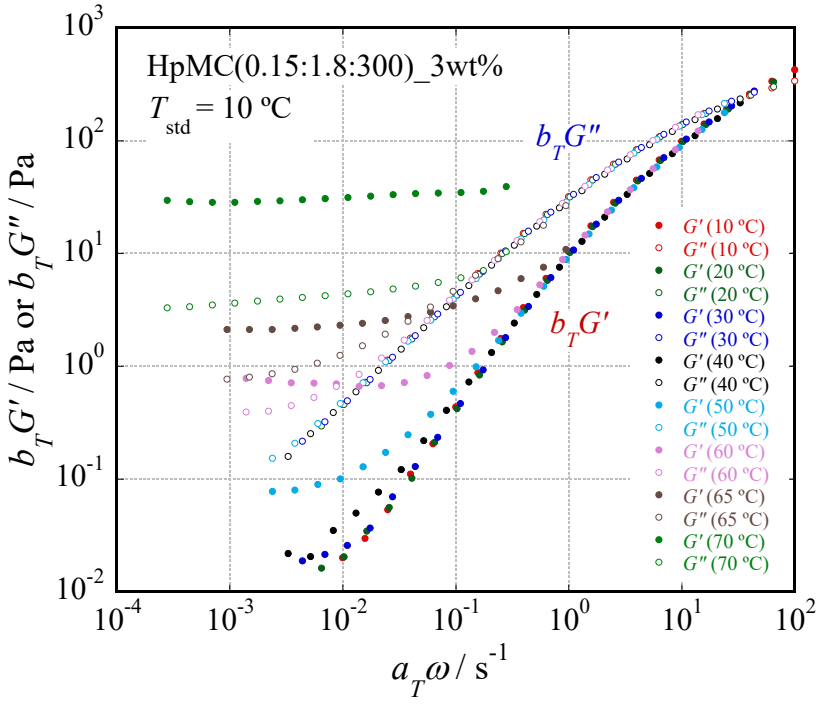

Figure 3.3 Master curves of G' and G'' for an aqueous solution of HpMC(0.15:1.8:300) at c = 3 wt% obtained by shifting data along both frequency and modulus axes taking the data of HpMC(0.15:1.8:300) at T = 10 ºC as the standards.

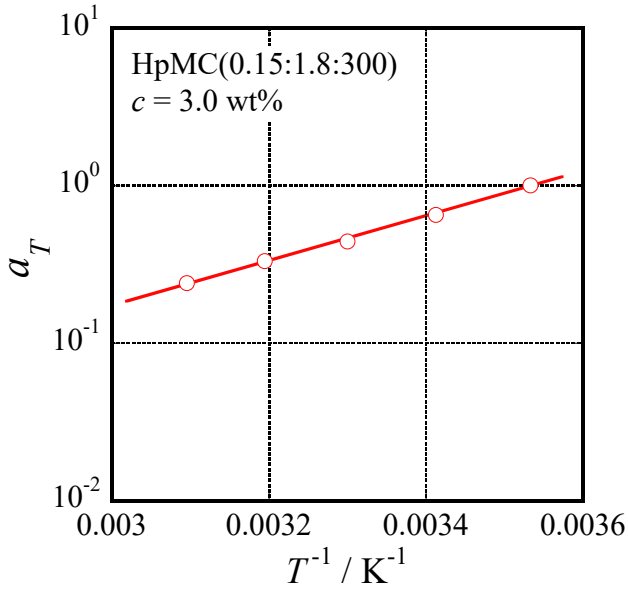

Figure 3.4 Dependence of a_T on the reciprocal of temperature, T^{-1}, for an aqueous solution of HpMC(0.15:1.8:300) at c = 3.0 wt%.

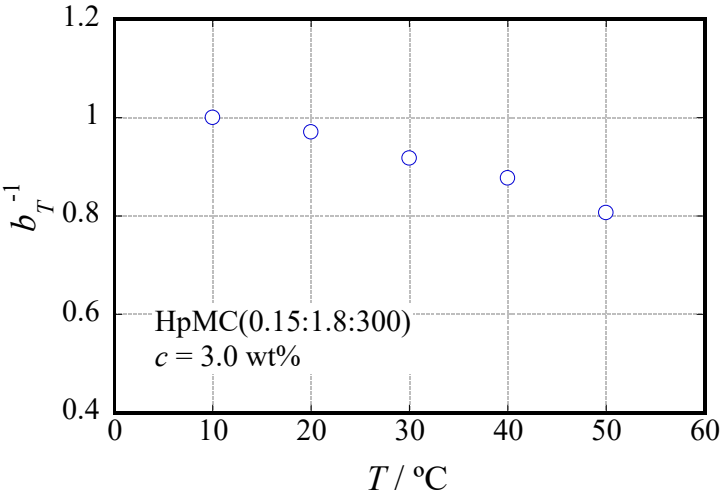

Figure 3.5 Temperature, T, dependence of the reciprocal value of the vertical shift factor, b_T^{-1}, for an aqueous solution of HpMC(0.15:1.8:300) at c = 3.0 wt%.

The small shoulder in G' curve observed as the slow mode in a low-frequency region at T = 10 ºC where HpMC molecules keep a sufficient hydration number, markedly grows with increasing T above 30 ºC as described before. Approaching to the clouding point of the aqueous HpMC(0.15:1.8:M_w) solution (T = 53 ºC as discussed in Chapter 2), the plateau in G' data remarkably

increases its strength and frequency area. The slow mode observed as plateaus in G' and G'' curves results in gel like behavior. The dehydration of HpMC molecules with increasing T induces molecular association cooperatively due to hydrophobic interaction between HpMC molecules. The plateaus in G' show little frequency dependence and dominates the viscoelastic behavior ($G' >> G''$) over a wide frequency range at T = 70 ºC. Then, people say that the aqueous HpMC solution demonstrates gelation behavior at the temperature.

It is reported that the critical gel behavior observed at a gelation temperature (T_{gel}) for many polymeric materials showing gelation is characterized by a scaling relationship between the dynamic moduli, G' and G'', and ω given by:

$$G' \sim G'' \sim \omega^n \qquad (3\text{-}2)$$

where n is the relaxation exponent.[15] Arvidson et al.[4] determined the gelation temperature of methylcellulose in aqueous solution by using this relationship. However, aqueous solution of HpMC(0.15:1.8:300) never showed the critical gelation behavior given by eq. 3-2 examined in this study. The aqueous HpMC(0.15:1.8:300) solution forms a weak network structure even at the low temperature of T = 10 ºC. Although the values of G' and G'' remarkably increase with increasing T due to the gelation, the values in a frequency range higher than 10^0 s^{-1} reduce only slightly over a T range from 10 to 50 ºC as seen in Figures 3.3 and 3.5. In the temperature range lower than 50 ºC, most HpMC molecules behave in the standard manner as controlled by activation energy without forming molecular association. However, a distinct reduction in the G' and G'' curves was observed in the T range higher than 50 ºC in a high frequency range. The number of mobile HpMC molecules decreases and the molecules take parts in the formation of the network structure above 50 ºC. Finally, the strong network constructs throughout the solution and the aqueous HpMC solution demonstrates gelation behavior at T = 70 ºC. Figure 3.6 represents the schematic illustration of the gelation mechanism of HpMC molecules in aqueous solution.

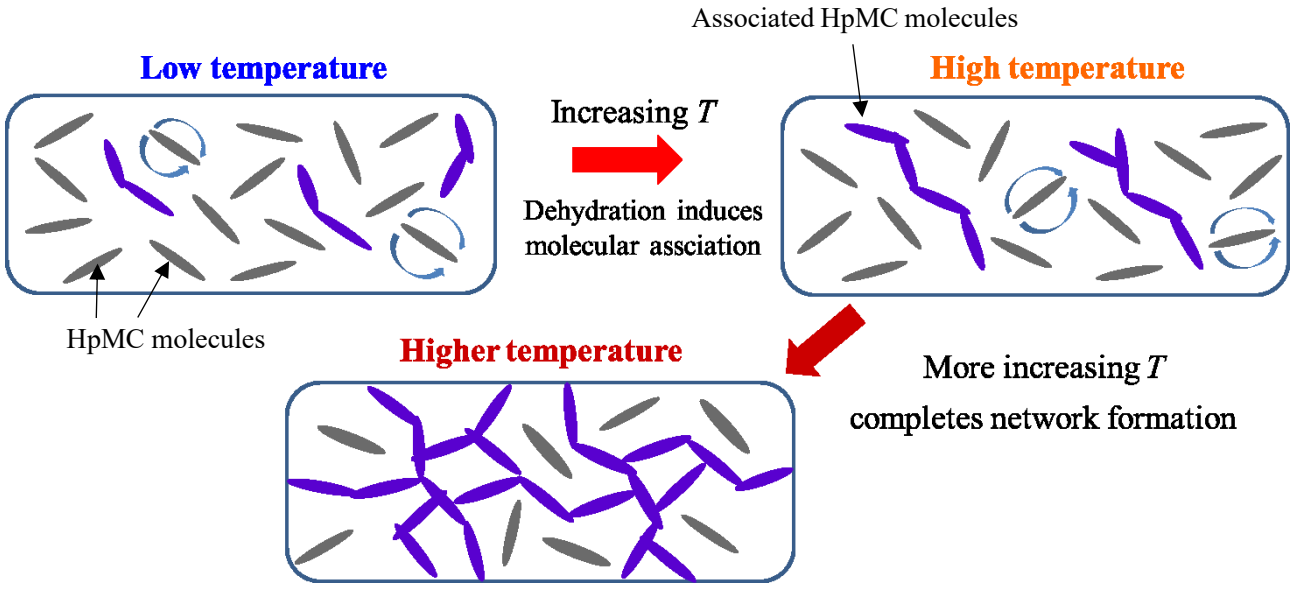

Figure 3.6 Schematic representation for the formation of network structure and gelation in aqueous HpMC systems with increasing temperature.

Figure 3.7 shows the obtained master curves of G' and G'' for an aqueous solution of MC(1.8:300) at c = 3 wt% obtained by using time-temperature superposition taking the data of 10 ºC as the standards. The aqueous MC solution behaves as gel over the entire frequency range examined at T = 50 ºC. It is likely that the gelation mechanism of aqueous MC solution is the same as that of HpMC. Then, MC never demonstrated the critical gelation behavior with increasing T. However, a temperature showing G' shoulder growth clearly in the aqueous MC solution is substantially lower than that of the aqueous HpMC solution. The fact that the hydration number of MC decreases more rapidly with increasing T than that of HpMC as described in Chapter 2 is one of the reasons. Furthermore, the shoulder in G' observed in the MC system grows more rapidly with increasing T than that in the HpMC system. It is reported that aqueous solution of MC forms stronger gel than HpMC.[16] Consequently, the dehydration behavior with increasing T causes the growth of the network structure, and mechanical strength of the formed gel is controlled by the density of the formed network.

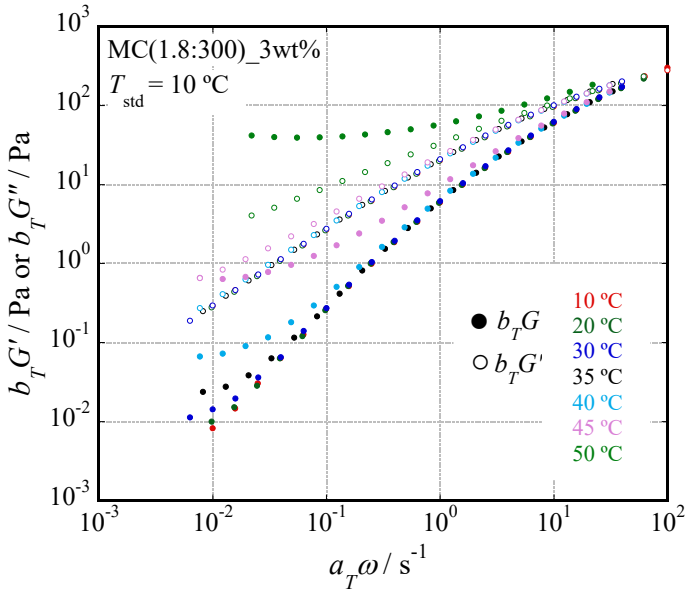

Figure 3.7 Master curves of G' and G'' for an aqueous solution of MC(1.8:300) at c = 3 wt% obtained by shifting data along both frequency and modulus axes taking the data of MC(1.8:300) at T = 10 ºC as the standards.

3.3.3 Concentration Dependence of Viscoelastic Behavior for Aqueous HpMC Solution

To clarify the conformation of HpMC molecules dissolved in aqueous solution, concentration dependence of viscoelastic behavior for aqueous HpMC systems was investigated. Shahin et al.[3] reported the concentration dependence of the relaxation time τ defined as the reciprocal of the frequency showing $G' = G''$ and the elastic modulus G_{el} defined as the G' value observed at the frequency of $10\tau^{-1}$. However, a new method proposed in this study assuming time-concentration superposition principle to determine the concentration, c, dependence of the average relaxation time, τ_w, and the average modulus (the reciprocal value of steady state compliance), J_e^{-1}, is more accurate, because the superposition uses the whole frequency dependence of viscoelastic spectra obtained by frequency sweeps. Figure 3.8 shows ω dependence of G' and G'' for aqueous HpMC(0.15:1.8:300) solutions at 5 kinds of concentrations at 10 ºC: c = 1.5, 2, 3, 4 and 5 wt%. To discuss the c dependence of viscoelastic behavior for the system, I assume the time-concentration

superposition principle on the ω dependence of G' and G'' data at different concentrations. Figure 3.9 shows the master curves for G' and G'' of the HpMC solution obtained by using the superposition taking the data of 3 wt% as the standards. The horizontal and vertical shift factors are a_c and b_c, respectively, which are necessary to perform the superposition. The superposition worked well in the aqueous HpMC solution over all c range examined in this study. Figure 3.10 shows concentration dependence of a_c and b_c necessary to complete the superposition resulting to the master curves seen in Figure 3.9. The horizontal shift factor a_c increases with increasing concentration in the manner of $a_c \propto c^{2.8}$. On the other hand, the vertical shift factor b_c decreases with increasing concentration as $b_c \propto c^{-1.3}$. The shift along frequency axis corresponds to a change in the average relaxation time, τ_w. On the other hand, the shift along moduli axis corresponds to a change in the average modulus (the reciprocal value of steady state compliance), J_e^{-1}. Therefore, the relationship between τ_w and c is given as $\tau_w \propto c^{2.8}$, and the other relationship between J_e^{-1} and c as $J_e^{-1} \propto c^{1.3}$.

The time-concentration superposition principle was also applied to aqueous solutions of HpMC(0.15:1.8:75), HpMC(0.15:1.8:150) and HpMC(0.15:1.8:220) at T = 10 ºC. Figure 3.11 shows master curves of G' and G'' for aqueous solutions of HpMC(0.15:1.8:$M_w/10^3$) at T = 10 ºC obtained by using the superposition. The superposition worked well in the three HpMC samples over all c range examined in this study. Table 3.2 summarizes c dependence of exponents for τ_w and J_e^{-1} for all the HpMC samples examined in this study. All the HpMC samples showed essentially the same c dependence exponents for τ_w and J_e^{-1} ($\tau_w \propto c^{\sim 2.8}$ and $J_e^{-1} \propto c^{\sim 1.3}$).

In addition to the HpMC, MC samples without the substitution by Hp group, but with the identical degree of substitution by methyl group showed essentially the same concentration dependence of τ_w and J_e^{-1}; $\tau_w \propto c^{2.7 - 2.9}$ and $J_e^{-1} \propto c^{1.2 - 1.4}$. Therefore, concentration dependence of τ_w and J_e^{-1} for the MC and HpMC samples examined in this study is independent of molecular weight and the substituent condition.

In the case of entangled flexible polymer chains system, concentration dependence of τ_w and J_e^{-1} is theoretically predicted as $\tau_w \propto c^{1.5}$ and $J_e^{-1} \propto c^{9/4}$, and the relationships $\tau_w \propto c^{b-2}$ and $J_e^{-1} \propto c^2$ (the value of b is dependent on the polymer species) have been experimentally confirmed.[8,10] On the other hand, concentration dependence of τ_w and J_e^{-1} for entangled rigid rod-like particles is theoretically predicted as $\tau_w \propto c^2$ and $J_e^{-1} \propto c^1$.[8] In addition, Morse[9] theoretically predicted that c dependence of J_e^{-1} for entangled semiflexible polymers is given as $J_e^{-1} \propto c^{1.33}$ or $c^{1.4}$. Unfortunately, the prediction for entangled semiflexible polymers is mentioned only J_e^{-1} and not τ_w. The obtained exponent values of concentration dependence of J_e^{-1} for MC and HpMC in aqueous solution, 1.2 – 1.3, in this study, are closer to theoretically predicted values for entangled semiflexible polymers ($J_e^{-1} \propto c^{1.33}$ or $c^{1.4}$) and rigid rod-like particles ($J_e^{-1} \propto c^1$) than that of entangled flexible polymer chains ($J_e^{-1} \propto c^2$ or $J_e^{-1} \propto c^{9/4}$). Bodvik et al.[17] have reported that the SAXS results for aqueous solution of hydroxypropylmethyl cellulose at 25 ºC indicated a rod-like conformation of HpMC molecules in aqueous solution. Consequently, concentration dependence of J_e^{-1} for aqueous MC and HpMC solutions reveals that MC and HpMC molecules behave as semiflexible polymer chains or rigid rod-like particles in aqueous solution.

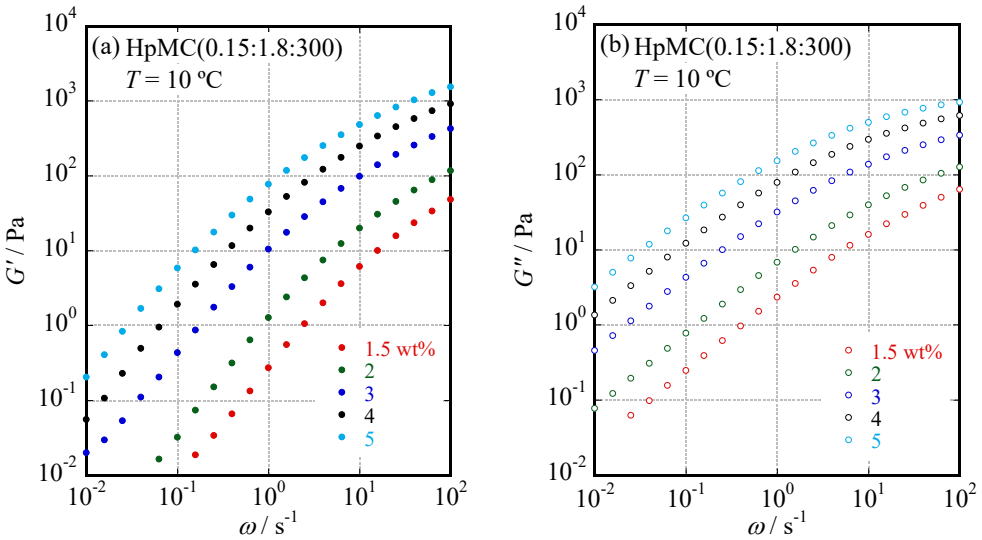

Figure 3.8 Concentration, c, dependence of storage modulus G' (a) and loss modulus G'' (b) obtained in an ω range from 10^{-2} to 10^2 s^{-1} for aqueous solutions of HpMC(0.15:1.8:300) at T = 10 ºC at several concentrations ranged from 1.5 to 5 wt%.

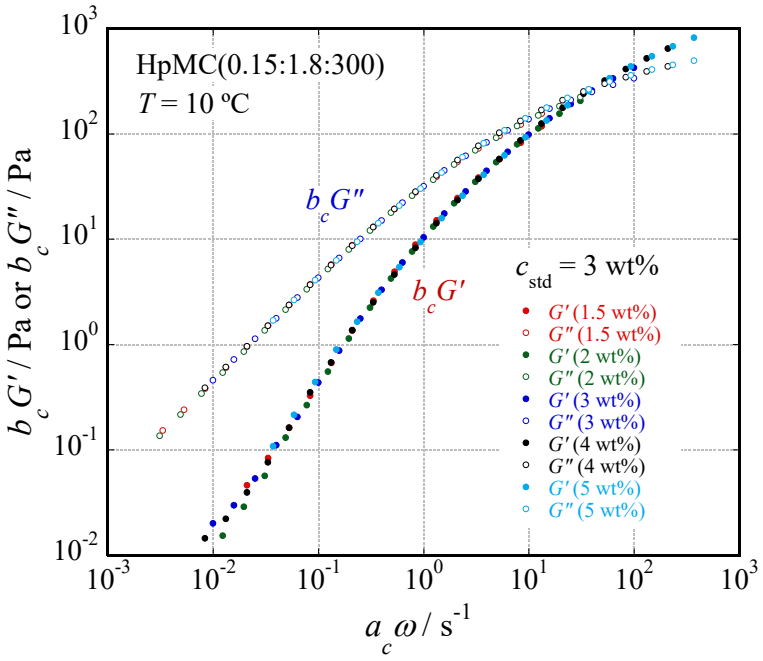

Figure 3.9 Master curves of G' and G'' for aqueous solutions of HpMC(0.15:1.8:300) at $T = 10$ ºC obtained by using time-concentration superposition principle taking the data of HpMC(0.15:1.8:300) at $c = 3$wt% as the standards. The horizontal and vertical shift factors are a_c and b_c, respectively.

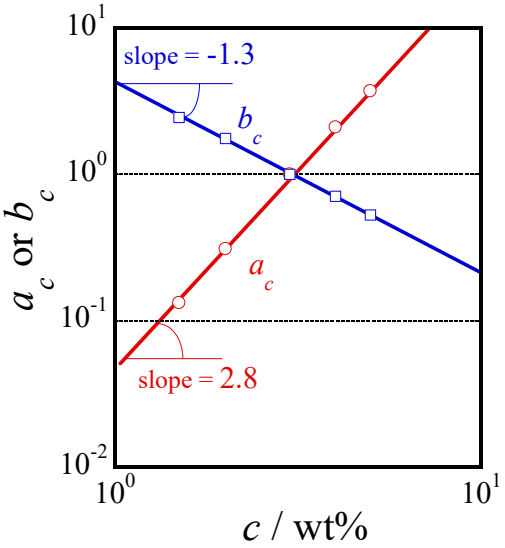

Figure 3.10 Concentration dependence of shit factors, a_c and b_c, for aqueous solutions of HpMC(0.15:1.8:300) at $c = 1.5 – 5$ wt% and $T = 10$ ºC taking the data at $c = 3$wt% as the standards.

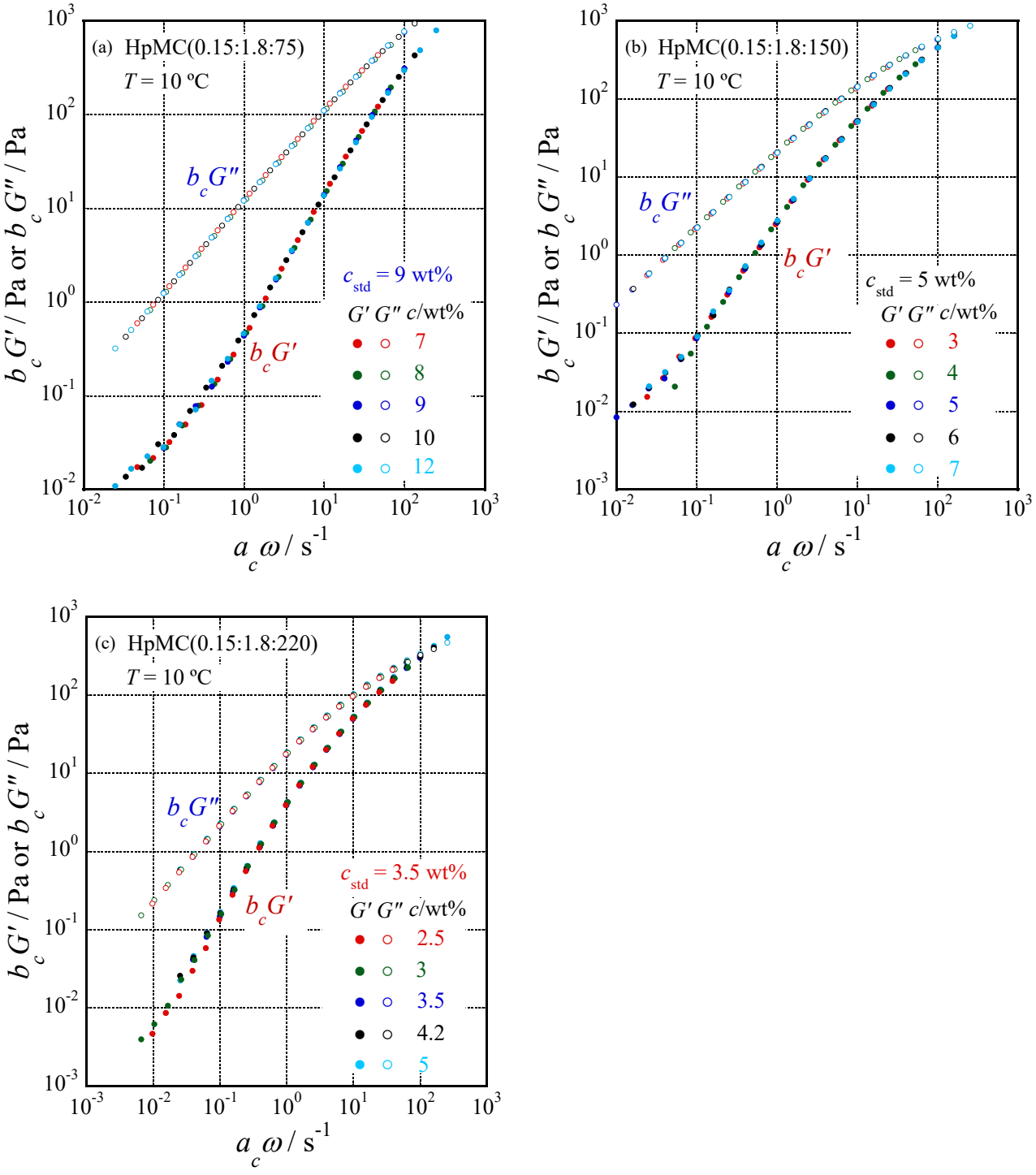

Figure 3.11 Master curves of G' and G'' for aqueous solutions of HpMC(0.15:1.8:75) (c = 9 wt% as the standards) (a), HpMC(0.15:1.8:150) (c = 5 wt% as the standards) (b) and HpMC (0.15:1.8:220) (c = 3.5 wt% as the standards) (c) obtained by using the time-concentration superposition principle.

Table 3.2 Exponent numbers, n and m, of the concentration, c, for the average relaxation time, τ_w ($\propto c^n$), and the average modulus, J_e^{-1} ($\propto c^m$), for HpMC(0.15:1.8:$M_w/10^3$).

Samples	n	m
HpMC(0.15:1.8:75)	2.8	1.3
HpMC(0.15:1.8:150)	2.8	1.3
HpMC(0.15:1.8:215)	2.7	1.3
HpMC(0.15:1.8:300)	2.8	1.3

3.3.4 Molecular Weight Dependence of Viscoelastic Behavior for Aqueous HpMC Solution

There have been no reports on the molecular weight dependence of viscoelastic behavior for aqueous HpMC systems. To discuss the conformation of HpMC molecules in aqueous solution in detail, the molecular weight dependence of the average relaxation time, τ_w, and the average modulus, J_e^{-1}, was investigated. In the previous section, it is concluded that the concentration dependence of τ_w and J_e^{-1} for HpMC(0.15:1.8:$M_w/10^3$) is independent of molecular weight. Then, a time-molecular weight superposition principle is applied to aqueous HpMC(0.15:1.8:$M_w/10^3$) systems assuming that the relaxation mechanism of HpMC molecules is identical independently of molecular weight. Figure 3.12 shows the master curves of G' and G'' for aqueous solutions of HpMC(0.15:1.8:75), HpMC(0.15:1.8:150), HpMC(0.15:1.8:220) and HpMC(0.15:1.8:300) at T = 10 ºC obtained by using the time-concentration and time-molecular weight superposition principles taking the data of HpMC(0.15:1.8:300) at c = 3 wt% as the standards. The horizontal and vertical shift factors are termed a_M and b_M, respectively. The time-concentration and time-molecular weight superpositions worked well in the aqueous HpMC solution over entire molecular weight range examined, 75×10^3

$\leq M_w \leq 300 \times 10^3$. Figure 3.13 shows molecular weight, M_w, dependence of shit factors, a_M and b_M, for aqueous solutions of HpMC(0.15:1.8:$M_w/10^3$) at $T = 10$ ºC taking the data of HpMC(0.15:1.8:300) at c = 3 wt% as the standards assuming that the concentration dependence of τ_w and J_e^{-1} for all HpMC(0.15:1.8:$M_w/10^3$) samples are $\tau_w \propto c^{2.8}$ and $J_e^{-1} \propto c^{1.3}$. The horizontal and vertical shift factors increase with increasing molecular weight in the manner of $a_M \propto M_w^{5.5}$ and $b_M \propto M_w^{1.3}$. Then, the relationships can be described to be $\tau_w \propto M_w^{5.5}$ and $J_e^{-1} \propto M_w^{-1.3}$. Therefore, the obtained dependence of τ_w and J_e^{-1} on c and M_w for HpMC is given as $\tau_w \propto c^{2.8}M_w^{5.5}$ and $J_e^{-1} \propto c^{1.3}M_w^{-1.3}$. Using the number density of polymer chains ν (= c/M_w or c/M_n) in the system to describe the experimentally obtained τ_w and J_e^{-1} for HpMC, the relationships $\tau_w \propto \nu^{2.8}M_w^{8.3}$ and $J_e^{-1} \propto \nu^{1.3}$ is obtained.

As described above, empirical concentration, c, and molecular weight, M_w, dependence of τ_w and J_e^{-1} for entangled flexible polymer chains is reported to be $\tau_w \propto c^{b-2}M_w^{3.4}$ and $J_e^{-1} \propto c^2M_w^0$, where the value of b is dependent on polymer species.[10] The M_w dependence of τ_w for HpMC, $\tau_w \propto M_w^{5.5}$, is much stronger than that for entangled flexible polymer chains. Moreover, although J_e^{-1} for flexible polymer chains is independent of M_w, the aqueous HpMC systems show a decrease in J_e^{-1} with increasing M_w. On the other hand, according to Morse prediction of J_e^{-1} for entangled semiflexible polymers, the relationship is described as $J_e^{-1} \propto c^{1.33}L_p^{-0.2}$ or $J_e^{-1} \propto c^{1.4}L_p^{-0.33}$, where L_p means persistence length of polymer chains.[9] As discussed above, the aqueous HpMC systems demonstrate that HpMC molecules behave as semiflexible polymer chains or rigid rod-like particles in aqueous solution. However, the prediction by Morse does not include the dependence on molecular weight. Since the aqueous HpMC systems show clear M_w dependence of J_e^{-1}, the Morse's prediction is not accepted in the system. In the case of entangled rigid rod-like particles, c and M_w dependence of τ_w and J_e^{-1} is theoretically predicted as $\tau_w \propto c^2M_w^7$ and $J_e^{-1} \propto c^1M_w^{-1}$ or $\tau_w \propto \nu^2M_w^9$ and $J_e^{-1} \propto \nu^1$ using ν.[8] The obtained ν and M_w dependence of τ_w for HpMC, $\tau_w \propto \nu^{2.8}M_w^{8.3}$, is close to that for entangled rigid rod-like particles, $\tau_w \propto \nu^2M_w^9$. However, the M_w dependence of τ_w for the experimental results is slightly smaller than that for rigid rod-like particles. It is likely that the HpMC

molecules cannot keep the rigidity as fully stretched rods, but the molecules form a rod-like structure constructed by folding like hairpins, and the folding number depends on M_w. Sagawa et al.[18] reported that the number of folding in each HpMC molecule is estimated to be one for a sample with M_w = 75×10^3 and two for $M_w = 300 \times 10^3$ in aqueous solution by using dynamic light scattering techniques. On the other hand, the obtained dependence of J_e^{-1} on ν in aqueous HpMC solution, $J_e^{-1} \propto \nu^{1.3}$, is rather similar to that for rigid rod-like particles, $J_e^{-1} \propto \nu^1$. Therefore, the obtained c, ν and M_w dependence of τ_w and J_e^{-1} for HpMC in aqueous solution reveals that HpMC molecules behave as rod-like particles possessing high rigidity in aqueous solution.

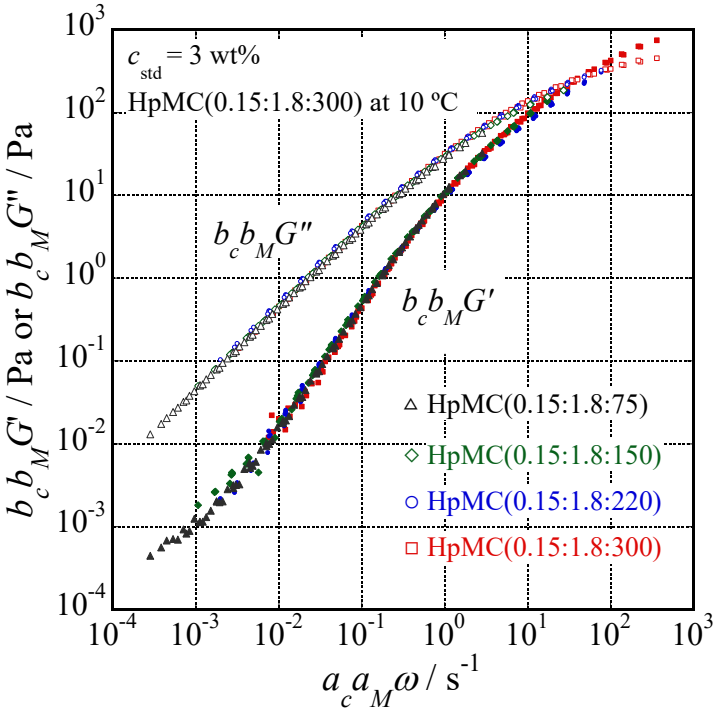

Figure 3.12 Master curves of G' and G'' for aqueous solutions of HpMC(0.15:1.8:75), HpMC(0.15:1.8:150), HpMC(0.15:1.8:220) and HpMC(0.15:1.8:300) at T = 10 ºC obtained by using time-concentration and time-molecular weight superpositions taking the data of HpMC(0.15:1.8:300) at c = 3 wt% as the standards.

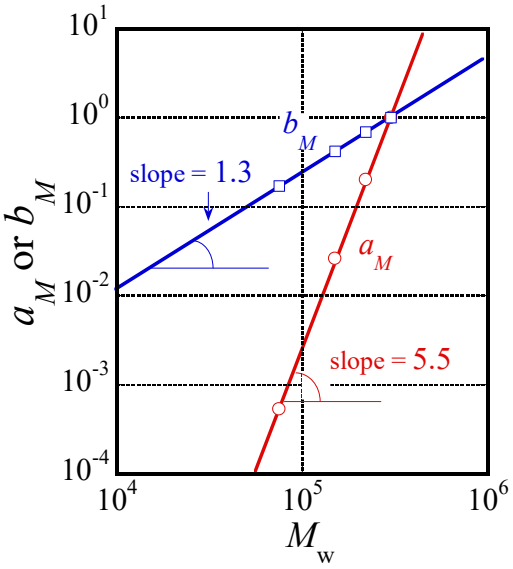

Figure 3.13 Molecular weight dependence of shit factors a_M and b_M for aqueous solutions of HpMC(0.15:1.8:M_w/10^3) at T = 10 ºC taking the data of HpMC(0.15:1.8:300) at c = 3 wt% as the standards.

3.3.5 Origin of Viscoelasticity in Aqueous HpMC Solution

The origin of viscoelasticity for aqueous solutions of MC and HpMC has not been fully understood so far. To investigate the origin of viscoelasticity of the HpMC system, dynamic viscoelastic measurements were performed over a wide ω range at the low temperature of T = 10 ºC which is far from the gelation temperature and provides the sufficiently hydrated state for HpMC molecules. Figure 3.14 shows ω dependence of G' and G'' for 7 wt% aqueous solutions of HpMC(0.15:1.8:75) (a) and HpMC(0.15:1.8:150) (b), and 3 wt% aqueous solutions of HpMC(0.15:1.8:220) (c) and HpMC(0.15:1.8:300) (d) at 10 ºC, respectively. In the case of entangling flexible polymer chain system, the molecular weight between entanglement points (M_e) gives a clear physical meaning of the site of polymer chain strand which behaves as an elastic spring in the entangling flexible polymer system. The value of M_e can be easily calculated from plateau modulus, G_N, by using next equation:[8]

$$M_e = \frac{cRT}{G_N} \qquad (3\text{-}3)$$

where R is the gas constant. In the case of aqueous HpMC solution, G_N values cannot be clearly determined because of the limitation of a measurable frequency. The frequency range covered by the measuring system was too low to determine G_N values directly in the aqueous HpMC solution examined even in the solution of the longest HpMC(0.15:1.8:300). Then, the reciprocal value of steady state compliance, J_e^{-1} is used instead of G_N in this study. It is known that the relationship between J_e^{-1} and G_N is given by $2J_e^{-1} = G_N$ for approximately monodisperse ($M_w/M_n \sim 1$) polymer samples. From this relationship and Equation 3-3, M_e can be calculated by using next equation:

$$M_e = \frac{cRT}{2J_e^{-1}} \qquad (3\text{-}4)$$

The dispersity of HpMC is not low, but $M_w/M_n = 2 \sim 3$ as reported by the providing chemical company. The relationship between J_e^{-1} and G_N is unclear for moderately polydisperse polymer samples such as $M_w/M_n = 2 \sim 3$. However, eq. 3-4 is employed to evaluate the value of M_e for HpMC as a characteristic parameter in the unit of [g mol^{-1}] in this study. The value of J_e^{-1} was determined from crossing points between straight lines of G' and G'' in the double logarithmic plot, which mean $G' \propto \omega^2$ and $G'' \propto \omega$ (as seen in Figure 3.14(a)). The determined M_e values for each sample are summarized in Table 3.3. M_e values for all samples are systematically larger than the whole weight-average molecular weight, M_w. In the case of entangling flexible polymer systems, the value of M_e should be much smaller than M_w. Therefore, one can conclude that the origin of elasticity for HpMC in aqueous solution is not the formation of entanglements between flexible polymer chains. Although the estimation of G_N values is not accurate at this point, the G_N for the aqueous HpMC(0.15:1.8:300) solution at c = 3.0 wt% will be determined to be ca. 10^3 Pa ($\approx 30\ J_e^{-1}$) as seen in Figure 3.9. Then, the relationships $M_e \approx 68{,}000$ and $M_e/M_w \approx 0.23$ are obtained. The latter relationship is followed in other

HpMC systems. The fact that the M_e value depends on the M_w strictly denies the origin of elasticity in the aqueous HpMC systems is the entanglement between flexible chains.

To clarify that the origin of the elasticity in the system is the rotational relaxation of rigid rod-like particles formed in the system, the meaning of the obtained M_e value via eq. 3-4 should be considered here. According to a theory for monodisperse rod-like particle suspensions proposed by Doi and Edwards,[8] plateau modulus, G_N, is given by an equation $G_N = (3/5)\nu RT$, where ν means the number density defined using the molecular weight of particles as $\nu = c/M$, irrespective of the presence of entanglements. Then, an equation $M = (3/5)cRT/G_N$ similar to eq. 3-3 is obtained. Although the estimated value M (= 41000 g mol^{-1}) is less than M_w (= 3×10^5 g mol^{-1}) or M_n (= 88000 g mol^{-1}) for HpMC(0.15:1.8:300), the ratio of $M/M_n = 0.47$ is close to unity reveals that the HpMC molecules behave as rod-like particles and the number density controls the elasticity of the system. The reason for $M < M_n$ is possibly related to the bending motions of HpMC molecules. The same consideration on the relation of M/M_n is possible in other HpMC samples with different M_n. To discuss the origin of elasticity for HpMC more precisely, it is quite helpful to use HpMC samples with monodisperse ($M_w/M_n \sim 1$) molecular weight distribution.

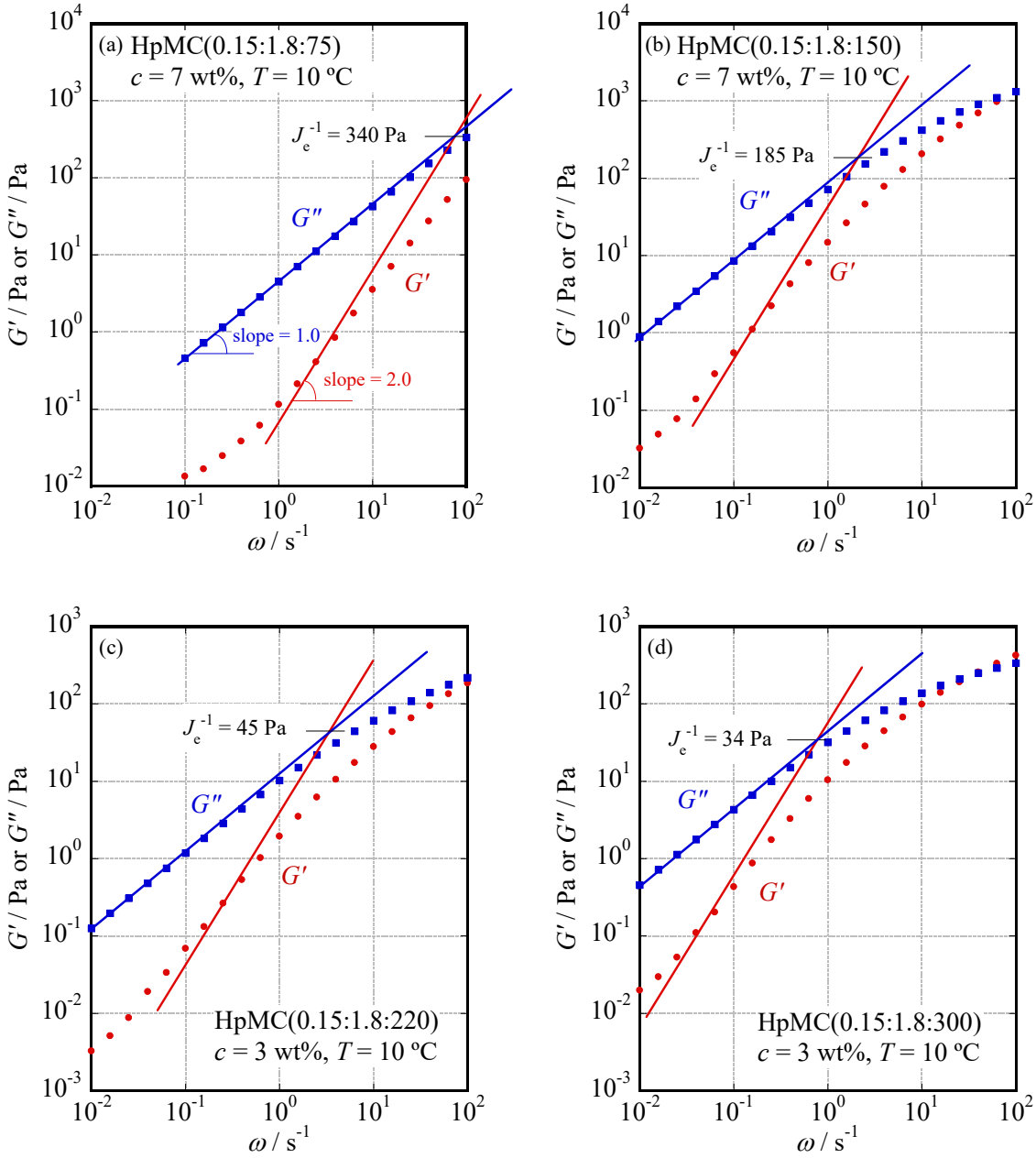

Figure 3.14 Angular frequency, ω, dependence of G' and G'' for aqueous solutions of HpMC(0.15:1.8:75) (a) and HpMC(0.15:1.8:150) (b) at c = 7 wt% and T = 10 ºC, and aqueous solutions of HpMC(0.15:1.8:220) (c) and HpMC(0.15:1.8:300) (d) at c = 3 wt% and T = 10 ºC.

Table 3.3 Reciprocal value of steady state compliance, J_e^{-1}, molecular weight between entanglements, M_e obtained via eq. 3-4, weight-average molecular weight, M_w, and M_e/M_w for aqueous HpMC solution.

Samples	c [g/100 mL]	J_e^{-1} [Pa]	M_e[g/mol]	M_w[g/mol]	M_e/M_w
HpMC (0.15:1.8:75)	7	340	240,000	75000	3.2
HpMC (0.15:1.8:150)	7	185	440,000	150,000	2.9
HpMC (0.15:1.8:220)	3	45	780,000	220,000	3.6
HpMC (0.15:1.8:300)	3	34	1,030,000	300,000	3.5

3.4 Conclusions

The gelation mechanism of methyl cellulose, MC, and hydroxypropylmethyl cellulose, HpMC, in aqueous solution was investigated for a temperature range from T = 10 to 70 ºC using viscoelastic measurements. Although the MC and HpMC samples possess high hydration number (12 ~ 13 per glucopyranose unit) at T = 10 ºC as described in Chapter 2, a small part of MC and HpMC polymer chains forms a weak network structure possessing a long relaxation time. The weak network structure gradually grows to a strong network structure due to dehydration of polymer chains with increasing T. The dehydration with increasing T induces molecular association cooperatively. The strong network spreads throughout the solution, and MC and HpMC demonstrate gelation behavior with additional increasing T. Aqueous solutions of MC and HpMC do not show the critical gel behavior, which is usually observed in many gel forming systems.

The conformation of HpMC in aqueous solution was investigated in a molecular weight range from $M_w = 75 \times 10^3$ to 300×10^3 at 10 ºC by using viscoelastic measurements. Time-concentration and time-molecular weight superposition principles worked well in the aqueous HpMC solution over all concentration and molecular weight range examined in this study. Concentration, c,

the number density of polymer chains, ν, and M_w dependence of the average relaxation time, τ_w, and the average modulus (the reciprocal value of steady state compliance), J_e^{-1}, for HpMC is obtained from the shift factors along frequency and moduli axes. The experimentally obtained relationships for HpMC, $\tau_w \propto \nu^{2.8} M_w^{8.3}$ and $J_e^{-1} \propto \nu^{1.3}$, are quite similar to the theoretically predicted relationships for entangled rigid rod-like particles, $\tau_w \propto \nu^2 M_w^9$ and $J_e^{-1} \propto \nu^1$. Therefore, HpMC molecules behave as rod-like particles possessing high rigidity in aqueous solution.

References

(1) Wang, Q.; Li, L. Effects of Molecular Weight on Thermoreversible Gelation and Gel Elasticity of Methylcellulose in Aqueous Solution. *Carbohydr. Polym.* **2005**, *62* (3), 232–238.

(2) Silva, S. M. C.; Pinto, F. V.; Antunes, F. E.; Miguel, M. G.; Sousa, J. J. S.; Pais, A. A. C. C. Aggregation and Gelation in Hydroxypropylmethyl Cellulose Aqueous Solutions. *J. Colloid Interface Sci.* **2008**, *327* (2), 333–340.

(3) Shahin, A.; Nicolai, T.; Benyahia, L.; Tassin, J. F.; Chassenieux, C. Evidence for the Coexistence of Interpenetrating Permanent and Transient Networks of Hydroxypropyl Methyl Cellulose. *Biomacromolecules* **2014**, *15* (1), 311–318.

(4) Arvidson, S. A.; Lott, J. R.; McAllister, J. W.; Zhang, J.; Bates, F. S.; Lodge, T. P.; Sammler, R. L.; Li, Y.; Brackhagen, M. Interplay of Phase Separation and Thermoreversible Gelation in Aqueous Methylcellulose Solutions. *Macromolecules* **2013**, *46* (1), 300–309.

(5) McAllister, J. W.; Schmidt, P. W.; Dorfman, K. D.; Lodge, T. P.; Bates, F. S. Thermodynamics of Aqueous Methylcellulose Solutions. *Macromolecules* **2015**, *48* (19), 7205–7215.

(6) McAllister, J. W.; Lott, J. R.; Schmidt, P. W.; Sammler, R. L.; Bates, F. S.; Lodge, T. P. Linear and Nonlinear Rheological Behavior of Fibrillar Methylcellulose Hydrogels. *ACS Macro Lett.* **2015**, *4* (5), 538–542.

(7) Lodge, T. P.; Maxwell, A. L.; Lott, J. R.; Schmidt, P. W.; McAllister, J. W.; Morozova, S.; Bates, F. S.; Li, Y.; Sammler, R. L. Gelation, Phase Separation, and Fibril Formation in

Aqueous Hydroxypropylmethylcellulose Solutions. *Biomacromolecules* **2018**, *19* (3), 816–824.

(8) M. Doi and S. F. Edwards. *The Theory of Polymer Dynamics*; Oxford, 1986.

(9) Morse, D. D. Tube Diameter in Tightly Entangled Solutions of Semiflexible Polymers. *Phys. Rev. E - Stat. Physics, Plasmas, Fluids, Relat. Interdiscip. Top.* **2001**, *63* (3), 1–22.

(10) Ferry, J. D. *Viscoelastic Properties of Polymers*, 3rd ed.; Wiley & Sons: New York, 1980.

(11) Del Giudice, F.; Tassieri, M.; Oelschlaeger, C.; Shen, A. Q. When Microrheology, Bulk Rheology, and Microfluidics Meet: Broadband Rheology of Hydroxyethyl Cellulose Water Solutions. *Macromolecules* **2017**, *50* (7), 2951–2963.

(12) Heo, Y.; Larson, R. G. Universal Scaling of Linear and Nonlinear Rheological Properties of Semidilute and Concentrated Polymer Solutions. *Macromolecules* **2008**, *41* (22), 8903–8915.

(13) Tassieri, M.; Evans, R. M. L.; Barbu-Tudoran, L.; Khaname, G. N.; Trinick, J.; Waigh, T. A. Dynamics of Semiflexible Polymer Solutions in the Highly Entangled Regime. *Phys. Rev. Lett.* **2008**, *101* (19), 1–5.

(14) Hardy, R. C.; Cottington, R. L. Viscosity of Deuterium Oxide and Water in the Range 5 ° to 125° C. *J. Res. Natl. Bur. Stand.* **1949**, *42* (6), 573–578.

(15) Chambon, F.; Winter, H. H. Linear Viscoelasticity at the Gel Point of a Crosslinking PDMS with Imbalanced Stoichiometry. *J. Rheol. (N. Y. N. Y).* **1987**, *31* (8), 683–697.

(16) Sarkar, N. Kinetics of Thermal Gelation of Methylcellulose and Hydroxypropylmethylcellulose in Aqueous Solutions. *Carbohydr. Polym.* **1995**, *26* (3), 195–203.

(17) Bodvik, R.; Dedinaite, A.; Karlson, L.; Bergström, M.; Bäverbäck, P.; Pedersen, J. S.; Edwards, K.; Karlsson, G.; Varga, I.; Claesson, P. M. Aggregation and Network Formation of Aqueous Methylcellulose and Hydroxypropylmethylcellulose Solutions. *Colloids Surfaces A Physicochem. Eng. Asp.* **2010**, *354* (1–3), 162–171.

(18) Sagawa, N.; Yamanishi, N.; Shikata, T. A Viscoelastic Study of Dilute Aqueous Solution of Chemically Modified Cellulose Ethers Using Dynamic Light Scattering Techniques. *Nihon Reoroji Gakkaishi* **2017**, *45* (1), 57–63.

Chapter 4: Dynamic Viscoelastic Behavior of Hydroxyethyl Cellulose and Hydroxypropyl Cellulose in Aqueous Solution

4.1 Introduction

In this chapter, I focus on the rheological behavior of aqueous solutions of hydroxyethyl cellulose, HeC, and hydroxypropyl cellulose, HpC, to understand temperature dependence of the dynamics of the HeC and HpC in aqueous systems and to clarify the conformation of these cellulose ether molecules in aqueous solution. Aqueous HpC solution demonstrates phase separation and gelation behavior with increasing temperature and its physicochemical properties have been studied by using various techniques, such as nuclear magnetic resonance (NMR) measurement,[1] cloud-point observation,[2] infrared (IR) and near infrared (NIR) spectroscopy[3] and rheological measurements.[4,5] Carotenuto et al.[4] have reported that phase transition of concentrated aqueous HpC solution is controlled by temperature, the rate of temperature change and concentration, and the solution demonstrates the critical gel behavior, G' and $G'' \propto \omega^n$.[6] Costanzo et al.[5] have investigated the effect of the concentration and heating rate on sol-gel transition of aqueous HpC solution by using rheological measurements. Although they have investigated frequency dependence of G' and G'' for aqueous HpC solution, the viscoelastic behavior in a low frequency range, $\omega \sim 10^{-2}$ s^{-1}, was not focused on. In the previous chapter, I showed that aqueous solutions of methyl cellulose, MC, and hydroxypropylmethyl cellulose, HpMC, demonstrate a small shoulder in G' data in a low frequency range and the growth of the shoulder with increasing temperature is the essential reason for the gelation of the solutions. Then, in this chapter, I will discuss the temperature dependence of dynamic viscoelastic behavior for aqueous HpC solution including the low frequency range, $\omega \sim 10^{-2}$ s^{-1}, in relation to the hydration behavior of HpC molecules. Moreover, the obtained temperature dependence

of rheological behavior for aqueous HpC solution will be compared with that for aqueous solutions of MC and HpMC.

It is reported that aqueous HeC system does not show a cloud point with increasing temperature even in a high temperature range.[7] There are several reports on the characteristic rheological behavior of aqueous HeC solutions.[8–10] Benyounes et al.[8] have investigated the flow properties of aqueous HeC solutions over a wide range of shear rates and reported that the solutions were not thixotropic. Giudice et al.[9] have investigated the viscoelastic properties of HeC solutions by using various rheological techniques over a wide concentration and frequency range. Ouaer et al.[10] have determined the intrinsic viscosity and the critical overlap concentration of HeC molecules in aqueous solution. These studies were performed around the room temperature of T = 20 – 25 ºC because it has been believed that the high water solubility of HeC molecules is not affected by temperature. That is why there have been no reports on the temperature dependence of viscoelastic behavior for aqueous HeC systems. However, the HeC samples in aqueous solution clearly demonstrate dehydration behavior with increasing temperature as discussed in Chapter 2. Hence, it is necessary to clarify the temperature dependence of rheological behavior for aqueous HeC solutions in relation to their hydration/dehydration behavior. In this chapter, the temperature dependence of viscoelastic behavior for aqueous HeC solutions is investigated over a wide temperature range from 10 to 70 ºC.

Although there are several reports on the rheological behavior of aqueous HeC solutions as mentioned above, few studies have focused on the conformation of HeC molecules in aqueous solution. Giudice et al.[9] have discussed the conformation of HeC molecules with a molecular weight $M_w \sim 600 \times 10^3$ in aqueous solution by using various rheological techniques and concluded that the HeC molecules behave like a linear-flexible polymer chains in aqueous system. However, the number of examined HeC sample species was only one kind of molecular weight, and the concentration and molecular weight dependence of viscoelastic behavior for aqueous HeC solution was not fully

discussed. In this chapter, the viscoelastic behavior for aqueous solutions of several HeC samples with wide molecular weights ranged from $M_w = 220 \times 10^3$ to 1420×10^3 was investigated at a low temperature of 1 ºC. The obtained concentration and molecular weight dependence of the viscoelastic behavior for aqueous HeC solutions will be fully discussed to clarify the conformation of HeC molecules in aqueous solution.

4.2 Experimental

Materials: A series of hydroxyethyl cellulose (HeC) samples were kindly supplied by Daicel Corporation (Osaka) and The Dow Chemical Company (Midland), and hydroxypropyl cellulose (HpC) samples were kindly supplied by Nippon Soda Co., Ltd. (Tokyo). These cellulose ether samples were coded in the same manner as in Chapter 2. Table 4.1 summarizes the characteristics of HeC and HpC samples examined in this chapter. The HeC and HpC samples were used without further purification. Highly deionized water with a specific resistance higher than 18.2 MΩ cm obtained by a Direct-Q 3UV system (Millipore-Japan, Tokyo) was used as the solvent for the aqueous sample solution.

The concentrations, c, of aqueous HeC and HpC solutions for the viscoelastic measurements are ranged from 0.5 to 8 wt%.

Table 4.1 Characteristics of HeC and HpC samples used in this Chapter

Sample codes	Molar substitution number by hydroxyethyl groups	Molar substitution number by hydroxypropyl groups	$M_w/10^3$
HeC(1.3:$M_w/10^3$)	1.3	—	220, 520, 820, 1300, 1420
HeC(2.0:760)	2.0	—	760
HpC(2.8:830)	—	2.8	830

Methods

Dynamic viscoelastic measurements: Dynamic viscoelastic measurements were conducted using a rheometer MCR301(Anton Paar) equipped with a coaxial cylinder (internal radius: 16.7mm, external radius: 18mm, height: 25mm) and a Peltier temperature control. The measurements were performed at strain amplitude of $\gamma = 10$ % over an angular frequency range from $\omega = 10^{-2}$ to 10^{2} s^{-1} and in a temperature range from $T = 1$ to 70 °C. The waiting time before measurements at each temperature was 20 minutes and a thin liquid layer of tetradecane was placed on the top surface of the samples to prevent the evaporation of the solvent water.

Gel permeation chromatography: The GPC system was equipped with a column (Shodex OHpak SB-806M HQ) and a refractive index detector (Optilab rEX, Wyatt Technology, U.S.A.). The eluent of water containing 0.1 M $NaNO_3$ was delivered by a pump at a constant flow rate of 1.0 mL/min. The concentrations of the samples were 0.02, 0.05 and 0.1 w/v %, and injected volume was 200 μL.

Intrinsic viscosity measurements: Intrinsic viscosities for polymer samples were calculated from the concentration reduced specific viscosity data determined using an Ubbelohde viscometer TN-102-03 (Takao Manufacturing CO., LTD., Japan). The measurements were performed in a water bath kept at the temperature of $T = 25$ °C with the accuracy of ± 0.2 °C using a temperature controlling unit.

4.3 Results and Discussion

4.3.1 Viscoelastic Behavior for Aqueous Solutions of HeC and HpC Samples

Figure 4.1(a) shows the obtained angular frequency, ω, dependence of storage modulus, G',

and loss modulus, G'', for an aqueous solution of HeC(1.3:520) at the concentration of c = 3 wt% and the temperature of T = 10 ºC as a typical example. The aqueous HeC solution behaves as a typical flowing fluid showing G' proportional to ω^2 and G'' to ω in an ω range lower than $\omega = 2.5 \times 10^{-2}$ s^{-1}. This flowing behavior suggests that all solute cellulose molecules in the examined system are in the relaxed state in the low frequency range. Then, the HeC samples well dissolve into water in a low temperature range. Figure 4.1(b) shows the ω dependence of G' and G'' for an aqueous solution of HpC(2.8:830) at c = 3 wt% and T = 10 ºC. Unfortunately, flowing behavior, $G' \propto \omega^2$ and $G'' \propto \omega$ cannot be observed because of the limitation of measurable low frequencies. The frequency range covered by our measuring system was too high to observe flowing behavior directly in the examined aqueous HpC solution.

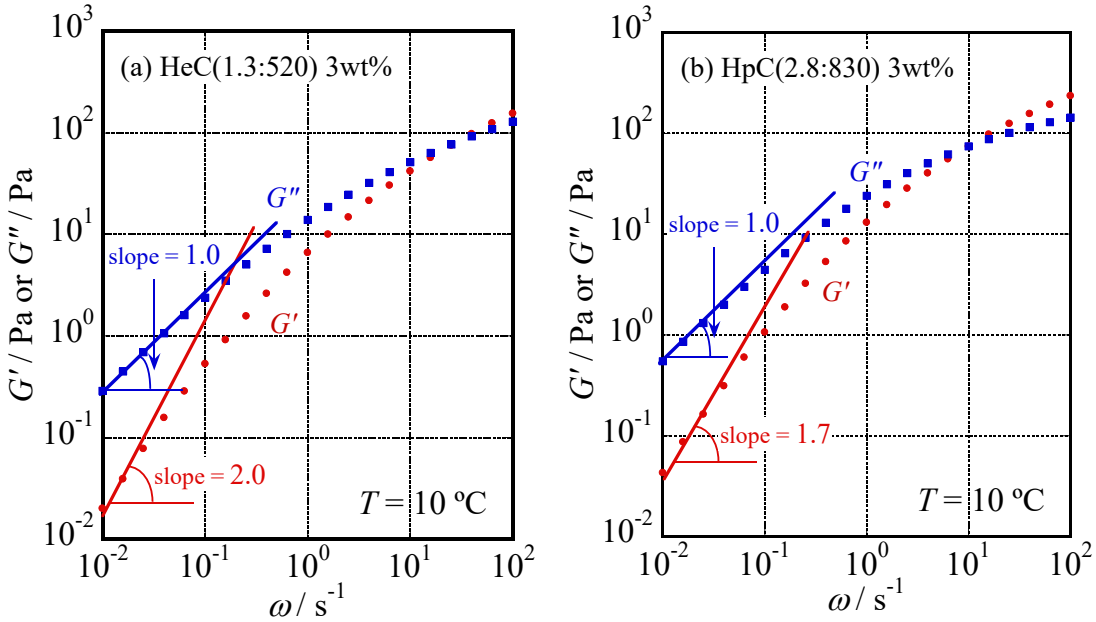

Figure 4.1 Angular frequency, ω, dependence of storage and loss modulus, G' and G'', for aqueous solutions of HeC(1.3:520) (a) and HpC(2.8:830) (b) at c = 3 wt% and T = 10 ºC.

4.3.2 Temperature Dependence of Viscoelastic Behavior for Aqueous Solution of HpC

In the Chapter 2, it is reported that the temperature dependence of dehydration behavior and

the critical hydration number for HpC in aqueous solution differ from that for methyl cellulose, MC, and hydroxypropylmethyl cellulose, HpMC, in aqueous solution. Then, in order to clarify the gelation mechanism of aqueous HpC solution, the T dependence of G' and G'' for an aqueous solution of HpC was investigated over a T range from 10 ºC up to the observed cloud point. Figure 4.2 shows dynamic viscoelastic behavior for the aqueous solution of HpC(2.8:830) at 3 wt% in a T range from 10 to 48 ºC. Although the flowing behavior of the aqueous HpC(2.8:830) solution was not able to be observed at T = 10 ºC, the flowing behavior was observed at T = 30 ºC. This observation suggests that all HpC molecules in aqueous solution in a lower temperature range, $T \leq 30$ ºC, are in the relaxed state in the low frequency range and do not form a network structure. I speculate that this is because the hydration number of HpC is much larger than that of MC and HpMC in the low T range as described in Chapter 2. However, a shoulder of G' is observed in a high temperature range, $T > 40$ ºC, i.e., the aqueous HpC system forms a network structure in the T range. Finally, the aqueous HpC solution showed a cloud point at T = 47 ºC.

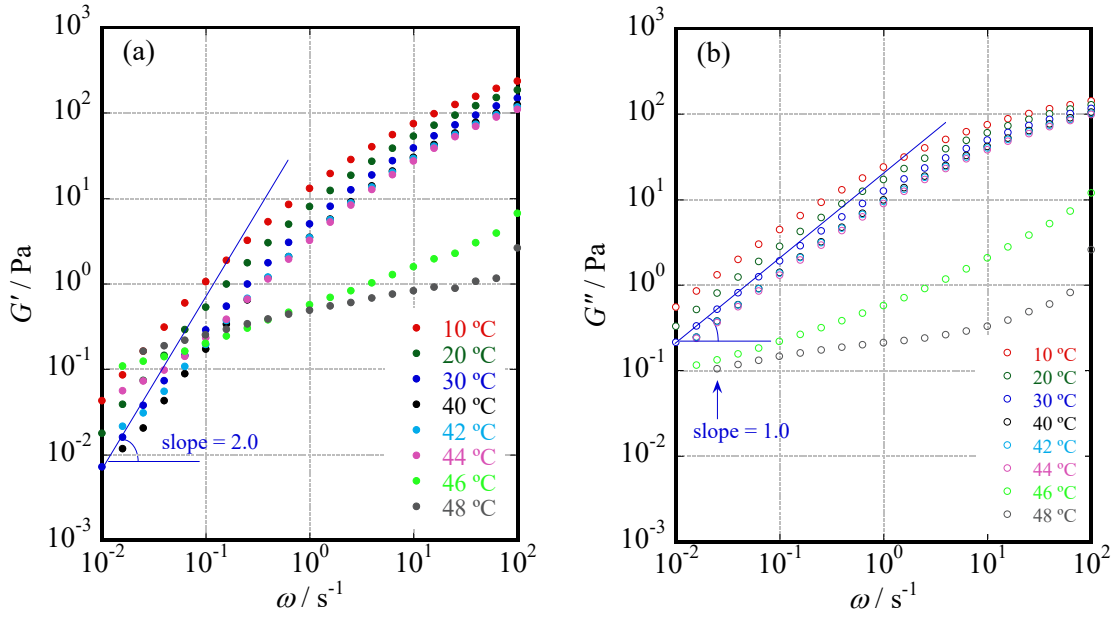

Figure 4.2 Temperature, T, dependence of storage modulus G' (a) and loss modulus G'' (b) as function of ω for an aqueous solution of HpC(2.8:830) obtained at c = 3 wt% over a temperature range from 10 to 48 ºC.

Here, we tried to apply the time-temperature superposition principle to the obtained viscoelastic spectra for the aqueous solution of HpC(2.8:830) seen in Figure 4.2 to discuss the T dependence of viscoelastic behavior in more detail. The superposition procedure was applied to both G' and G'' curves taking the data of 10 ºC as the standards. Figure 4.3 shows the obtained master curves of G' and G'' for the solution. The horizontal (ω axis) shift factor and the vertical (modulus axis) shift factor are defined as a_T and b_T, respectively. The time-temperature superposition works well in the data of the aqueous HpC solution especially in a high-frequency (fast mode) range in a temperature range from 10 to 44 ºC. Figure 4.4(a) shows the dependence of a_T on the reciprocal of temperature, T^{-1}, necessary to obtain the master curves in Figure 4.3 in a T range from 10 to 44 ºC. The obtained T dependence of a_T in a T range from 10 to 40 ºC showed Arrhenius type one. The activation energy of the fast mode in the temperature range, E_f*, was evaluated from the slope of a solid line in Figure 4.4(a) to be E_f* = 32.7 kJ mol^{-1}. However, there exists a break point in the slope of a_T data at T = 40 ºC where a shoulder in G' is observed. These observations suggest that the relaxation mechanism of the aqueous HpC solution above 40 ºC alters from that in a lower T range. The slope of a dotted line for a_T data in a high temperature range from 40 to 44 ºC provides the activation energy of the fast mode, E_{fH}*, of 12 kJ mol^{-1}. The E_{fH}* value is much smaller than the value of E_f* in a low temperature range and close to the activation energy of viscosity of pure water, E_w*, calculated to be E_w* = 15.4 kJ mol^{-1} by using viscosity data of water.[11] It is likely that the intermolecular interactions between HpC molecule and water molecule decrease with increasing T. The hydration number of HpC decreases with increasing T as discussed in Chapter 2. Moreover, it is reported that the HpC molecules in aqueous solution demonstrate coil-to-globule transition with increasing T.[3] Consequently, the activation energy of relaxation time for HpC molecules would decrease in a high temperature range from 40 to 44 ºC.

A vertical shift factor b_T was also necessary to obtain the master curves of G' and G'' for the aqueous HpC(2.8:830) solution. Figure 4.4(b) shows T dependence of the reciprocal value of b_T in a

T range from 10 to 44 ºC in which the superposition worked well. The vertical shift factor b_T was not necessary in a T range from T = 10 to 40 ºC where all HpC molecules in the system do not form a network structure but behave simply as entangled polymer chains. However, the b_T^{-1} value decreased steeply with increasing T above 40 ºC. This observation strongly suggests that the HpC molecules in aqueous solution begin to form a network structure rapidly above T = 40 ºC.

Although the HpC molecules in aqueous system do not form a network structure in a T range from 10 to 40 ºC, a distinct shoulder of G' is clearly observed above 40 ºC. The magnitude of the shoulder increased with increasing T as observed in aqueous HpMC(0.15:1.8:300) and MC(1.8:300) solutions as described in Section 3.4.2. However, the shoulder of G' for aqueous HpC systems grows much rapidly with increasing T than that for HpMC and MC. The aqueous HpC solution shows a cloud point at 47 ºC. Finally, the plateaus in G' data show weak frequency dependence and dominate the viscoelastic behavior ($G' > G''$) over a wide frequency range at T = 48 ºC. Then, the aqueous HpC solution demonstrates gel like behavior at the temperature. However, the strength of the gel for the aqueous HpC solution at 3 wt% does not strengthen with increasing T as the case of aqueous MC and HpMC solutions at 3 wt% as discussed in Chapter 3. The chain length of substitution groups of HpC, hydroxypropyl groups, are longer than that of MC, methyl groups, and HpMC, mainly substituted by methyl groups. Then, the distance between HpC chains is longer than MC and HpMC, and the HpC molecules cannot form rigid bundles. Consequently, the aqueous HpC solution cannot form a strong network structure with increasing T.

In order to clarify the gelation mechanism of aqueous HpC solution in detail, I investigated the T dependence of G' and G'' for an aqueous solution of HpC around gelation temperature. Figure 4.5 shows dynamic viscoelastic behavior for the aqueous solution of HpC(2.8:830) at 3 wt% in a T range from 45 to 48 ºC. The magnitude of the shoulder for G', which is observed in a low frequency range at 45 ºC, strengthens with increasing T as seen in Figure 4.5(a). Simultaneously, G' and G'' in a high frequency range remarkably decreased. Finally, the aqueous HpC solution turns to a gel at 47

ºC as seen in Figure 4.5(b). Although the shoulders of G' observed in a low frequency range for aqueous solutions of MC and HpMC exceed G'' values at temperatures lower than that showing gelation behavior as described in Chapter 3, the shoulder of G' for aqueous HpC solution never exceeds G'' until showing gelation behavior. Moreover, the aqueous HpC solution shows the critical gel behavior, G' and $G'' \propto \omega^n$,[6] at 46 ºC as seen in Figure 4.5(b). The exponent, n, for the frequency dependence of G' and G'' at 46 ºC is ~ 0.47 as seen in a dotted line in Figure 4.5(b). This observed critical gel behavior suggests that the sizes of HpC associations formed in aqueous solution are ranged from smallest HpC molecules to infinitely large clusters. Then, the cooperativity of molecular association in the aqueous HpC system during the gelation process is much lower than that in aqueous MC and HpMC systems as discussed in Chapter 3. Consequently, it is concluded that the gelation mechanism of aqueous HpC solutions is essentially different from that of aqueous solutions of MC and HpMC.

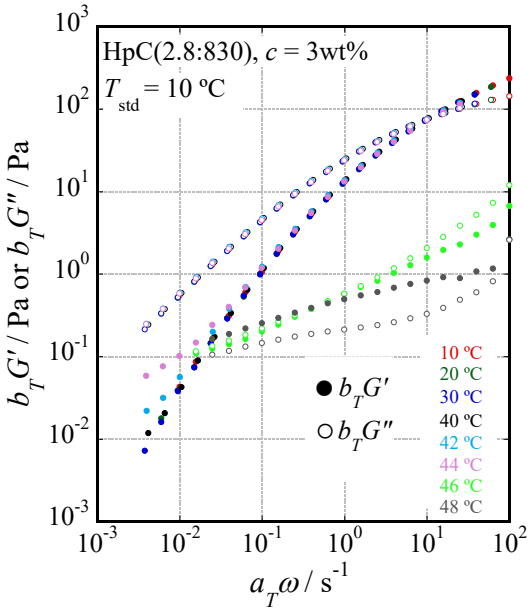

Figure 4.3 Master curves of G' and G'' for an aqueous solution of HpC(2.8:830) at c = 3 wt% obtained by shifting data along both frequency and modulus axes taking the data at T = 10 ºC as the standards.

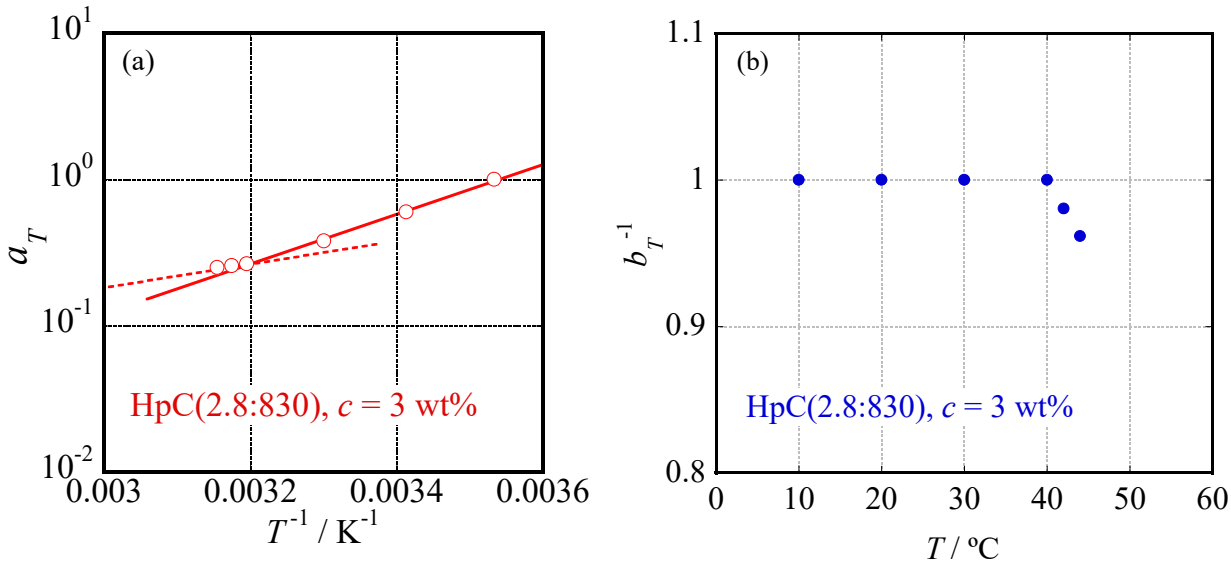

Figure 4.4 The reciprocal of temperature, T^{-1}, dependence of a_T (a) and temperature, T, dependence of the reciprocal of the vertical shift factor, b_T^{-1}, (b) for an aqueous solution of HpC(2.8:830) at c = 3.0 wt%.

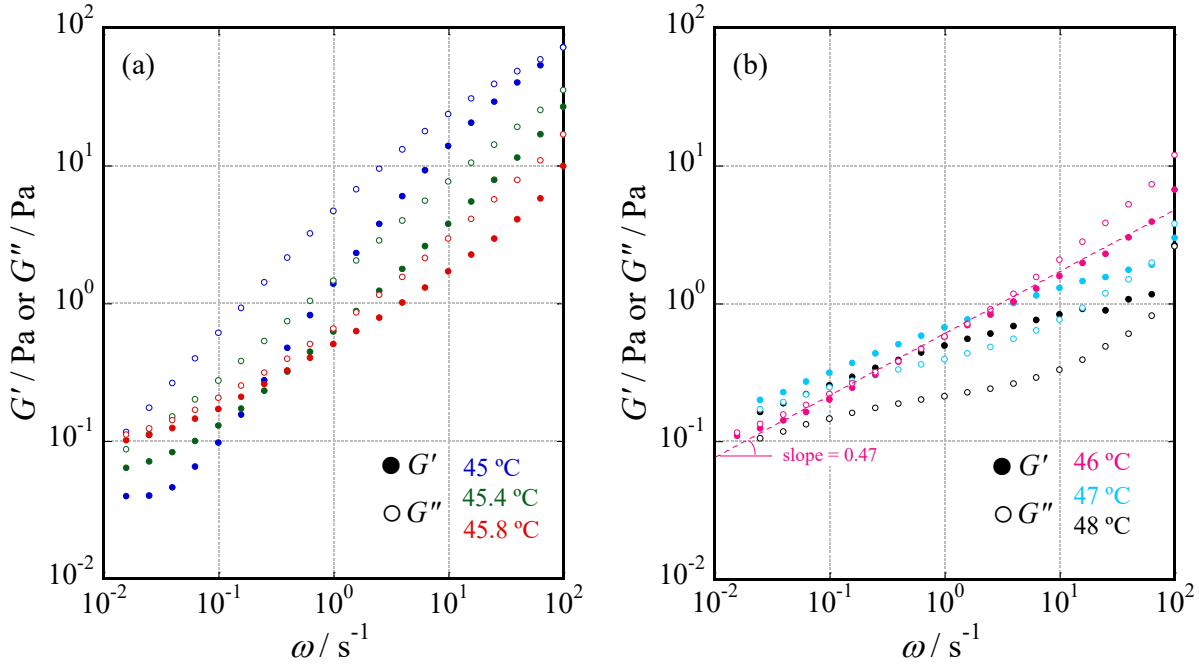

Figure 4.5 Temperature, T, dependence of G' and G'' as function of ω for an aqueous solution of HpC(2.8:830) obtained at c = 3 wt% in a T range from 45 to 45.8 ºC (a) and 46 to 48 ºC (b). The slope of dotted line, 0.47, shows an exponent for the ω dependence of G' and G'' at 46 ºC.

4.3.3 Temperature Dependence of Viscoelastic Behavior for Aqueous Solution of HeC

The aqueous HeC solution showed the typical flowing behavior in a low-frequency range at T = 10 ºC as seen in the Section 4.3.1. It is reported that the HeC samples keep high water solubility over a wide temperature range even at a high temperature.[7] However, the HeC samples in aqueous solution also clearly show dehydration behavior with increasing T as discussed in Chapter 2. The T dependence of G' and G'' for HeC in aqueous solution was investigated over a wide T range from 10 to 70 ºC. Figure 4.6 shows the ω dependence of G' and G'' for an aqueous solution of HeC(1.3:820) at 3 wt% in a T range from 10 to 70 ºC. The flowing behavior of the aqueous HeC(1.3:820) solution cannot be observed clearly even at 10 ºC due to a limitation of measurable frequency. The frequency range covered by my measuring system was not enough low to observe the flowing behavior directly in the examined aqueous HeC solution. However, it is likely that the HeC(1.3:820) chains in aqueous systems are in the relaxed state in a lower frequency range at 10 ºC similar to the HeC(1.3:520) chains as observed in Figure 4.1(a), because the hydration behavior of the HeC molecules is essentially controlled by the substituent condition of HeC as discussed in Chapter 2. Then, the viscoelastic data of the aqueous HeC(1.3:820) solution demonstrate that all HeC chains in the aqueous system behave as simply entangled chains in a temperature range, $T \leq 40$ ºC. However, a shoulder of G' is observed in a high temperature range, $T > 40$ ºC, i.e., the aqueous HeC system forms a network structure in the temperature range. The magnitude of the shoulder increased with increasing T.

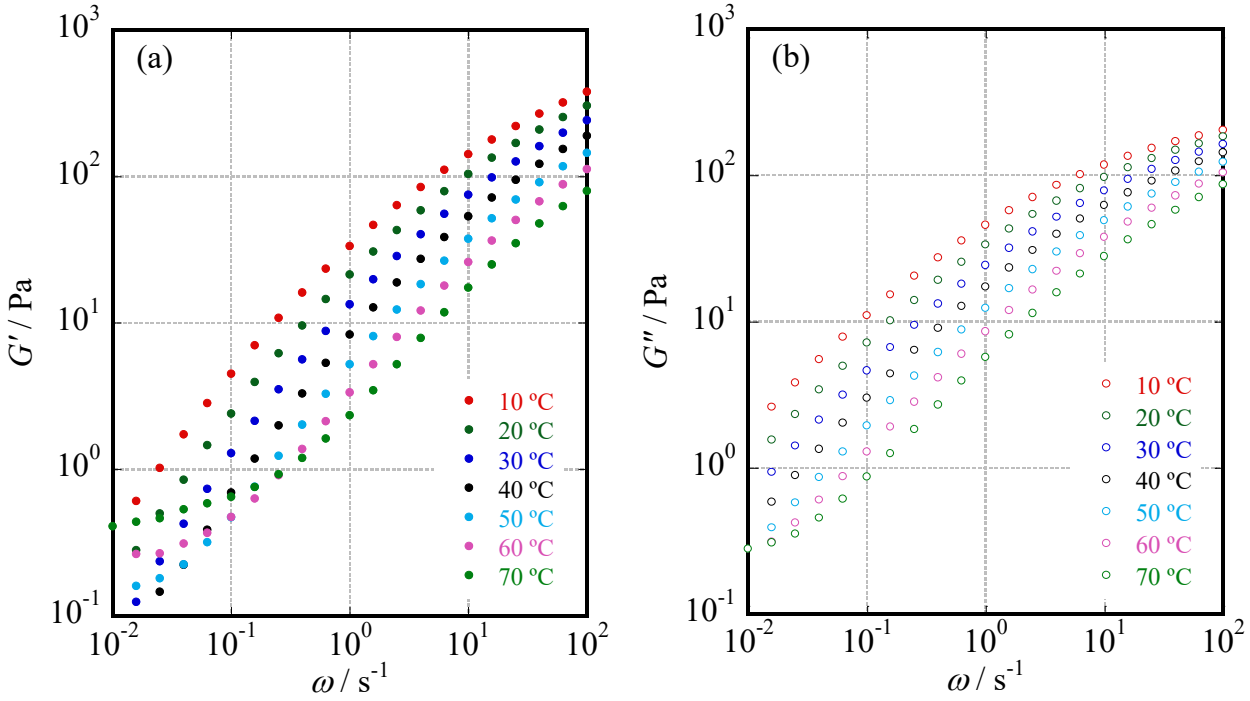

Figure 4.6 Temperature, T, dependence of storage modulus G' (a) and loss modulus G'' (b) obtained by frequency sweep experiments for an aqueous solution of HeC(1.3:820) at c = 3 wt% over a temperature range from 10 to 70 ºC.

In order to discuss the temperature dependence of viscoelastic behavior observed in Figure 4.6 in detail, I tried to apply the time-temperature superposition principle to the frequency, ω, dependence of G' and G'' for an aqueous solution of HeC(1.3:820) seen in Figure 4.6. Figure 4.7 shows the master curves of G' and G'' for the HeC solution obtained by using the superposition taking the data of 10 ºC as the standards. The time-temperature superposition worked well in the data for the aqueous HeC solution especially in a high-frequency (fast mode) region in a T range from 10 to 70 ºC. Figure 4.8(a) shows the dependence of the horizontal shift factor a_T on the reciprocal of temperature, T^{-1}, necessary to obtain the master curves in Figure 4.7 for the aqueous solution of HeC(1.3:820) at c = 3 wt% in a T range from 10 to 70 ºC. The obtained T dependence of a_T showed Arrhenius type one. The activation energy of the fast mode, E_f*, was evaluated from the slope of a straight line in Figure 4.8(a) to be E_f* = 40.7 kJ mol^{-1}. The E_f* value is substantially larger than the

value of E_w*, ca. 15 kJ mol^{-1}, and E_m * of aqueous HpMC system, ca. 24 kJ mol^{-1}. Although, the substitution group of HeC, hydroxyethyl group, bears hydroxy group, the main substitution group of HpMC, methyl group, does not have hydroxy group. As a result, the intermolecular hydrogen bond formation, which possesses finite lifetime, between HeC molecules is greater than that of HpMC molecules. Moreover, dehydration of the HeC samples in aqueous solution with increasing T is much weaker than that of HpMC, and the hydration number of HeC is larger than that of HpMC over all examined temperature range as discussed in Chapter 2. Then, the interaction between HeC and water molecules is stronger than that between HpMC and water molecules. Consequently, the E_f* value is larger than the values of E_w* and E_m * for HpMC.

The vertical shift factor b_T was also used to obtain the master curves of G' and G'' for the aqueous HeC(1.3:820) solution. Figure 4.8(b) shows T dependence of the reciprocal value of b_T for HeC(1.3:820) and HeC(2.0:760) in a temperature range from 10 to 70 ºC. The value of b_T^{-1} for HeC(1.3:820) kept unity in a temperature range from T = 10 to 40 ºC. This means that all HeC molecules in the aqueous system in the T range behave in the standard manner as controlled by activation energy without forming intermolecular association. Although the value of b_T^{-1} began to decrease with increasing temperature above T = 40 ºC, the decrease of b_T^{-1} for HeC(1.3:820) from 10 to 70 ºC was only ca. 0.05. Then, a small part of HeC chains forms a network structure in a high T range, but most HeC molecules in the aqueous systems behave freely in the T range similar to the HeC molecules in a low T range. The T dependence of b_T^{-1} for HeC(2.0:760) is essentially same as that of HeC(1.3:820). However, the temperature for HeC(2.0:760) where the b_T^{-1} value shows decreasing is higher than that for HeC(1.3:820) by 10 ºC. The reason for this discrepancy would be the higher hydration number of HeC(2.0:M_w/10^3) than that of HeC(1.3:M_w/10^3) as already discussed in Chapter 2.

Although it is reported that the HeC samples possess high water solubility in a wide temperature range even at a high temperature by using viscometric measurements,[7] a distinct shoulder

of G' for aqueous HeC(1.3:820) solution at 3 wt% is observed at T = 50 ºC. The strain applied to the aqueous HeC systems used in dynamic viscoelastic measurements is much smaller than that used in the steady state viscosity measurements. Thus, the shoulder in G' data can be observed without breaking the structure in the systems by using dynamic viscoelastic measurements. The strength of the shoulder of G' for aqueous HeC(1.3:820) solution increased with increasing T similar to aqueous solutions of HpMC(0.15:1.8:300) and MC(1.8:300) as discussed in Chapter 3, but an increase of the strength for the HeC solution with increasing T was much weaker than that for HpMC and MC in aqueous system. Moreover, the aqueous HeC solution never demonstrates gelation behavior even at T = 70 ºC as the aqueous HpMC and MC solution. The dehydration behavior of HeC(1.3:$M_w/10^3$) in aqueous solution with increasing T was much gentler than that of MC and HpMC as seen in Chapter 2. From these, the progress of network formation in aqueous HeC solution with increasing T is much slower than that of MC and HpMC. Therefore, the aqueous HeC solution does not demonstrate gelation behavior even at high temperatures. Figure 4.9 shows the schematic representation for the formation of network structure of HeC molecules in aqueous solution.

Figure 4.10 shows the master curves of G' and G'' for an aqueous solution of HeC(2.0:760) at c = 3 wt% obtained by using time-temperature superposition principle taking the data of 10 ºC as the standards. The mechanism of network forming for aqueous HeC(2.0:760) system is essentially same as that for the HeC(1.3:820) solution. However, the shoulder growth temperature for aqueous HeC(2.0:760) solution is higher than that for HeC(1.3:820) by 10 ºC. This is because that the hydration number of HeC(2.0:760) in aqueous solution is larger than that of HeC(1.3:820) over entire temperature range examined as discussed in Chapter 2.

As discussed in this chapter and Chapter 3, the aqueous solutions of all examined water soluble cellulose ether samples, WSCEs (MC, HpMC, HpC and HeC), have a same property of forming network structure with increasing temperature. However, the gelation mechanism of aqueous HpC solution essentially differs from that of aqueous solutions of MC and HpMC. The reason would

be that the hydrophobicity of the substitution groups for HpC is slightly higher than that of MC and HpMC. On the other hand, aqueous HeC solution does not demonstrate gelation behavior even in a high temperature range because of the gentle dehydration behavior with increasing temperature. These observations reveal that the substitution groups of WSCEs control their hydration/dehydration behavior and intermolecular interaction between WSCE molecules, and these properties determine the temperature dependent viscoelastic behavior for aqueous WSCEs systems.

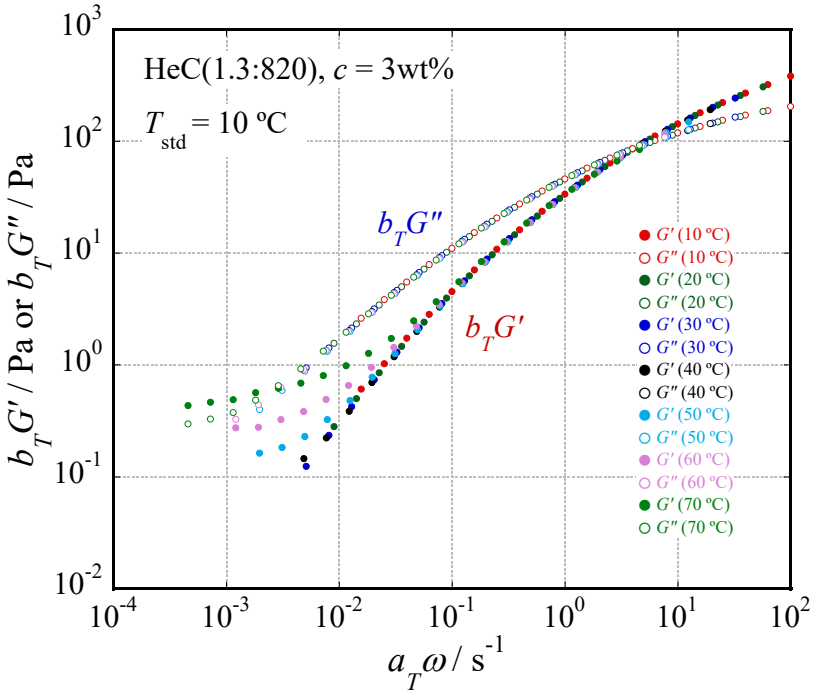

Figure 4.7 Master curves of G' and G'' for the aqueous solution of HeC(1.3:820) at c = 3 wt% obtained by shifting data along both frequency and modulus axes taking the data of HeC(1.3:820) at T = 10 ºC as the standards.

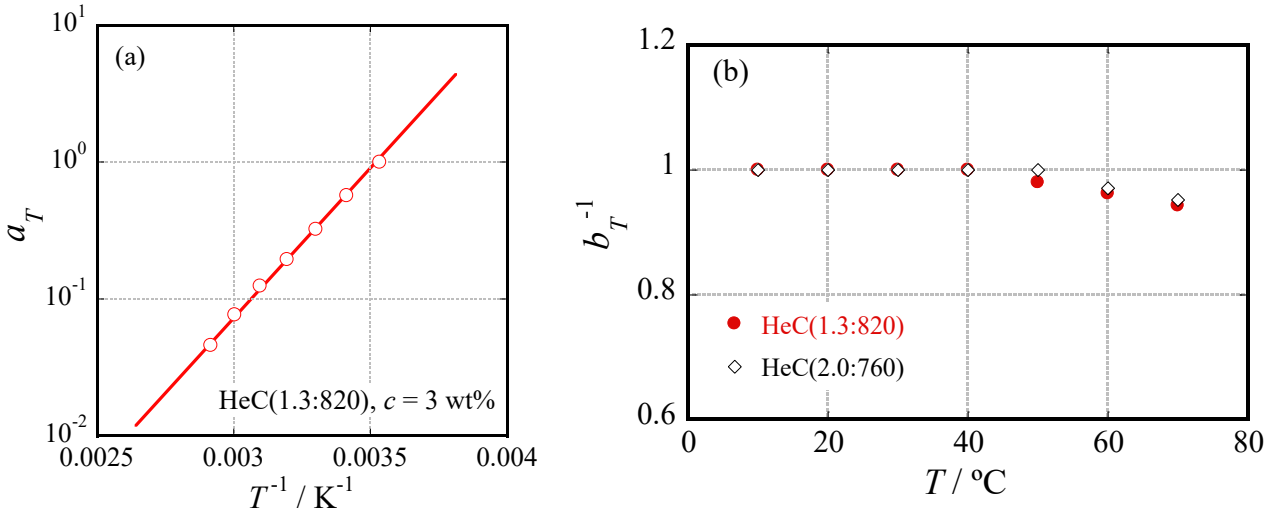

Figure 4.8 The reciprocal of temperature, T^{-1}, dependence of a_T for an aqueous solution of HeC(1.3:820) at c = 3 wt% (a), and temperature, T, dependence of the reciprocal of the vertical shift factor, b_T^{-1}, for aqueous solutions of HeC(1.3:820) and HeC(2.0:760) at c = 3 wt% (b).

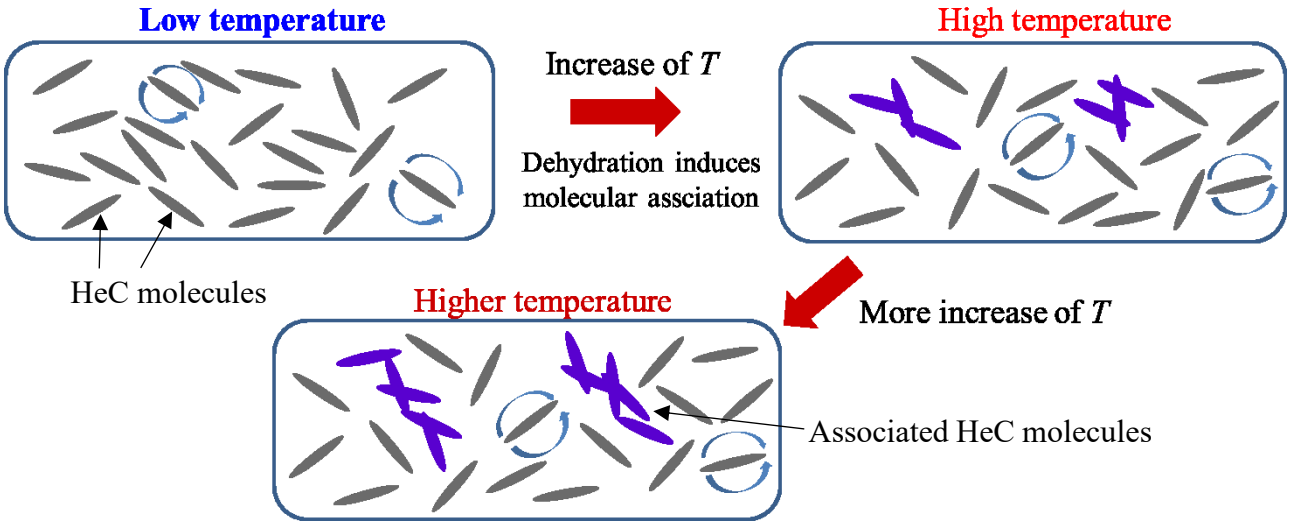

Figure 4.9 Schematic representation for the formation of a network structure in aqueous HeC systems with increasing temperature.

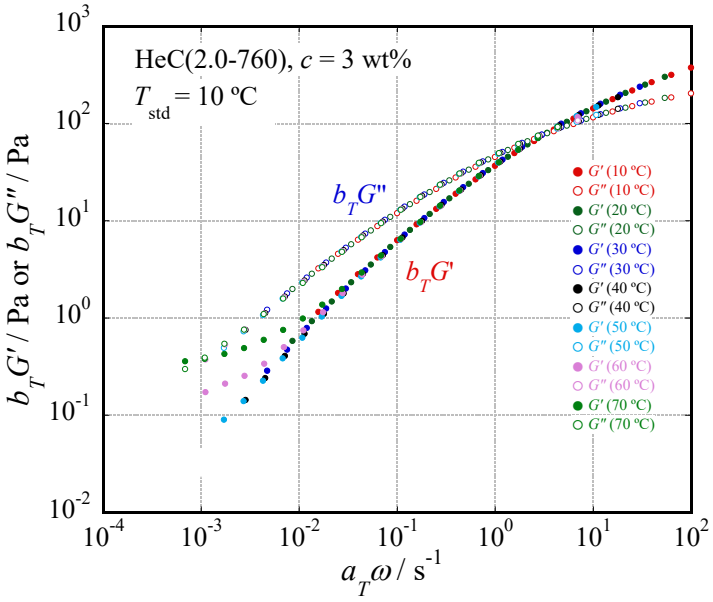

Figure 4.10 Master curves of G' and G'' for an aqueous solution of HeC(2.0:760) at c = 3 wt% obtained by shifting data along both frequency and modulus axes taking the data of HeC(2.0:760) at T = 10 ºC as the standards.

4.3.4 Origin of Viscoelasticity in Aqueous HeC Solution

Giudice et al.[9] reported that HeC molecules dissolved in aqueous solution behaved as flexible polymers. However, they examined only one kind of HeC sample (M_w ~ 600 kDa) and did not discuss the value of molecular weight between entanglement points, M_e, in their viscoelastic data. To investigate the origin of viscoelasticity of the HeC system in detail, dynamic viscoelastic measurements were performed over a wide ω range at a low temperature of T = 1 ºC where all HeC molecules in the aqueous systems behave simply as entangled polymer chains and the molecules are in the sufficiently hydrated state. Figures 4.11(a) to (e) show ω dependence of G' and G'' for an 8 wt% aqueous solution of HeC(1.3:220) and 2.5 wt% aqueous solutions of HeC(1.3:520), HeC(1.3:820), HeC(1.3:1300) and HeC(1.3:1420) at T = 1 ºC, respectively. The value of M_e can be calculated from plateau modulus, G_N, by using the equation 3-3 defined in Chapter 3.[12] In the case of

aqueous HeC solution, G_N values cannot be precisely determined because of the limitation of a measurable frequency range. The frequency range covered by our measuring system was too low to determine G_N values directly in the aqueous HeC solution examined. However, substantially accurate G_N values for the aqueous solutions of HeC(1.3:820), HeC(1.3:1300) and HeC(1.3:1420) at c = 2.5 wt% and T = 1 ºC are determined to be ca. 660, 780 and 1000 Pa, respectively.

In the case of entangled rigid rod-like particle systems, the origin of elasticity for the systems is only the rotational mode of particles dispersed in the systems. Then, the G_N values decrease with increasing molecular weight, M, in the manner of M^{-1} because the number density of the particles decreases with increasing M. On the other hand, in the case of entangled flexible polymer chain systems, the elasticity for the systems is governed by the number density of polymer chain strands which behave as elastic springs, and the weight of one polymer chain strand corresponds to the molecular weight between entanglement points, M_e. The M_e values for entangled flexible polymer chains at the same weight concentration are independent of M values of the polymer chains. Then, the G_N values for entangled flexible polymer chain systems at the same concentration condition are also independent of the value of M, i.e., $G_N \propto M^0$. If the alternation of conformation for polymer molecules from rigid rod-like particles to flexible chains occurs with increasing molecular weight, the relationship between the values of G_N and M for the entangled polymer systems would demonstrate the systematic correlation. This is because in addition to the rotational mode of particles, the polymer chain strand between two entanglement points works as an elastic spring.

In the case of aqueous HeC solution, the G_N value increases with increasing the weight and number average molecular weight, M_w and M_n, as seen in Table 4.2. This relationship reveals that the flexibility of the HeC molecules increases with increasing molecular weight. The obtained M_e values via eq. 3-3 and the ratio of M_e/M_n for the aqueous solutions of HeC(1.3:820), HeC(1.3:1300) and HeC(1.3:1420) at c = 2.5 wt% and T = 1 ºC are summarized in Table 4.2. When HeC molecules are rigid rod-like particles, the value of M obtained by using an equation $M = (3/5)cRT/G_N$ as discussed

in Chapter 3 and the ratios of M/M_n for HeC(1.3:820), HeC(1.3:1300) and HeC(1.3:1420) in aqueous solution are evaluated as summarized in Table 4.2. In the case of HeC(1.3:820), although the estimated value M (= 5.16 × 10^4 g mol^{-1}) is less than M_w (= 8.2 × 10^5 g mol^{-1}) or M_n (= 2.1 × 10^5 g mol^{-1}), the ratio of M/M_n = 0.25 is too large to conclude that the origin of elasticity in the aqueous HeC(1.3:820) systems is the entanglement between flexible chains. On the other hand, the estimated values of M and M_e is much less than M_w and M_n for HeC(1.3:1300) and HeC(1.3:1420) as seen in Table 4.2. These results suggest that the origin of elasticity in the aqueous HeC(1.3:1300) and HeC(1.3:1420) systems is the entanglement between flexible chains. To discuss the origin of elasticity for HeC more precisely, it is quite helpful to use HeC samples with a monodisperse ($M_w/M_n \sim 1$) molecular weight distribution.

In the Section 3.3.5, the M_e values of HpMC in aqueous systems are evaluated by using eq. 3-4. However, the reciprocal value of steady state compliance, J_e^{-1}, for aqueous HeC solutions cannot be determined because the frequency range where the solutions demonstrate $G' \propto \omega^2$ and $G'' \propto \omega$ is too low to observe directly except for aqueous solutions of HeC(1.3:220) and HeC(1.3:520). Then, I use the next equation 4-1 instead of eq. 3-4:

$$M_e^* = \frac{cRT}{G_{cross}} \qquad (4\text{-}1)$$

where G_{cross} means the value at a crossing point of G' and G'' as seen in Figure 4.11. Equation 4-1 is employed to evaluate the value of M_e^* for HeC in aqueous solution as a characteristic parameter in the unit of [g mol^{-1}] in this study. The determined M_e^* values for each sample are summarized in Table 4.2. The ratio of M_e^*/M_w for HeC(1.3:220) and HeC(1.3:520) demonstrates little dependence on M_w as seen in Table 4.2. This observation means that the M_e^* values for HeC(1.3:220) and HeC(1.3:520) depend on the M_w. Then, the origin of elasticity in the aqueous HeC(1.3:220) and HeC(1.3:520) systems is not the entanglement between flexible chains similarly to the aqueous HpMC systems as discussed in Chapter 3. Although the M_e^* values for aqueous HeC(1.3:520) and

HeC(1.3:820) solutions at 2.5 wt% slightly increase with increasing M_w, the values for aqueous solutions of HeC in a high M_w range, $M_w \geq 820 \times 10^3$, at 2.5 wt% decrease with increasing M_w as seen in Table 4.2. Then, the values of G_{cross} for aqueous solutions of HeC in the high M_w range increase with increasing M_w. The reason for this increase in the G_{cross} would be the transition of conformation for polymer chains from rigid rod-like particles to flexible polymer chains with increasing M_w as discussed above. Consequently, the molecular weight dependence of M_e* values suggests that although the HeC molecules in aqueous solution possess high rigidity in the low M_w range, $M_w \leq 520 \times 10^3$, the flexibility of the HeC molecules in the high M_w range, $M_w \geq 820 \times 10^3$, increases with increasing molecular weight.

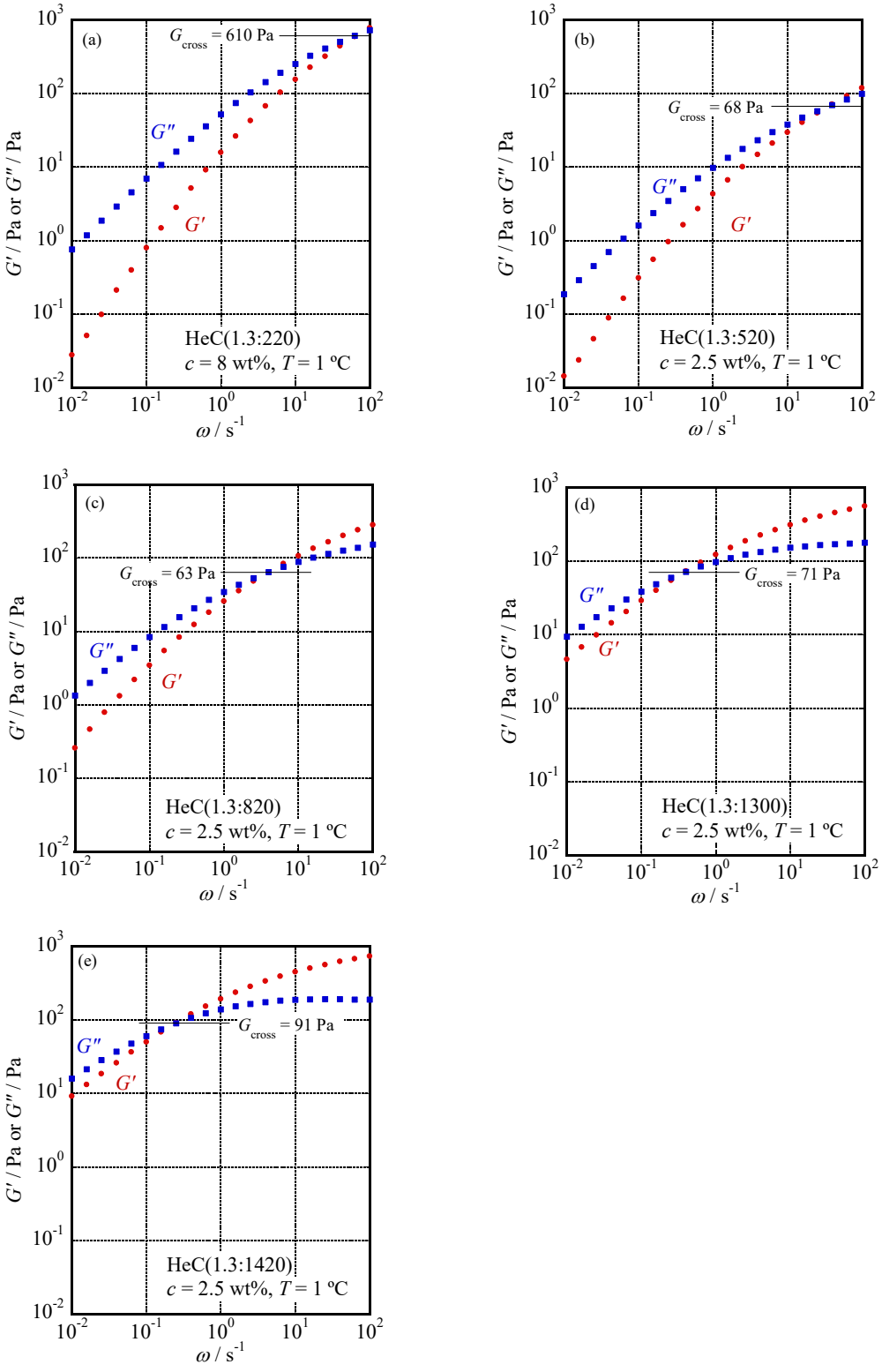

Figure 4.11 Angular frequency, ω, dependence of G' and G'' for an aqueous solution of HeC(1.3:220) (a) at c = 8 wt% and T = 1 ºC and aqueous solutions of HeC(1.3:520) (b), HeC(1.3:820) (c), HeC(1.3:1300) (d) and HeC(1.3:1420) (e) at c = 2.5 wt% and T = 1 ºC.

Table 4.2 Characteristic values for HeC samples in aqueous soltuion.

Samples	c [g/100 mL]	G_N [Pa]	G_{cross} [Pa]	M_e [g/mol]	M [g/mol]	M_e* [g/mol]	M_w [g/mol]	M_n [g/mol]	M_e/M_n	M/M_n	M_e*/M_w
HeC(1.3:220)	8	–	610	–	–	300000	220000	81000	–	–	1.4
HeC(1.3:520)	2.5	–	68	–	–	840000	520000	112000	–	–	1.6
HeC(1.3:820)	2.5	660	63	86000	51600	900000	820000	210000	0.41	0.25	1.1
HeC(1.3:1300)	2.5	780	71	73000	43800	800000	1300000	550000	0.13	0.08	0.6
HeC(1.3:1420)	2.5	1000	91	57000	34200	630000	1420000	630000	0.09	0.05	0.44

4.3.5 Concentration and Molecular Weight Dependence of Viscoelastic Behavior for Aqueous HeC Solution

To clarify the conformation of HeC molecules dissolved in aqueous solution, concentration and molecular weight dependence of viscoelastic behavior for aqueous HeC systems was investigated. In the previous section, the values of M_e, M and M_e* for HeC in aqueous systems suggest that the flexibility of HeC molecules increases with increasing their molecular weight. Then, I divided the molecular weight range into two region, $M_w \leq 820 \times 10^3$ (a) and $M_w > 820 \times 10^3$ (b). Firstly, viscoelastic behavior for aqueous HeC solutions in region (a) is discussed. Figure 4.12 shows ω dependence of G' and G'' for aqueous HeC(1.3:820) solutions at 4 kinds of concentrations at 1 ºC: c = 1.5, 2, 2.5 and 3 wt%. To discuss the c dependence of viscoelastic behavior for the system, I assume the time-concentration superposition principle on the ω dependence of G' and G'' data at different concentrations. Figure 4.13 shows the master curves for G' and G'' of the HeC solution obtained by using the superposition taking the data of 3 wt% as standards. The horizontal and vertical shift factor are a_c and b_c, respectively, which are necessary to perform the superposition. The superposition worked well in the aqueous HeC solution over all c range examined in this study. The obtained power laws of c dependence of a_c and b_c for HeC(1.3:820) are $a_c \propto 3.2$ and $b_c \propto -1.4$, respectively. Therefore, the relationship between τ_w and c is given as $\tau_w \propto c^{3.2}$, and the relationship between J_e^{-1} and c as $J_e^{-1} \propto c^{1.4}$.

The time-concentration superposition principle was also applied to aqueous solutions of HeC(1.3:220) and HeC(1.3:520) at T = 1 ºC. Figure 4.14 shows the master curves for G' and G'' of aqueous HeC(1.3:220) and HeC(1.3:520) solutions obtained by using the superposition. The superposition worked well in these HeC samples over all c range examined in this study. Table 4.3 summarizes c dependence of exponents for τ_w and J_e^{-1} in these HeC(1.3:M_w/10^3) samples in the region (a), $M_w \leq 820 \times 10^3$. The obtained exponents for c dependence of τ_w for HeC(1.3:M_w/10^3) samples were approximately 3.2 irrespective of the M_w value. On the other hand, the obtained exponents for

c dependence of J_e^{-1} increased from 1.1 to 1.4 with increasing M_w.

In the case of entangled flexible polymer chains system, concentration dependence of τ_w and J_e^{-1} are theoretically predicted as $\tau_w \propto c^{1.5}$ and $J_e^{-1} \propto c^{9/4}$, and the relationship $\tau_w \propto c^{b-2}$ and $J_e^{-1} \propto c^2$ (the value of b is dependent on polymer species) has been experimentally confirmed.[12,13] On the other hand, concentration dependence of τ_w and J_e^{-1} for entangled rigid rod-like particles is theoretically predicted as $\tau_w \propto c^2$ and $J_e^{-1} \propto c^1$.[12] In addition, Morse theoretically predicted that c dependence of J_e^{-1} for entangled semiflexible polymers is given as $J_e^{-1} \propto c^{1.33}$ or $c^{1.4}$.[14] The obtained c dependence of J_e^{-1} for HeC in aqueous solution, 1.1 – 1.4, are closer to theoretically predicted power laws for rigid rod-like particles, $J_e^{-1} \propto c^1$, and for entangled semiflexible polymers, $J_e^{-1} \propto c^{1.33}$ or $c^{1.4}$, than an experimentally confirmed power law for entangled flexible polymer chains, $J_e^{-1} \propto c^{9/4}$. In the case of HeC(1.3:220), the obtained exponent for c dependence of J_e^{-1}, 1.1, is quite close to the theoretically predicted exponent for rigid rod-like particles. Moreover, the obtained power number for HeC(1.3:820), 1.4, is very close to Morse's prediction for entangled semiflexible polymers. These results strongly suggest that the conformation of HeC(1.3:$M_w/10^3$) in aqueous solution depends on its molecular weight even in a low molecular weight range (a), $M_w \leq 820 \times 10^3$.

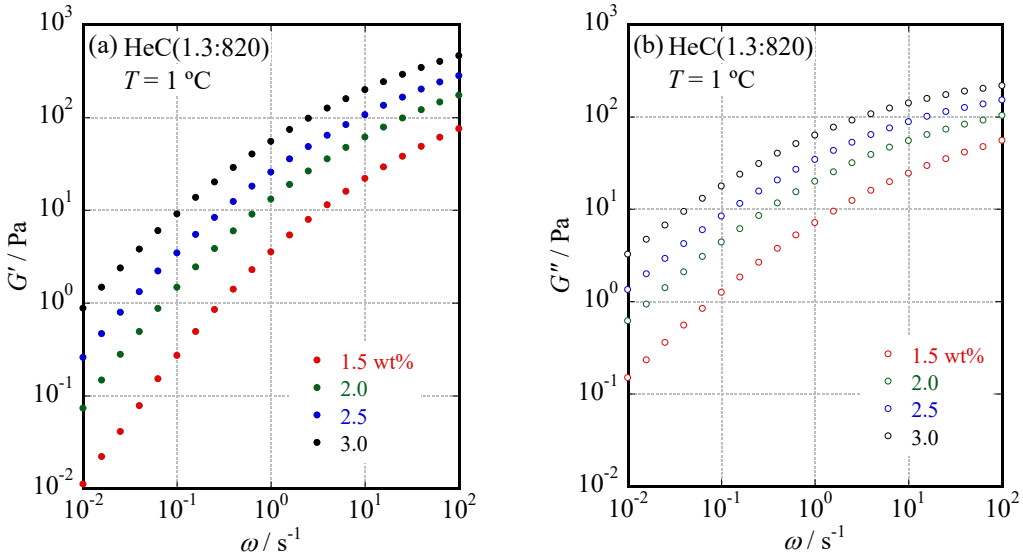

Figure 4.12 Concentration, c, dependence of storage modulus, G', (a) and loss modulus, G'', (b) obtained in an ω range from 10^{-2} to 10^2 s^{-1} for aqueous solutions of HeC(1.3:820) at T = 1 °C at several concentrations ranged from 1.5 to 3 wt%.

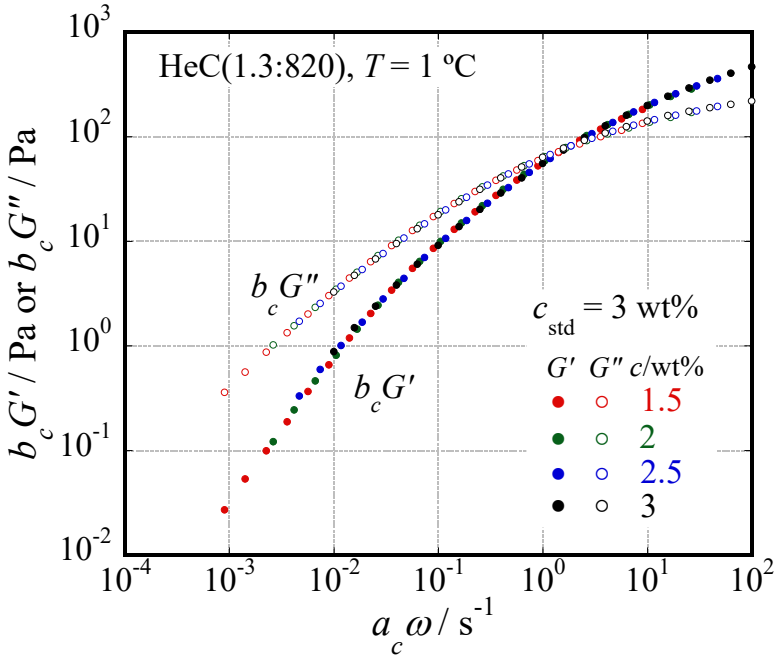

Figure 4.13 Master curves of G' and G'' for aqueous solutions of HeC(1.3:820) at $T = 1$ ºC obtained by using time-concentration superposition principle taking the data of HeC(1.3:820) at $c = 3$wt% as the standards. The horizontal and vertical shift factors are a_c and b_c, respectively.

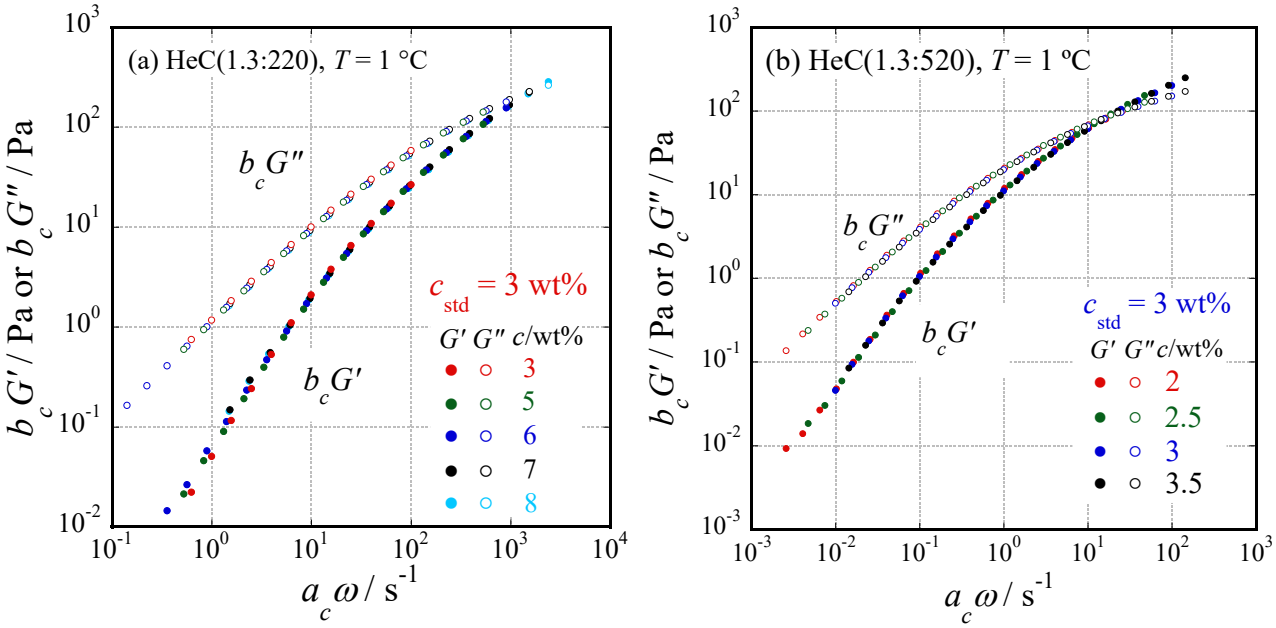

Figure 4.14 Master curves of G' and G'' for aqueous solutions of HeC(1.3:220) (a) and HeC(1.3:520) (b) at $T = 1$ ºC obtained by using the time-concentration superposition principle taking the data of $c = 3$ wt% as the standards.

Table 4.3 Exponent numbers, n and m, of the concentration, c, for the average relaxation time, τ_w ($\propto c^n$), and the average modulus, J_e^{-1} ($\propto c^m$), for HeC(1.3:$M_w/10^3$).

Samples	n	m
HeC(1.3:220)	3.2	1.1
HeC(1.3:520)	3.2	1.2
HeC(1.3:820)	3.3	1.4

Figure 4.15 shows other master curves of G' and G'' for aqueous solutions of HeC(1.3:220), HeC(1.3:520) and HeC(1.3:820) at T = 1 ºC obtained by using the time-concentration and time-molecular weight superposition principles taking the data of HeC(1.3:820) at c = 3 wt% as the standards. The horizontal and vertical shift factors are termed a_M and b_M, respectively. The time-concentration and also time-molecular weight superpositions worked well in the aqueous HeC solutions over entire molecular weight range examined, $220 \times 10^3 \leq M_w \leq 820 \times 10^3$ except for the data in a frequency range lower than $a_c a_M \omega \sim 10^{-3}$. The reason for the deviation from the superposition of the data in the frequency range would be the difference between the molecular weight distribution (M_w/M_n) in HeC(1.3:220), HeC(1.3:520) and HeC(1.3:820). The determined M_w/M_n values of HeC(1.3:220), HeC(1.3:520) and HeC(1.3:820) are 2.67, 4.67 and 3.95, respectively, by using the gel permeation chromatography (GPC) measurements. It is likely that the increase of M_w/M_n value leads to broader spectra of dynamic viscoelasticity (the ω dependence of G' and G'') due to a wider distribution of relaxation times. In fact, the agreement of the master curves for the data of HeC(1.3:520) and HeC(1.3:820), which possess the similar M_w/M_n value, obtained by using the superposition is rather well over all ω range examined in this study. However, the deviation from the superposition of the data in the low frequency range is quite little, and the superposition substantially worked well in the aqueous HeC solutions over entire molecular weight and frequency range examined. To obtain the final master curves seen in Figure 4.15, I used master curves obtained by

using the time-concentration superposition as seen in Figures 4.13 and 4.14 taking the data of c = 3 wt% as the standards. Then, the shift factors necessary to obtain the final master curves seen in Figure 4.15 are dependent on only molecular weight of HeC molecules. Figure 4.16 shows M_w dependence of the shit factors a_M and b_M necessary to complete the superposition. I found the presence of a break point in the slopes of a_M and b_M data at $M_w = 520 \times 10^3$ particularly in M_w dependence of b_M in Figure 4.16. Then, the M_w dependence of a_M would be divided into additional two regions: $M_w \leq 520 \times 10^3$, region (a-1), and $520 \times 10^3 \leq M_w \leq 820 \times 10^3$, region (a-2), to discuss the conformation of HeC molecules in aqueous solution.

In the region (a-1), the obtained exponents for M_w dependence of a_M and b_M are 5.7 and -1.3, respectively, as seen in a solid line in Figure 4.16. Then, the relationship can be described to be $\tau_w \propto M_w^{5.7}$ and $J_e^{-1} \propto M_w^{-1.3}$. Therefore, the totally obtained dependence of τ_w and J_e^{-1} on c and M_w for HeC is given as $\tau_w \propto c^{3.2} M_w^{5.7}$ and $J_e^{-1} \propto c^{1.1\text{-}1.2} M_w^{-1.3}$. Using the number density of polymer chains ν (= c/M_w or c/M_n) in the system to describe the experimentally obtained τ_w and J_e^{-1} for HeC, the relationship $\tau_w \propto \nu^{3.2} M_w^{8.9}$ and $J_e^{-1} \propto \nu^{\sim 1.2}$ is obtained.

The M_w dependence of τ_w for HeC ($\tau_w \propto M_w^{5.7}$) is much stronger than that for entangled flexible polymer chains, $\tau_w \propto M_w^{3.4}$.[13] Moreover, although J_e^{-1} for flexible polymer chains are independent of M_w, the aqueous HeC systems show a decreasing in J_e^{-1} with increasing M_w. As discussed above, the aqueous HeC systems demonstrate that HeC molecules behave as rigid rod-like particles or semiflexible polymer chains in aqueous solution. However, the prediction by Morse does not include the dependence on molecular weight. Then, M_w dependence of J_e^{-1} cannot be discussed with the Morse's prediction. In the case of entangled rigid rod-like particles, c and M_w dependence of τ_w and J_e^{-1} are theoretically predicted as $\tau_w \propto c^2 M_w^7$ and $J_e^{-1} \propto c^1 M_w^{-1}$ or $\tau_w \propto \nu^2 M_w^9$ and $J_e^{-1} \propto \nu^1$ using ν. The obtained ν and M_w dependence of τ_w for HeC, $\tau_w \propto \nu^{3.2} M_w^{8.9}$, is close to that for entangled rigid rod-like particles, $\tau_w \propto \nu^2 M_w^9$ especially in the M_w dependence of τ_w. However, the ν dependence of τ_w for HeC is obviously stronger than that for the theoretical prediction for entangled

rigid rod-like particles. The intermolecular hydrogen bond formation between HeC molecules discussed in the Section 4.3.3 should be one of the reasons for the increase in the exponent value of the relationship. On the other hand, the obtained dependence of J_e^{-1} on ν in aqueous HeC solution, $J_e^{-1} \propto \nu^{\sim 1.2}$, is rather similar to that for rigid rod-like particles, $J_e^{-1} \propto \nu^1$. Therefore, the obtained c, ν and M_w dependence of τ_w and J_e^{-1} for HeC in aqueous solution reveals that HeC molecules in the region (a-1), $M_w \leq 520 \times 10^3$, behave as rod-like particles possessing high rigidity in aqueous solution.

In the region (a-2), $520 \times 10^3 \leq M_w \leq 820 \times 10^3$, the obtained exponents for M_w dependence of a_M and b_M are 4.7 and ca. 0, respectively, as seen in a dotted line in Figure 4.16. Then, the relationship can be described to be $\tau_w \propto M_w^{4.7}$ and $J_e^{-1} \propto M_w^{\sim 0}$. Therefore, the obtained dependence of τ_w and J_e^{-1} on c and M_w for HeC is given as $\tau_w \propto c^{3.2} M_w^{4.7}$ and $J_e^{-1} \propto c^{1.2\text{-}1.4} M_w^{\sim 0}$. As discussed above, the aqueous HeC systems demonstrate that HeC molecules belonging to the region (a-1) behave as rigid rod-like particles in aqueous solution. However, the obtained M_w dependence of J_e^{-1} show little M_w dependence, $J_e^{-1} \propto M_w^{\sim 0}$. Then, the HeC chains in the M_w region (a-2) no longer behave as rigid rod-like particles. On the other hand, although the prediction by Morse does not include the dependence on molecular weight, the c dependence of J_e^{-1} for HeC is quite close to that for semiflexible polymers predicted by Morse as discussed above.[14] In addition, the exponents of M_w dependence of τ_w for HeC decreased from 5.7 to 4.7 with increasing M_w as seen in Figure 4.16. The exponent of M_w for τ_w approaches that for experimentally confirmed flexible polymers, $\tau_w \propto M_w^{3.4}$.[13] These results propose that HeC molecules in aqueous systems cannot keep their rigidity and the flexibility of the molecules becomes pronounced with increasing M_w. Therefore, the obtained dependence of τ_w and J_e^{-1} on c and M_w for HeC in aqueous solution, $\tau_w \propto c^{3.2} M_w^{4.7}$ and $J_e^{-1} \propto c^{1.2\text{-}1.4} M_w^{\sim 0}$, reveals that HeC molecules in the region (a-2), $520 \times 10^3 \leq M_w \leq 820 \times 10^3$, possess flexibility in aqueous solution.

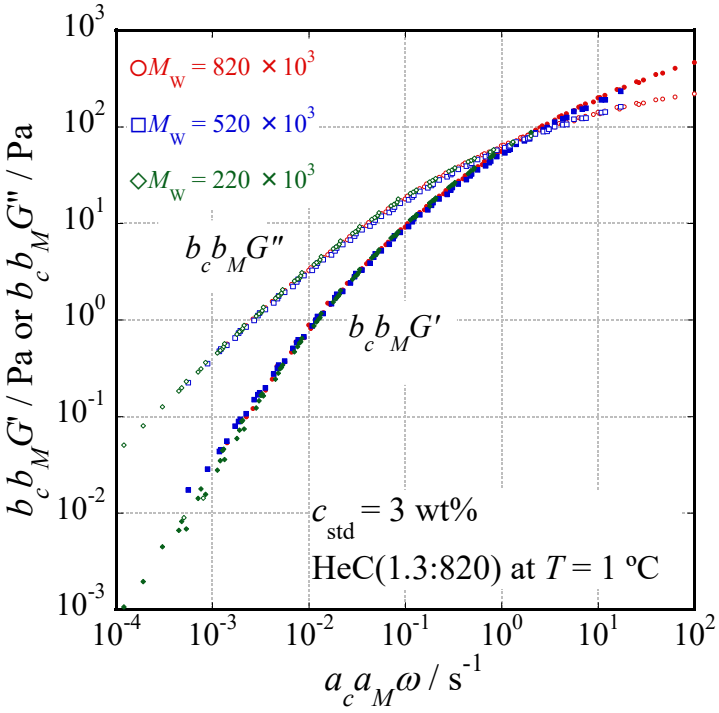

Figure 4.15 Total master curves of G' and G'' for aqueous solutions of HeC(1.3:220), HeC(1.3:520) and HeC(1.3:820) at T = 1 ºC obtained by using time-concentration and time-molecular weight superpositions taking the data of HeC(1.3:820) at c = 3 wt% as the standards.

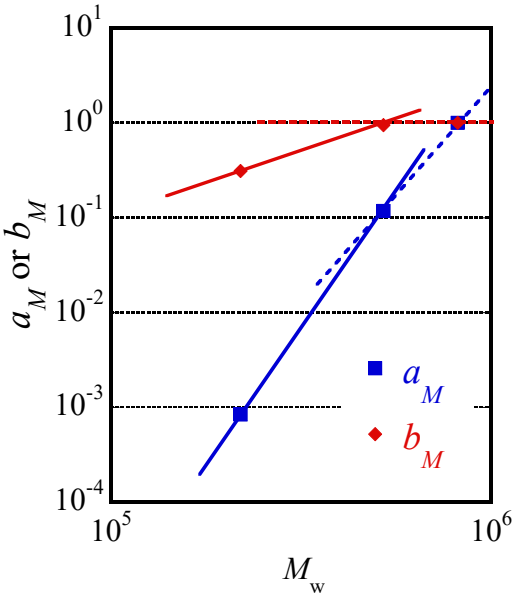

Figure 4.16 Molecular weight dependence of shit factors a_M and b_M for aqueous solutions of HeC(1.3:M_w /10^3) at T = 1 ºC taking the data of HeC(1.3:820) at c = 3 wt% as the standards.

The concentration dependence of viscoelastic behavior for aqueous HeC solutions in the high M_w region (b), $M_w \geq 1{,}300 \times 10^3$, was also investigated in detail. Figure 4.17 shows master curves of G' and G'' for aqueous solutions of HeC(1.3:1300) and HeC(1.3:1420) obtained by using time-concentration superposition. The superposition worked well in the aqueous HeC solutions over all concentration range examined in this study. The obtained exponents for c dependence of τ_w and J_e^{-1} for HeC(1.3:1300) were 2.7 and 1.6, respectively. On the other hand, the obtained exponents of c for τ_w and J_e^{-1} for HeC(1.3:1420) were 2.7 and 1.7, respectively. Figure 4.18 shows the M_w dependence of c for τ_w and J_e^{-1} for all HeC samples examined in this study. The exponents of c for J_e^{-1} of HeC(1.3:M_w /10^3) increase with increasing M_w. The dotted line meaning 2.0 in the Figure 4.18 shows the exponent of c for J_e^{-1} for experimentally confirmed entangled flexible polymer chains.[13] The obtained exponents of c for J_e^{-1} of HeC approache the exponent value, 2.0, of entangled flexible polymer chains with increasing M_w. On the other hand, the obtained power law of c for τ_w for HeC decreased from 3.2 to 2.7 with increasing M_w. Doi and Edwards[12] theoretically predicted that the power of c for τ_w as $\tau_w \propto c^{1.5}$ for entangled flexible polymers. The exponent of 1.5 is smaller than that for entangled rigid rod-like particles, $\tau_w \propto c^2$. The similar tendency would appear in the power of c for τ_w for HeC(1.3:M_w/10^3) with increasing M_w. Therefore, the obtained concentration dependence of τ_w and J_e^{-1} for aqueous HeC solutions reveals that the flexibility of HeC chains becomes pronounced with increasing M_w.

To clarify the molecular weight dependent conformation of the HeC molecules in aqueous solution, M_w dependence of viscoelastic behavior for aqueous HeC(1.3:M_w /10^3) solutions was investigated. Figure 4.19 shows the master curves of G' and G'' for aqueous solutions of HeC(1.3:520), HeC(1.3:820), HeC(1.3:1300) and HeC(1.3:1420) at c = 2 wt% and T = 1 ºC obtained by using time-molecular weight superposition taking the data of HeC(1.3:820) as the standards. The horizontal and vertical shift factors are termed a_M and b_M, respectively. The superposition worked well in the aqueous solutions of these four HeC samples. Figure 4.20 shows the obtained M_w dependence of a_M and b_M

for aqueous solutions of the HeC samples at 2 wt%. The value of b_M decreased with increasing M_w in a high molecular weight range, $M_w \geq 820 \times 10^3$. Then, the J_e^{-1} values for aqueous HeC solutions at the same weight concentration increased with increasing M_w in the M_w range. The reason for this increase in the J_e^{-1} would be the alternation of conformation for HeC chains from rigid rod-like particles to flexible polymer chains with increasing M_w as discussed in Section 4.3.4. Then, another plateau will appear in M_w dependence of b_M for the HeC molecules in a much higher M_w region in Figure 4.20 and then, the value of M_e obtained from the viscoelastic data of HeC in the high molecular weight region approaches the true value of M_e for the HeC samples in aqueous solution.

On the other hand, the obtained M_w exponents of 4.5 for τ_w of HeC in the region (b), $M_w \geq 820 \times 10^3$, are slightly smaller than the value of 4.7 in the region (a-2), $520 \times 10^3 \leq M_w \leq 820 \times 10^3$. It is likely that the power number of the M_w dependence of τ_w for HeC approaches that for experimentally obtained entangled flexible polymers, $\tau_w \propto M_w^{3.4}$,[13] with increasing M_w due to the flexibility of HeC chains. However, the decrease of the exponent for HeC with increasing M_w from 520×10^3 to 1420×10^3 was only 0.2. A difference between the exponents for HeC having high M_w, $\tau_w \propto M_w^{4.5}$, and that for entangled flexible polymers, $\tau_w \propto M_w^{3.4}$, is still large. The reason for this discrepancy would be assigned to the limitation of molecular weight resolution ability of a GPC column in a high molecular weight region used in this study. Figure 4.21 shows the molecular weight distribution profiles for HeC(1.3:1300) and HeC(1.3:1420) obtained by GPC measurements. The determined weight fraction distributions in a high molecular weight side did not show well separated profiles. As a result, the molecular weights of HeC(1.3:1300) and HeC(1.3:1420) seem to be underestimated. If the molecular weight resolution of GPC column in a high molecular weight region is improved, the true value of molecular weight for HeC(1.3:1300) and HeC(1.3:1420) will be obtained. Then, the slope of the M_w dependence of a_M seen in Figure 4.20 becomes gentle, and the exponent of M_w for τ_w of HeC having high molecular weight in aqueous systems approaches that of entangled flexible polymer chains, $\tau_w \propto M_w^{3.4}$.

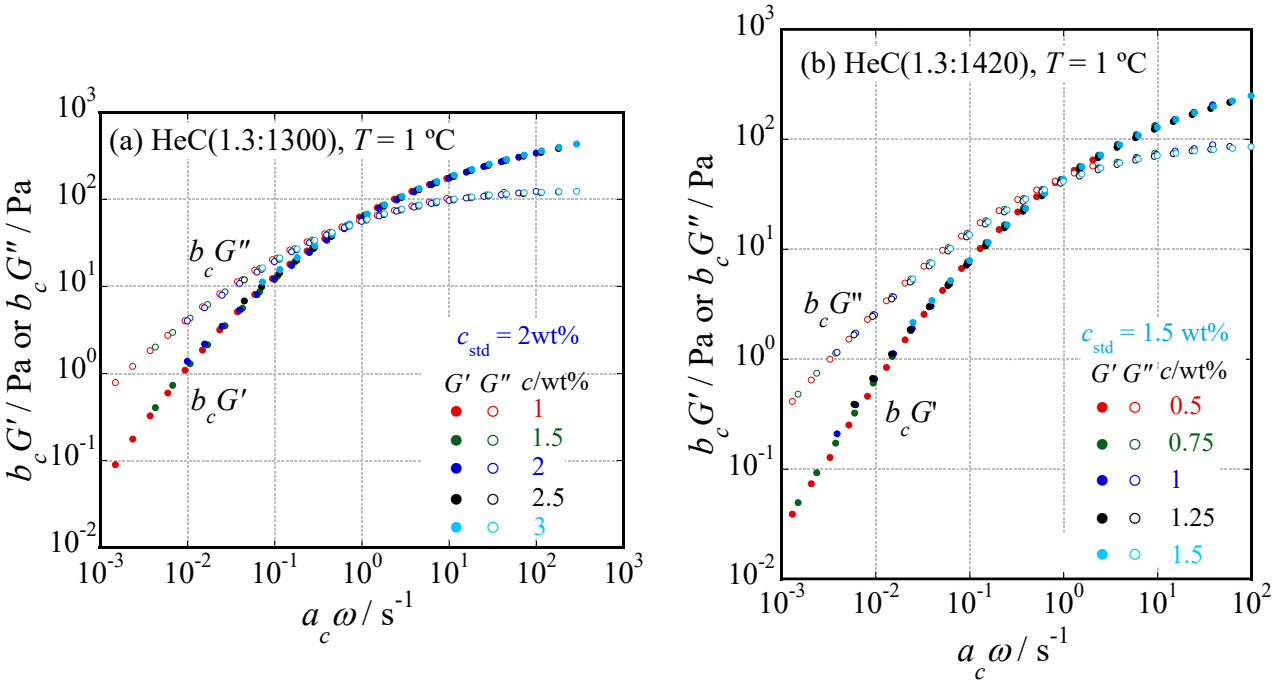

Figure 4.17 Master curves of G' and G'' for aqueous solutions of (a) HeC(1.3:1300) and (b) HeC(1.3:1420) at $T = 1$ °C obtained by shifting data along both frequency and modulus axes taking the data of $c = 2$ wt% (HeC(1.3:1300)) and 1.5 wt% (HeC(1.3:1420)) as the standards.

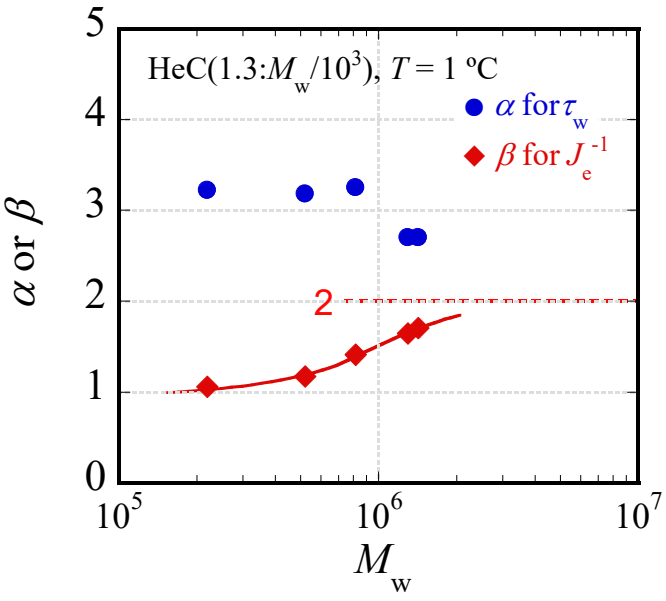

Figure 4.18 Molecular weight dependence of exponents, α and β, for the concentration dependence of relaxation time, τ_w ($\propto c^{\alpha}$), and average modulus, J_e^{-1} ($\propto c^{\beta}$), for aqueous solutions of HeC(1.3:M_w/10^3) at $T = 1$ °C.

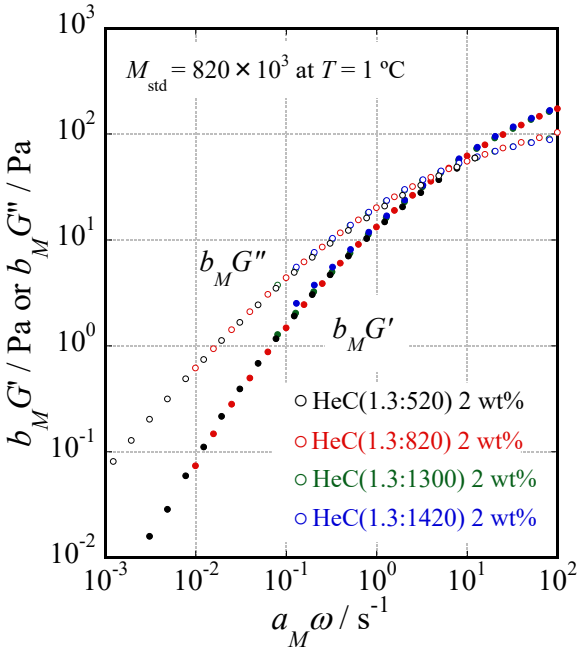

Figure 4.19 Master curves of G' and G'' for aqueous solutions of HeC(1.3:520), HeC(1.3:820), HeC(1.3:1300) and HeC(1.3:1420) at c = 2 wt% and T = 1 ºC obtained by using time-molecular weight superposition taking the data of HeC(1.3:820) at c = 2 wt% and T = 1 ºC as the standards.

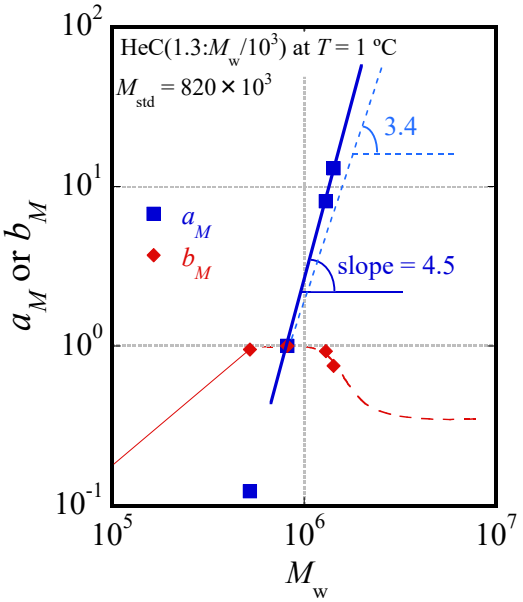

Figure 4.20 Molecular weight, M_w, dependence of the shift factors a_M and b_M for HeC(1.3:$M_w/10^3$) in aqueous solution at c = 2 wt% and T = 1 ºC obtained by time-molecular weight superposition taking the data of HeC(1.3:820) as the standards. The dashed blue line represents M_w dependence of a_M for the behavior of well-known flexible polymers.[13]

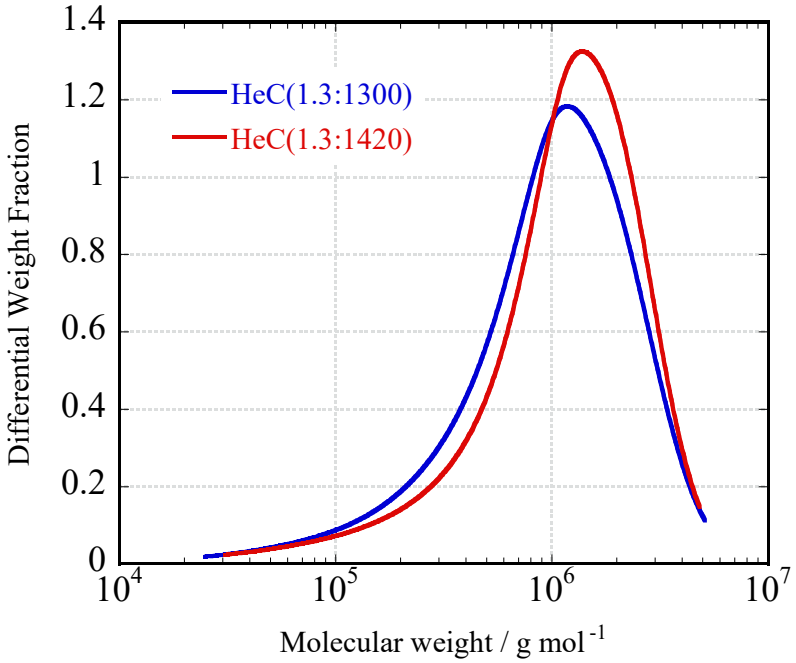

Figure 4.21 Molecular weight distribution of HeC(1.3:1300) and HeC(1.3:1420) obtained by GPC techniques.

4.3.6 Difference of Viscoelastic Behavior between Aqueous HeC Solution and Aqueous HpMC Solution

In this section, the differences of viscoelastic behavior between aqueous HeC solution and aqueous HpMC solution at low temperature will be discussed. In the previous section, concentration and molecular weight dependence of viscoelastic behavior for aqueous HeC solution demonstrated that the HeC molecules with a low molecular weight, $M_w = 220 \times 10^3$, behave as rod-like particles in aqueous system. In the Chapter 3, the viscoelastic behavior for aqueous HpMC solution suggests that the HpMC molecules with a molecular weight, $M_w = 220 \times 10^3$, also behave as rod-like particles in aqueous system. Figure 4.22(a) shows the obtained ω dependence of G' and G'' for aqueous solutions of HeC(1.3:220) and HpMC(0.15:1.8:220) at c = 5 wt% and T = 10 ºC. Although these samples possess almost same molecular weight of 220×10^3 and degree of polymerization of 1000 and 1100 for HeC(1.3:220) and HpMC(0.15:1.8:220), respectively, the longest relaxation time of aqueous

HpMC(0.15:1.8:220) solution at c = 5 wt% and T = 10 ºC is much longer than that of aqueous HeC(1.3:220) solution at the same concentration and temperature. Figure 4.22(b) shows the master curves of G' and G'' for aqueous solutions of HeC(1.3:220) and HpMC(0.15:1.8:220) at c = 5 wt% and T = 10 ºC obtained by shifting the data of HeC (1.3:220) only along frequency axis taking the data of HpMC(0.15:1.8:220) at c = 5 wt% and T = 10 ºC as the standards. The horizontal shift factor is termed a_s. The value of a_s needed to obtain the master curves is 0.062, i.e., the average relaxation time of aqueous HpMC(0.15:1.8:220) solution at c = 5 wt% and T = 10 ºC is ca. 16 times as long as that of aqueous HeC(1.3:220) solution at the same concentration and temperature.

Moreover, in order to determine the intrinsic viscosity, $[\eta]$, of HeC(1.3:220) and HpMC(0.15:1.8:220), I used the next equations:[15]

$$\eta_{sp} = \frac{\eta - \eta_s}{\eta_s} \qquad (4\text{-}2)$$

$$[\eta] = \lim_{c \to 0} \frac{\eta_{sp}}{c} \qquad (4\text{-}3)$$

where η_{sp}, η, η_s and c are the specific viscosity, the viscosity of polymer solution, the viscosity of solvent and the polymer concentration in the unit of g mL^{-1}, respectively. The values of η_{sp} for these solutions are experimentally determined by using an Ubbelohde viscometer. Figure 4.23 shows the c dependence of $\eta_{sp}c^{-1}$ for aqueous solutions of HeC(1.3:220) and HpMC(0.15:1.8:220) at 25 ºC. The $[\eta]$ values of HeC(1.3:220) and HpMC(0.15:1.8:220) were evaluated to be 225 mL/g and 510 mL/g, respectively, from the intercept values of η_{sp}/c. Then, the volume occupied by HpMC(0.15:1.8:220) in dilute aqueous solution is much larger than that by HeC(1.3:220) in the same state. However, the average modulus of these aqueous solutions is independent of the substitution condition at the same concentration and temperature. These observations suggest that both HeC and HpMC molecules with a molecular weight of 220 × 10^3 behave as rod-like particles in aqueous solution, and the number of folding in each HeC molecule to keep the rod-like conformation would be larger than the case of

HpMC.[18] The reason for the large folding number is likely that the distance between backbone of the folding cellulose of HeC is larger than that of HpMC due to the longer chain length of the substitution groups of HeC and its higher hydration number than HpMC as discussed in Chapter 2. Consequently, the differences of the viscoelastic behavior between aqueous solutions of HeC and HpMC indicate that the substitution by hydroxyethyl groups has great influence not only on the hydration behavior of cellulose ethers but also their conformation.

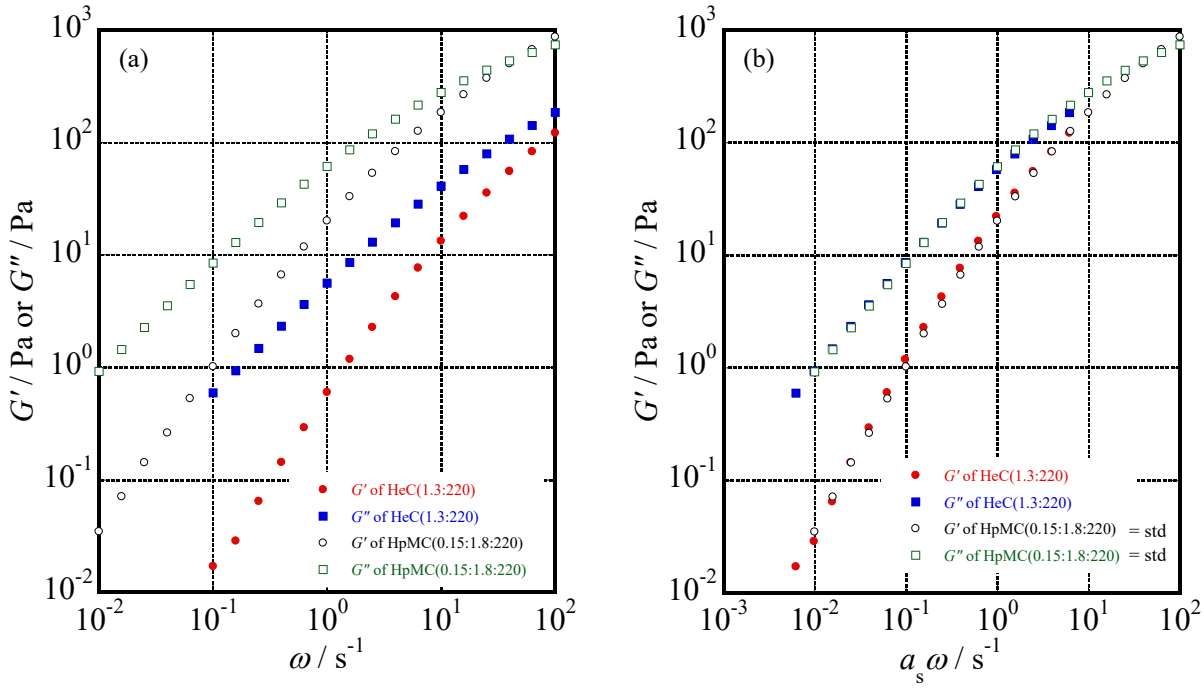

Figure 4.22 (a) Angular frequency, ω, dependence of G' and G'' for aqueous solutions of HeC(1.3:220) and HpMC(0.15:1.8:220) at c = 5 wt% and T = 10 ºC. (b) Master curves of G' and G'' for aqueous solutions of HeC(1.3:220) and HpMC(0.15:1.8:220) at c = 5 wt% and T = 10 ºC obtained by shifting the data of HeC(1.3:220) along frequency axis taking the data of HpMC(0.15:1.8:220) at c = 5 wt% and T = 10 ºC as the standards.

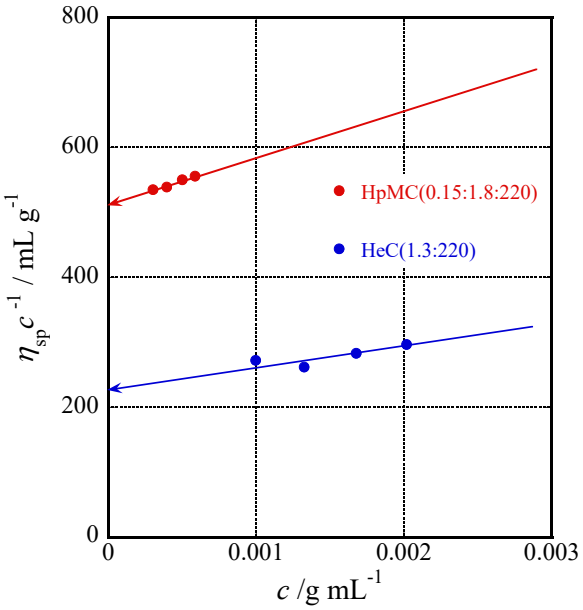

Figure 4.23 Dependence of concentration reduced specific viscosity, $\eta_{sp} c^{-1}$, on the concentration for aqueous solutions of HeC(1.3:220) and HpMC(0.15:1.8:220) at $T = 25$ ºC.

4.4 Conclusions

Temperature dependence of viscoelastic behavior for aqueous solutions of hydroxypropyl cellulose, HpC, and hydroxyethyl cellulose, HeC, was investigated. HpC and HeC molecules in aqueous solution behave as simply entangled chains in a lower temperature range, $T \leq 40$ ºC. However, a part of HpC polymer chains forms a network structure with increasing T above $T = 40$ ºC. Although the network structure grows rapidly with increasing T, a shoulder of G' found in a lower frequency range never exceeds G'' values before showing gelation behavior. The aqueous HpC systems demonstrated the critical gel behavior at $T = 46$ ºC, and finally the systems showed gel like behavior at $T = 48$ ºC. The gelation mechanism of aqueous HpC system is essentially different from that of aqueous solutions of MC and HpMC. On the other hand, a part of HeC molecules in aqueous solution also forms a weak network structure with increasing temperature above $T = 40$ ºC. Although the

viscoelasticity in a low frequency range increases with increasing T, the aqueous HeC systems do not demonstrate gelation behavior even in a high T range. This is because the dehydration behavior of HeC in aqueous systems with increasing T is quite gentle as discussed in Chapter 2.

The conformation of HeC in aqueous solution was investigated for a molecular weight range from M_w = 220 × 10^3 to 1420 × 10^3 at T = 1 ºC by using viscoelastic measurements. Time-concentration and time-molecular weight superposition principles work well in the aqueous HeC systems. Concentration, c, the number density of polymer chains, ν, and M_w dependence of the average relaxation time, τ_w, and the average modulus (the reciprocal value of steady state compliance), J_e^{-1}, for aqueous HeC solutions was determined from the shift factors for frequency and modulus axes. The power laws for c, ν and M_w dependence of τ_w and J_e^{-1} altered with increasing M_w. Then, the M_w range was divided into three regions: (i) $M_w \leq 520 \times 10^3$, (ii) $520 \times 10^3 \leq M_w \leq 820 \times 10^3$ and (iii) $820 \times 10^3 < M_w$, and the conformation of HeC molecules in aqueous solution was discussed. In the first region (i), $M_w \leq 520 \times 10^3$, the experimentally obtained relationships for HeC, $\tau_w \propto \nu^{3.2} M_w^{8.9}$ and $J_e^{-1} \propto \nu^{1.2}$, are quite similar to the theoretically predicted relationships for entangled rigid rod-like particles, $\tau_w \propto \nu^2 M_w^9$ and $J_e^{-1} \propto \nu^1$. In the second region (ii), $520 \times 10^3 \leq M_w \leq 820 \times 10^3$, the obtained c dependence of J_e^{-1} for HeC, $J_e^{-1} \propto c^{1.2\text{-}1.4}$, is close to the theoretically predicted one for entangled semiflexible polymers, $J_e^{-1} \propto c^{1.33}$ or $J_e^{-1} \propto c^{1.4}$. Moreover, the obtained M_w dependence of J_e^{-1} shows little frequency dependence, $J_e^{-1} \propto M_w^{\sim 0}$. In the third region (iii), $820 \times 10^3 < M_w$, the c dependence of J_e^{-1} for HeC, $J_e^{-1} \propto c^{1.6\text{-}1.7}$, approaches the experimentally confirmed one for entangled flexible polymers, $J_e^{-1} \propto c^{2.0}$. Consequently, the HeC molecules in aqueous system alter their rigidity and increase their flexibility with increasing molecular weight.

References

(1) Ibbett, R. N.; Philp, K.; Price, D. M. 13C n.m.r. Studies of the Thermal Behaviour of Aqueous Solutions of Cellulose Ethers. *Polymer (Guildf).* **1992**, *33* (19), 4087–4094.

(2) Vshivkov, S. A.; Rusinova, E. V. Phase Diagrams of a Hydroxypropyl Cellulose-Water System under Static Conditions and in the Shear Field. *Polym. Sci. Ser. B* **2007**, *49* (7–8), 209–212.

(3) Jing, Y.; Wu, P. Study on the Thermoresponsive Two Phase Transition Processes of Hydroxypropyl Cellulose Concentrated Aqueous Solution: From a Microscopic Perspective. *Cellulose* **2013**, *20* (1), 67–81.

(4) Carotenuto, C.; Grizzuti, N. Thermoreversible Gelation of Hydroxypropylcellulose Aqueous Solutions. *Rheol. Acta* **2006**, *45* (4), 468–473.

(5) Costanzo, S.; Pasquino, R.; Donato, R.; Grizzuti, N. Effect of Polymer Concentration and Thermal History on the Inverse Thermogelation of Hydroxypropylcellulose Aqueous Solutions. *Polymer (Guildf).* **2017**, *132*, 157–163.

(6) Winter, H. H.; Mours, M. Rheology of Polymers Near Liquid-Solid Transitions. *Adv. Polym. Sci.* **1997**, *134*, 164–234.

(7) CELLOSIZE Hydroxyethyl Cellulose https://nshosting.dow.com/doc-archive/industry/building_construction/Cellosize_brochure.pdf.

(8) Benyounes, K.; Remli, S.; Benmounah, A. Rheological Behavior of Hydroxyethylcellulose (HEC) Solutions. *J. Phys. Conf. Ser.* **2018**, *1045* (1), 012008.

(9) Del Giudice, F.; Tassieri, M.; Oelschlaeger, C.; Shen, A. Q. When Microrheology, Bulk Rheology, and Microfluidics Meet: Broadband Rheology of Hydroxyethyl Cellulose Water Solutions. *Macromolecules* **2017**, *50* (7), 2951–2963.

(10) Ouaer, H.; Gareche, M. The Rheological Behaviour of a Water-Soluble Polymer (HEC) Used in Drilling Fluids. *J. Brazilian Soc. Mech. Sci. Eng.* **2018**, *40* (8), 380.

(11) Hardy, R. C.; Cottington, R. L. Viscosity of Deuterium Oxide and Water in the Range 5 ° to 125° C. *J. Res. Natl. Bur. Stand. (1934).* **1949**, *42* (6), 573–578.

(12) M. Doi and S. F. Edwards. *The Theory of Polymer Dynamics*; Oxford, 1986.

(13) Ferry, J. D. *Viscoelastic Properties of Polymers*, 3rd ed.; Wiley & Sons: New York, 1980.

(14) Morse, D. D. Tube Diameter in Tightly Entangled Solutions of Semiflexible Polymers. *Phys. Rev. E - Stat. Physics, Plasmas, Fluids, Relat. Interdiscip. Top.* **2001**, *63* (3), 1–22.

(15) Clasen, C.; Kulicke, W. M. Determination of Viscoelastic and Rheo-Optical Material Functions of Water-Soluble Cellulose Derivatives. *Progress in Polymer Science (Oxford)*. 2001.

(16) Brown, W.; Henley, D.; Öhman, J. Studies on Cellulose Derivatives. Part II. The Influence of Solvent and Temperature on the Configuration and Hydrodynamic Behaviour of Hydroxyethyl Cellulose in Dilute Solution. *Die Makromol. Chemie* **1963**, *64* (1), 49–67.

(17) Dow chemicals. *Handbook on Methocel Cellulose Ether Products*; Dow chemicals, 1975.

(18) Sagawa, N.; Yamanishi, N.; Shikata, T. A Viscoelastic Study of Dilute Aqueous Solution of Chemically Modified Cellulose Ethers Using Dynamic Light Scattering Techniques. *Nihon Reoroji Gakkaishi* **2017**, *45* (1), 57–63.

Chapter 5: Summary and Conclusions

The water soluble cellulose ether samples, WSCEs, are widely used for various applications because of their unique excellent properties. However, the reason why WSCEs demonstrate temperature dependent water solubility and the conformation of WSCEs in aqueous solution have not been fully understood. The goals of this thesis are to understand the temperature dependent dynamics of the aqueous WSCEs systems from two different perspectives, water and solute molecules, and to clarify the structure of WSCEs dissolved in water.

In Chapter 2, the hydration numbers for WSCEs, such as methyl cellulose, MC, hydroxypropylmethyl cellulose, HpMC, and hydroxyetylmethyl cellulose, HeMC, hydroxyethyl cellulose, HeC, and hydroxypropyl cellulose, HpC, in aqueous solution were determined by using extremely high-frequency dielectric spectroscopic techniques. The critical hydration number for mainly methylated cellulose ether samples (MC, HpMC and HeMC) necessary to be dissolved in water was evaluated to be ca. 5 because the hydration numbers observed just below their lower critical soluble temperatures (LCST) were close to 5 irrespective of their molecular weights. In the case of HeC, the dehydration behavior with increasing temperature was obviously gentler than that of the mainly methylated cellulose ethers. The hydration numbers for the examined HeC samples were substantially larger than the critical hydration number, ca. 5, even at a high temperature of 70 ºC. Therefore, the HeC samples keep their high water solubility even in a high temperature range. On the other hand, although the hydration number of HpC obtained just below its LCST value of T = 45 ºC was much larger than the critical hydration number of ca. 5, the aqueous HpC solution demonstrated a cloud point at 46 ºC because of the intermolecular interaction between its substitution groups. It was concluded that larger hydration numbers of cellulose ethers than their critical hydration numbers

are necessary to keep their solubility in water over a wide temperature range. When the hydrophobicity of the substitution groups is slightly high, the required hydration number to be dissolved in water becomes substantially large.

In Chapter 3, the gelation mechanism for aqueous solutions of MC and HpMC was investigated by using dynamic viscoelastic measurements. A small part of MC and HpMC polymer chains formed a weak network structure possessing a long relaxation time. The weak network structure gradually grew to a strong network structure due to dehydration behavior with increasing temperature. Additional increase of temperature led to spreading the strong network throughout the solution, and MC and HpMC demonstrated gelation behavior. Aqueous solutions of MC and HpMC did not show the critical gel behavior, which is usually observed in many gel forming systems. The conformation of HpMC in aqueous system was investigated in a molecular weight range from M_w = 75×10^3 to 300×10^3 at 10 ºC by using viscoelastic measurements. The obtained dependence of the average relaxation time, τ_w, and the average modulus (the reciprocal value of steady state compliance), J_e^{-1}, on concentration, c, the number density of polymer chains, ν, and M_w for HpMC was quite similar to the theoretically predicted relationships for entangled rigid rod-like particles. Therefore, HpMC molecules behave as rod-like particles possessing high rigidity in aqueous solution.

In Chapter 4, dynamic viscoelastic properties for aqueous solutions of HpC and HeC were investigated. Although a weak network structure appeared and grew in aqueous HpC system with increasing temperature as in the aqueous MC and HpMC systems, the HpC system demonstrated the critical gel behavior at T = 46 ºC. Then, the gelation mechanism of aqueous HpC solution is essentially different from that of aqueous solutions of MC and HpMC. The reason for this discrepancy would be that the hydrophobicity of substitution groups for HpC is slightly higher than that for MC and HpMC. On the other hand, although the aqueous HeC system demonstrated a shoulder in storage modulus, G', with increasing temperature, the system never showed gelation behavior even at a high temperature of T = 70 ºC. This is because the dehydration behavior of HeC with increasing T is very

much gentler than that of other WSCEs. The obtained c, ν and M_w dependence of τ_w and J_e^{-1} for aqueous HeC solution suggested that the HeC molecules in aqueous system cannot keep their rigidity and the flexibility becomes pronounced with increasing molecular weight. The comparison of viscoelastic behavior between aqueous solutions of HeC and HpMC indicated that the substitution by hydroxyethyl groups significantly affects not only the hydration behavior of cellulose ethers, but also their conformation in aqueous solution.

List of Publications

"Hydration/Dehydration Behavior of Cellulose Ethers in Aqueous Solution"
Kengo Arai and Toshiyuki Shikata, *Macromolecules* **2017**, *50*, 5920-5928.

Related Papers

1. "Reason for the High Solubility of Chemically Modified Poly(vinyl alcohol)s in Aqueous Solution" Kengo Arai, Misumi Okuzono and Toshiyuki Shikata, *Macromolecules* **2015**, *48*, 1573-1578.
2. "Pronounced Dielectric and Hydration/Dehydration Behaviors of Monopolar Poly(N-alkylglycine)s in Aqueous Solution" Kengo Arai, Naoya Sagawa, Toshiyuki Shikata, Garrett L. Sternhagen, Xin Li, Li Guo, Changwoo Do, and Donghui Zhang, *J. Phys. Chem. B* **2016**, *120*, 9978-9986.
3. "Transport Properties of Commercial Cellulose Nanocrystals in Aqueous Suspension Prepared from Chemical Pulp via Sulfuric Acid Hydrolysis" Kengo Arai, Yoshiki Horikawa and Toshiyuki Shikata, *ACS OMEGA* **2018**, *3*, 139445-13951.
4. "Molecular motions, structure and hydration behaviour of glucose oligomers in aqueous solution" Kengo Arai and Toshiyuki Shikata, *Phys. Chem. Chem. Phys.* **2019**, *21*, 25379-25388.